Faculty of Science and Engineering
Department of Civil Engineering

Contributing Mass of Soil in Pile Lateral Vibrations

Amir Bahrami

This thesis is presented for the Degree of
Doctor of Philosophy
of
Curtin University

August 2014

Declaration

To the best of my knowledge and belief this thesis contains no material previously published by any other person except where due acknowledgment has been made.

This thesis contains no material which has been accepted for the award of any other degree or diploma in any university.

The following publications have been resulted from the work carried out for this degree.

Refereed journal paper

1. Bahrami, A. and Nikraz, H. 2013.Generalized Winkler support properties for far field modeling of laterally vibrating piles, Soil Dynamics and Earthquake Engineering, (manuscript submitted).

2. Bahrami, A. and Nikraz, H. 2012. Effect of Shaft Diameter of Pile on Lateral Winkler Springs' Stiffness. Journal of Earthquake Engineering. 16 (5): pp. 595-606.

Refereed conference papers

1. Bahrami, A. and Nikraz, H. 2013. A Mathematically Developed Dynamic Model for Laterally Loaded Piles, in Proceedings of the International Conference on State of the Art of Pile Foundation and Pile Case Histories, Jun 2-4 2013. Bandung, Indonesia: Pile 2013 International Conference Undertaken by IRSM.

2. Bahrami, Amir and Nikraz, Hamid. 2012. Initial Soil Springs Stiffness for laterally loaded Piles, in G Narsilio, A Arulrajah, and J Kodikara (ed), Proceedings of the 11th Australia - New Zealand Conference on Geomechanics (ANZ 2012), Jul 15 2012, pp. 1027-1032. Melbourne, Vic.: The Australian Geomechanical Society and New Zealand Geotechnical Society.

3. Bahrami, Amir and Nikraz, Hamid. 2011. Characteristics of Radiated Waves in Viscoelstic Soil Layer due to Lateral Flexural Vibration of Single Pile, in Mohamed A Shahin and Hamid R Nikraz (ed), International Conference on Advances in Geotechnical Engineering (ICAGE 2011), Nov 7 2011, pp. 997-1005.Perth, Australia: Australian Geomechanics Society

Signature: …….

Date: ……...

I would like to dedicate this thesis to my lovely wife, Molouk and my children Shaghayegh, Negar and Parham for their patience and support.

Abstract

A theoretical research on laterally vibrating piles is conducted towards solving elastodynamic equations in a semi-infinite elastic continuum. The soil and the pile are assumed to be linearly elastic under small deformations. Solution to the elastodynamic equations includes lateral and rotational deformations of the pile. Full continuity between the pile and the soil is assumed and the effect of shear stresses between the soil and the surface of the pile is accounted for.

The solution mathematically describes radiated waves from the pile into the soil media. Formulations for shear (SH) and pressure (P) waves are provided as the first phase of the solution of the elastodynamic equations.

Analogy with beam on elastic foundation lead to introduction of a generalized Winkler springs with complex-valued properties (impedance) which include stiffness, mass and damping values. The values of stiffness, mass and damping are presented in closed mathematical form for low, medium and high frequency limits. A static value is also derived for the stiffness of Winkler springs.

In order to verify the theoretically derived values, large numbers of finite element analyses are performed. These analyses are static and cover a wide range of variations in soil properties. Winkler spring stiffness is calculated for finite element analyses and correlated with the soil and pile properties which are presented as non-dimensional factors. The results are compared with the formulation obtained from the theoretical analysis. There is good agreement between the finite element and theoretical results obtained for Winkler spring stiffness, therefore the theory is deemed verified.

The problem of axially vibrating pile is also briefly approached and improvement is made on an existing theory. The approach is purely mathematical and removes some of the shortcomings of the existing solution.

Applications of the results obtained in different sections are illustrated via solved examples. The examples are chosen from published pile test results. The pile is back analyzed and test results are reproduced. Very good agreement between the published test results and analysis is found.

Acknowledgements

I would like to express my deepest gratitude to my supervisor, Professor Hamid Nikraz of Civil Engineering Department of Curtin University for his invaluable guidance and encouragement in all stages of this research.

I extend my thanks to Dr. Arul Arulrajah, the Associate Supervisor and Dr. Arumugam Sathasivan, the Chairperson for being members of the research team.

The financial support provided in forms of Australian Postgraduate Award (APA) and Curtin University Postgraduate Scholarship (CUPS) are hereby highly and gratefully acknowledged.

I wish to thank Ms. Camilla Brokking for her valuable effort on editing the final copy of this thesis.

Table of Contents

List of Figures

List of Tables

Notations and Nomenclature

A_p=	Cross-sectional area of pile
r_0 =	Shaft (outside) radius of pile (mm)
A, B, C, D, b, c, q, f =	Constants
$A_s = \pi r_0^2$	Shaft cross-sectional area
c_p=	Material viscous damping of the pile
c_s =	Geometric (viscous) damping of the soil
c_h =	Geometric (hysteresis) damping of the soil
D=	Pile diameter
E =	Young modulus of elasticity of homogeneous material (general)
E_s =	Modulus of elasticity of soil
E_p =	Modulus elasticity of pile
FDM=	Finite difference method
FEA=	Finite element analysis
FEM=	Finite element method
g =	Acceleration of gravity
$i = \sqrt{-1}$	Imaginary number basis
I_p =	Second moment of inertia of pile
$I_s = \frac{\pi}{4} r_0^4$	Second moment of inertia of pile shaft
k_s =	Lateral spring stiffness constant

k_θ =	Rotational spring stiffness constant
k_p =	Rate of change of spring stiffness with depth $k_s = k_p z^n$
K_{xx} =	Lateral translational stiffness of pile
K_{rr} =	Rotational stiffness of pile
$K_{rx} = K_{xr}$ =	Coupled rotational- translational stiffness of pile
K_h =	Free-head pile lateral stiffness
kN=	killo newtons
L =	Pile length
m=	Mass
$m_p = \rho_p A_p$	Mass per unit length of pile
m_s =	Contributing mass of the soil
M_0 =	Bending moment on pile head
MPa=	Mega Pascals
SDOF=	Single degree of freedom
T_0 =	Tangential force on pile head
r =	Radial component of cylindrical coordinates system
$\hat{r} = r / r_0$	Non-dimensional radial distance parameter
D/L =	Pile diameter to length ratio (inverse of pile slenderness)
t =	Time
u =	Soil deformation in radial direction in cylindrical coordinates system

$u_x =$	Soil deformation in x-direction in Cartesian coordinates system
$u_y =$	Soil deformation in y-direction in Cartesian coordinates system
$u_z =$	Soil deformation in z-direction in Cartesian coordinates system
$v =$	Soil deformation in tangential direction in cylindrical coordinates system
$w =$	Soil deformation in vertical direction in cylindrical coordinates system
$V_p = \sqrt{(\lambda + 2\mu)/\rho}$	Pressure wave velocity in soil
$V_s = \sqrt{\mu/\rho}$	Shear wave velocity in soil
$x, y, z =$	Cartesian coordinate axis
$\hat{z} = z/r_0$	Non-dimensional depth parameter
$X(z) =$	Pile lateral deflection 'X' as a function of depth 'z'
$\mu =$	Shear modulus of the soil (also 'G') (MPa)
$\rho =$	Soil density (kg/m^3)
$\rho_p =$	Density of pile material (kg/m^3)
$\nu =$	Poisson's ratio of soil
$\eta = \sqrt{\frac{1-2\nu}{2(1-\nu)}}$	
$\beta = \sqrt[4]{\frac{k_s}{4E_pI_p}}$	Inverse characteristic length of the pile, also load transfer proportion in vertically vibrating piles
$\gamma = \sqrt{\frac{k_\theta}{4E_pI_p}}$	
$\theta =$	Rotation parameter

$\sigma_{ii} =$	Normal stress component
$\varepsilon_i =$	Normal strain component
$\varepsilon_{ij} =$	Shear strain component
$\gamma_{ij} =$	Shear strain component
$\xi_p = c_p / 2m_p\omega$	Pile material damping ratio
$\xi_h =$	Geometrical hysteretic damping ratio
$\xi_s =$	Geometrical viscous damping ratio
$\xi_{sh} =$	Material hysteretic damping ratio of soil
$\Delta =$	Dilatation
$\Delta_0 =$	Pile head lateral deflection
$\theta_0 =$	Pile head rotation
$\lambda =$	Lamé's constant
$\omega =$	Rotational frequency
$\varpi = \omega / V_s$	Ratio of rotational frequency to shear wave velocity
$a_0 = \varpi r_0 = \omega r_0 / V_s$	Non-dimensional frequency factor
$\phi =$	Airy stress function, also an arbitrary potential function
$\psi =$	An arbitrary potential function

CHAPTER ONE

1 INTRODUCTION

1.1 Background

Piles are used to support structures and machinery where surface soil is not strong enough to resist the applied loads or settlement is an issue. Dynamic loads due to wind, sea waves (in case of offshore structures), earthquake and rotary equipment cause lateral vibration in the structure and consequently on piles. The dynamic interaction between piles and the soil has been a subject of research for the past few decades. The theory of elasticity was one of the earliest approaches to the problem and was expected to form a basic theory for the soil-pile interaction. Approaches to this issue can be divided into two main categories. The first category is approaches which implement numerical methods to solve the soil-pile interaction problem. The problem may be formulated either in terms of boundary integral equations (e.g. Pak 1985) which are solved via numerical methods or in terms of governing differential equations (Poulos 1971a) which are solved via finite difference or other appropriate methods. Parametric finite element studies (Randolph 1981) can also be included under this category. Although these methods can be numerically accurate, their coverage depends on the range of essential variables chosen for the numerical evaluation. The second category is those approaches providing rigorous solutions to the elasticity equations in closed form (Baranov 1967; Novak 1974; Nogami 1980). Due to the complexity of the problem, all of these solutions include simplifying assumptions that restrict the solutions to special cases. For example, a plane strain approach, which is the core of some computer programs, can only provide accurate results for very high frequencies of vibration (Novak, Sheta, El-Hifnawy, El-Marsafawi and Ramadan 1991).

The author is of the opinion that the existing elastic solutions fail to fully describe the nature of the soil-pile interaction in an elastic regime. This is due to the many simplifying assumptions that are included in the process of solution. It is necessary to have a more accurate and more general solution as a basis. Although such a solution may not be used in practical cases of pile foundation design, the insight it provides helps to gain a better understanding of the nature of the soil-pile interaction and has academic and educational value.

The present research aims to improve upon the existing theories of dynamic soil-pile interaction, with the objective of providing a closed-form solution to elastodynamic equations. By a closed-form solution the author means to express the deformations, stresses

and strains in the soil and the pile in terms of elementary or advanced functions. No integral equations are provided and none of the results or conclusions is subject to a numerical evaluation. Wherever the results are not easy to interpret due to the presence of complex values or special functions, simplifications are made with the aid of mathematical expansions or curve fitting techniques. The author believes that in order to have a solid theory, it is essential to express all of the important quantities in terms of elementary functions whose behaviour is readily understood.

1.2 Research significance

The present research improves a great deal upon the existing theories of soil-pile interaction. It provides new knowledge on the characteristics of SH-P waves radiated from a laterally vibrating pile, which is helpful for the estimation of the amount of vibration reaching the structures or constructions in the vicinity of the piled foundation.

From a practical point of view, the results of this research may be used to improve the accuracy of dynamic analyses of piled foundations by including the contributing mass of soil in the analysis. The research also increases understanding of the nature of the dynamic soil-pile interaction and provides insight into the problem; therefore it has academic and educational value.

1.3 Research objectives

This research intends to develop the existing theory of laterally loaded piles through the application of theory of elasticity methods. The research will be a theoretical study of laterally loaded piles under both static and dynamic loads in order to formulate the contributing mass of soil in lateral pile vibrations. Since the inertia effect which determines the contributing mass is mixed with the stiffness and damping of the soil, separating the mass component also leads to determination of the stiffness and damping of the soil.

1.4 Outline of thesis

The thesis is arranged in six chapters. The first chapter is an introduction in which the background and the significance of the research are explained. Chapter 2 consists of a review of the literature, and the theory of elasticity formulation for static and dynamic loads is discussed for general three-dimensional (3D) and special two-dimensional (2D) cases. Boundary conditions for the problem are also formulated in this chapter. The subjects are chosen such that they are referenced throughout the text. The theory of beams on elastic foundation is considered as the central spine of the present research. An extensive study on this topic is contained in section 2.2. Statically loaded piles are referenced in section 2.3 and

existing elastic solutions for dynamically loaded piles are discussed in depth in section 2.4. This section is organized by the names of the contributors and in chronological order, both to facilitate a better understanding of the development of the theory and to give due credit to the contributors.

Chapter 3 is an independent finite element study of the statically loaded piles. The objective of this research is to study the stiffness of the soil interacting with the pile. Large numbers of analyses are performed and many new aspects of the soil-pile interaction are examined, including the effect of shaft diameter on Winkler spring stiffness. The results from this chapter are used to help verify the theory developed in chapter 4.

Chapter 4 is the main part of the thesis and focuses on the development of a rigorous theory describing soil-pile interaction. Section 4.1 deals with the solution of the elastodynamic equations in three dimensions for a laterally vibrating pile and the interaction between the soil and the pile. This section is the core of the theory and most of the findings of this research are derived in this section. Section 4.2 is a brief study of vertically vibrating piles in an attempt to improve upon an existing solution. Although it seems to be a digression from the topic, this section also includes findings on the contributing mass of soil which helps the completeness of the study.

Chapter 5 is dedicated to the contributing mass of the soil. This chapter contains the findings from chapter 4 focused on the contributing mass of the soil, and discusses the value of the contributing mass for different soil and pile types.

Chapter 6summarizes and concludes the outcomes of the research.

CHAPTER TWO

2 LITERATURE REVIEW

This chapter provides necessary material on the theory of elasticity which is used within this thesis. Therefore, only the formulas, equations and relationships which are used in the present study are given in this chapter.

The notations chosen for this chapter and within the text are more 'engineering' than 'scientific', i.e. tensor algebra and indicial notations are not used. The use of the simpler notation of engineering theory of elasticity will make the study more comprehensible and easier to follow.

2.1 Elastostatic formulation

Elastostatic equations in cylindrical coordinates are used in this study. Differential equations of static equilibrium in terms of displacement components in the soil media are presented. Radial, tangential and vertical components of displacement are shown as *u, v* and *w*, respectively. Wherever reference to displacement components in Cartesian coordinates is made, they are shown as 'u_x, u_y and u_z'. The relationships between the Cartesian and cylindrical components of displacement are given below:

$$u_x = u(r,\theta,z)\cos\theta - v(r,\theta,z)\sin\theta \qquad (2.1\text{–}1)$$

$$u_y = u(r,\theta,z)\cos\theta + v(r,\theta,z)\sin\theta \qquad (2.1\text{–}2)$$

$$u_z = w(r,\theta,z) \qquad (2.1\text{–}3)$$

In the above equations, the displacement components are expressed as a function of cylindrical coordinates ' (r,θ,z) . They could also be expressed in terms of Cartesian coordinates ' (x,y,z) .

Strains are represented as space derivatives of displacements. Small strain theory is used (Salencon 2001):

$$\varepsilon_r = \frac{\partial u}{\partial r} \qquad (2.1\text{–}4)$$

$$\varepsilon_\theta = \frac{1}{r}\frac{\partial v}{\partial \theta} + \frac{\partial u}{\partial r} \tag{2.1–5}$$

$$\varepsilon_z = \frac{\partial w}{\partial z} \tag{2.1–6}$$

$$\varepsilon_{r\theta} = \frac{1}{2}\left(\frac{\partial v}{\partial r} - \frac{v}{r} + \frac{1}{r}\frac{\partial u}{\partial \theta}\right) \tag{2.1–7}$$

$$\varepsilon_{zr} = \frac{1}{2}\left(\frac{\partial u}{\partial z} + \frac{\partial w}{\partial r}\right) \tag{2.1–8}$$

$$\varepsilon_{\theta z} = \frac{1}{2}\left(\frac{\partial v}{\partial \theta} + \frac{1}{r}\frac{\partial w}{\partial \theta}\right) \tag{2.1–9}$$

Material is considered homogeneous, linearly elastic. The generalized Hooke's law for linear isotropic elastic solids is applicable. Normal stresses σ and shear stresses τ are written in terms of strains as:

$$\sigma_r = \lambda(\varepsilon_r + \varepsilon_\theta + \varepsilon_z) + 2\mu\varepsilon_r \tag{2.1–10}$$

$$\sigma_\theta = \lambda(\varepsilon_r + \varepsilon_\theta + \varepsilon_z) + 2\mu\varepsilon_\theta \tag{2.1–11}$$

$$\sigma_z = \lambda(\varepsilon_r + \varepsilon_\theta + \varepsilon_z) + 2\mu\varepsilon_z \tag{2.1–12}$$

$$\tau_{r\theta} = 2\mu\varepsilon_{r\theta} \tag{2.1–13}$$

$$\tau_{zr} = 2\mu\varepsilon_{zr} \tag{2.1–14}$$

$$\tau_{\theta z} = 2\mu\varepsilon_{\theta z} \tag{2.1–15}$$

Where λ is Lamé's constant and μ is shear modulus or modulus of rigidity. In some texts, G is used for the latter (Timoshenko and Goodier 1970). The following relationships exist between Lamé's constants, Young's modulus of elasticity E and Poisson's ratio ν (e.g. Hetnarski and Ignaczak 2004):

$$\lambda = \frac{\nu E}{(1+\nu)(1-2\nu)} \tag{2.1–16}$$

$$\mu = \frac{E}{2(1+\nu)} \tag{2.1–17}$$

Elastostatic equations in cylindrical coordinates (in the absence of body forces) are written as follows:

$$\frac{\partial \sigma_r}{\partial r} + \frac{1}{r}\frac{\partial \tau_{r\theta}}{\partial \theta} + \frac{\partial \tau_{rz}}{\partial z} + \frac{\sigma_r - \sigma_\theta}{r} = 0 \tag{2.1–18}$$

$$\frac{\partial \tau_{r\theta}}{\partial r} + \frac{1}{r}\frac{\partial \sigma_\theta}{\partial \theta} + \frac{\partial \tau_{\theta z}}{\partial z} + 2\frac{\tau_{r\theta}}{r} = 0 \tag{2.1–19}$$

$$\frac{\partial \tau_{zr}}{\partial r} + \frac{1}{r}\frac{\partial \tau_{z\theta}}{\partial \theta} + \frac{\partial \sigma_z}{\partial z} + \frac{\tau_{zr}}{r} = 0 \tag{2.1–20}$$

Using the generalized Hooke's law and strain-deformation relationships, the equations of equilibrium can be expressed in terms of displacements:

$$(\lambda + 2\mu)\frac{\partial \Delta}{\partial r} - \frac{2\mu}{r}\frac{\partial \omega_z}{\partial \theta} + 2\mu\frac{\partial \omega_\theta}{\partial z} = 0 \tag{2.1–21}$$

$$(\lambda + 2\mu)\frac{1}{r}\frac{\partial \Delta}{\partial \theta} - 2\mu\frac{\partial \omega_r}{\partial z} + 2\mu\frac{\partial \omega_z}{\partial r} = 0 \tag{2.1–22}$$

$$(\lambda + 2\mu)\frac{\partial \Delta}{\partial z} - \frac{2\mu}{r}\frac{\partial (r\omega_\theta)}{\partial r} + \frac{2\mu}{r}\frac{\partial \omega_r}{\partial \theta} = 0 \tag{2.1–23}$$

Where

$$\Delta = \varepsilon_r + \varepsilon_\theta + \varepsilon_z = \frac{1}{r}\frac{\partial}{\partial r}(ru) + \frac{1}{r}\frac{\partial v}{\partial \theta} + \frac{\partial w}{\partial z} \tag{2.1–24}$$

is the dilatation, and:

$$\omega_r = \frac{1}{2}\left(\frac{1}{r}\frac{\partial w}{\partial \theta} - \frac{\partial v}{\partial z}\right) \tag{2.1–25}$$

$$\omega_\theta = \frac{1}{2}\left(\frac{\partial u}{\partial z} - \frac{\partial w}{\partial r}\right) \tag{2.1–26}$$

$$\omega_z = \frac{1}{2r}\left(\frac{1}{r}\frac{\partial}{\partial r}(rv) - \frac{\partial u}{\partial \theta}\right) \tag{2.1–27}$$

2.1.1 Elastodynamic formulation

Elastodynamic equations are derived from the elastostatic equations by adding the inertia term to the right-hand side:

$$(\lambda + 2\mu)\frac{\partial \Delta}{\partial r} - \frac{2\mu}{r}\frac{\partial \omega_z}{\partial \theta} + 2\mu\frac{\partial \omega_\theta}{\partial z} = \rho\frac{\partial^2 u}{\partial t^2} \tag{2.1–28}$$

$$(\lambda + 2\mu)\frac{1}{r}\frac{\partial \Delta}{\partial \theta} - 2\mu\frac{\partial \omega_r}{\partial z} + 2\mu\frac{\partial \omega_z}{\partial r} = \rho\frac{\partial^2 v}{\partial t^2} \tag{2.1–29}$$

$$(\lambda + 2\mu)\frac{\partial \Delta}{\partial z} - \frac{2\mu}{r}\frac{\partial (r\omega_\theta)}{\partial r} + \frac{2\mu}{r}\frac{\partial \omega_r}{\partial \theta} = \rho\frac{\partial^2 w}{\partial t^2} \tag{2.1–30}$$

Where ρ is the mass of unit volume of the soil.

2.1.2 Static two dimensional problems

The most important classical two-dimensional formulations are plane stress and plane strain (e.g. Sadd 2009). Plane strain elastodynamic equations can be derived from the general elastodynamic equations by setting *'w=0'* and considering that the displacement components *'u'* and *'v'* are independent to *'z'* coordinates. Note that in soil-pile interaction problems, the radial and tangential components of displacement are often set in the horizontal plane while the axial component is oriented vertically. Plane strain formulation is applicable to problems where one of the dimensions is much larger than the other two, such that the strain in the direction of the larger dimension is considered negligible.

$$(\lambda + 2\mu)\frac{\partial \Delta}{\partial r} - \mu\frac{1}{r^2}\left[\frac{\partial^2 (vr)}{\partial r \partial \theta} - \frac{\partial^2 u}{\partial \theta^2}\right] = 0 \tag{2.1–31}$$

$$(\lambda + 2\mu)\frac{1}{r}\frac{\partial \Delta}{\partial \theta} + \mu\frac{\partial}{\partial r}\left\{\frac{1}{r}\left[\frac{\partial}{\partial r}(vr) - \frac{\partial u}{\partial \theta}\right]\right\} = 0 \tag{2.1–32}$$

$$u = u(r,\theta), v = v(r,\theta), w = 0 \tag{2.1–33}$$

Static plane strain problems can be solved by employing the Airy stress function, which transforms the elastostatic equations into a bi-harmonic equation:

$$\nabla^4\phi = (\frac{\partial^2}{\partial r^2} + \frac{1}{r}\frac{\partial}{\partial r} + \frac{1}{r^2}\frac{\partial^2}{\partial \theta^2})^2\phi = 0 \qquad (2.1\text{–}34)$$

Where ϕ is the Airy stress function and is related to stress components by the following equations:

$$\sigma_r = \frac{1}{r}\frac{\partial\phi}{\partial r} + \frac{1}{r^2}\frac{\partial^2\phi}{\partial\theta^2} \qquad (2.1\text{–}35)$$

$$\sigma_\theta = \frac{\partial^2\phi}{\partial r^2} \qquad (2.1\text{–}36)$$

$$\tau_{r\theta} = -\frac{\partial}{\partial r}(\frac{1}{r}\frac{\partial\phi}{\partial\theta}) \qquad (2.1\text{–}37)$$

The general solution of the bi-harmonic equation in polar coordinates is given in (Sadd 2009). The solution is credited to Michell (1899) and is commonly called Michell's solution. The general solution is too lengthy and therefore it is not given in this text.

Plane stress formulation is suitable for thin members where stresses through the thickness can be considered negligible compared to other stress components. This formulation does not have much application for soil-pile interaction problems and its formulation is therefore not given here.

2.1.3 Dynamic two-dimensional problems

Plane strain formulation has had an important historical role (Baranov 1967; Novak 1974) in the theory of soil-pile interaction, and for this reason is given here::

$$(\lambda+2\mu)\frac{\partial\Delta}{\partial r} - \frac{\mu}{r^2}[\frac{\partial^2(v.r)}{\partial r\partial\theta} - \frac{\partial^2 u}{\partial\theta^2}] = \rho\frac{\partial^2 u}{\partial t^2} \qquad (2.1\text{–}38)$$

$$(\lambda+2\mu)\frac{1}{r}\frac{\partial\Delta}{\partial\theta} + \mu\frac{\partial}{\partial r}\{\frac{1}{r}[\frac{\partial}{\partial r}(v.r) - \frac{\partial u}{\partial\theta}]\} = \rho\frac{\partial^2 v}{\partial t^2} \qquad (2.1\text{–}39)$$

Where *u,v* and *w* are displacement components, and:

$$u = u(r,\theta,t), \quad v = v(r,\theta,t), \quad w = 0 \qquad (2.1\text{–}40)$$

The equations (2.1–38) and (2.1–39) can be simplified by introducing potential functions 'ψ' and 'ϕ', following Lamb's (1904) concept:

$$u = \frac{\partial \phi}{\partial r} + \frac{1}{r}\frac{\partial \psi}{\partial \theta} \tag{2.1–41}$$

$$v = \frac{1}{r}\frac{\partial \phi}{\partial \theta} - \frac{\partial \psi}{\partial r} \tag{2.1–42}$$

Substituting equations (2.1–41) and (2.1–42) into equations (2.1–38) and (2.1–39) leads to the following equations:

$$V_p^2 \nabla^2 \phi = \frac{\partial^2 \phi}{\partial t^2} \tag{2.1–43}$$

$$V_s^2 \nabla^2 \psi = \frac{\partial^2 \psi}{\partial t^2} \tag{2.1–44}$$

Where V_p and V_s are velocities of pressure and shear waves respectively. In a homogeneous elastic media the above wave velocities van be expressed in terms of elasticity constants:

$$V_p = \sqrt{\frac{\lambda + 2\mu}{\rho}}, \quad V_s = \sqrt{\frac{\mu}{\rho}} \tag{2.1–45}$$

Solutions of the equations (2.1–43) and (2.1–44) in application to lateral pile vibration are provided by Baranov (1967) and will be discussed in section 2.4.1.

2.1.4 Boundary conditions of the problem

It is essential to accurately determine the boundary conditions of a problem, in order to obtain a correct elasticity solution. The problem of a laterally loaded pile in an elastic half-space inherits the general boundary conditions of an elastic half-space problem. In addition, the connectivity between the soil and pile surface forms new boundary conditions to the problem.

In an elastic half-space, stresses (tractions) on the free surface should be zero, except possibly at a finite zone where external loads are applied. Additionally, the deformations must vanish at long distances from the pile. Mathematically, the limit of deformations at infinity should be zero.

The presence of a pile adds complicated boundary conditions to the problem. Assuming that the pile follows the Euler-Bernouli theory, the cross-sections of the pile should remain un-

deformed during bending of the pile. The deflection of the pile at any point is considered to be a combination of a horizontal translation and a rotation. From this point of view, the boundary conditions on the pile surface are different from a cavity problem (Kausel 2006). Figure 2-1 shows the components of the lateral deflection of a pile.

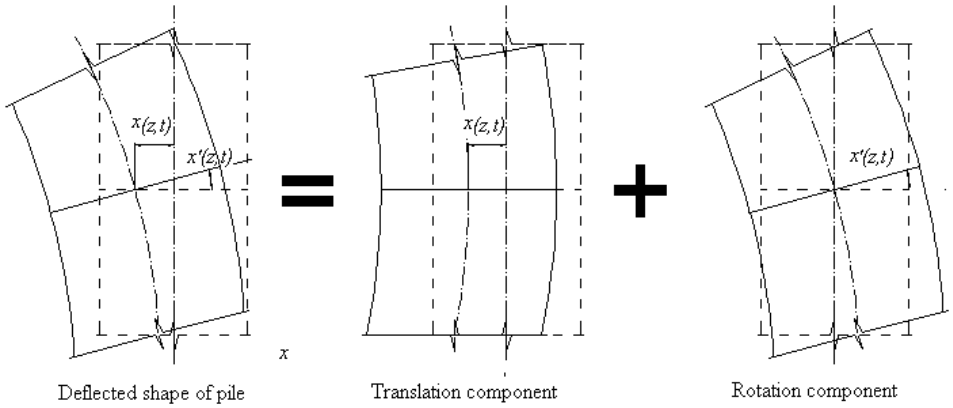

Figure 2-1 Components of the lateral deflection of a pile

Here pile deflection is arbitrarily chosen in the '*xz*' plane. The deflection is decomposed to a horizontal translation and a rotation. Figure 2-2 shows the translation and rotation of the pile cross-section in the horizontal *'xy'* plane. Connectivity conditions between the soil and the pile surface can be written as:

$$u(r_0,\theta,z,t) = X(z,t)\cos\theta \qquad (2.1\text{–}46)$$

$$v(r_0,\theta,z,t) = -X(z,t)\sin\theta \qquad (2.1\text{–}47)$$

$$w(r_0,\theta,z,t) = -r_0 X'(z,t)\cos\theta \qquad (2.1\text{–}48)$$

Where 'r_0', *'X(z,t)'* and *'X'(z,t)'* are radius, translation and rotation of an arbitrary cross-section of pile, respectively.

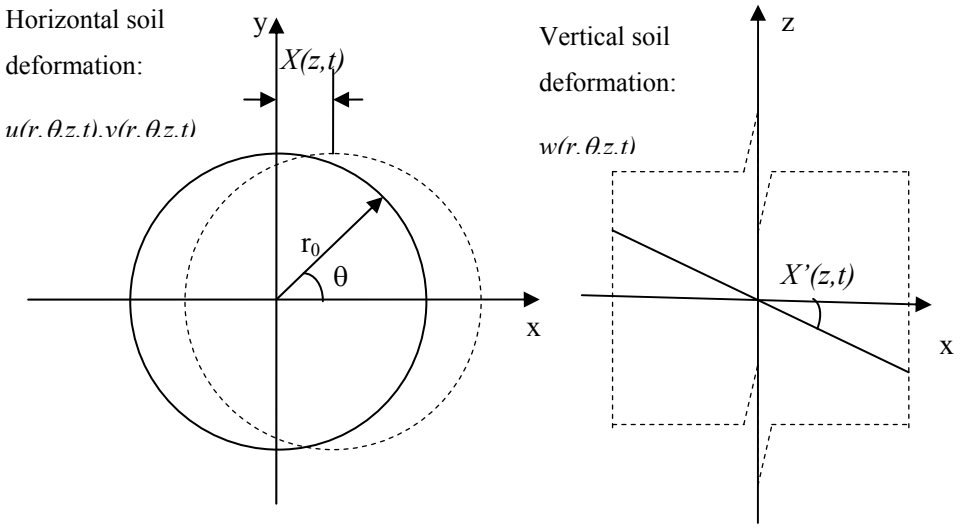

Figure 2-2 Translation and rotation of a circular pile cross-section

In a soil-pile interaction problem, loads are not applied at the half-space. An Euler-Bernouli pile bends under the action of a lateral load at its top.

2.1.5 Tangential force on the surface of a half-space

This class of problem is discussed in the literature for vertical and horizontal forces on the surface of two- and three-dimensional half-spaces for both static and dynamic cases. The problem of an infinitely long line force on the ground surface can be considered a two-dimensional problem.

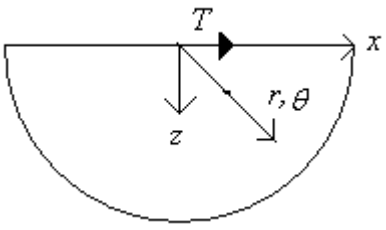

Figure 2-3: Two-dimensional half-space under a tangential load

Figure 2-3 shows a two-dimensional half-space under a tangential load *T* on its surface. The following formulations are taken from Johnson (1985):

$$u_x(x,z)=\frac{T}{2\pi\mu}[2(1-\nu)\ln\frac{z}{r}+(1-\frac{z^2}{r^2})] \tag{2.1–49}$$

$$u_z(x,z)=\frac{T}{2\pi\mu}[(1-2\nu)\tan^{-1}\frac{x}{z}+\frac{xz}{r^2}] \tag{2.1–50}$$

Where $r=\sqrt{x^2+z^2}$ is the radial distance to the point of application of the load. It can be seen that due to the presence of a logarithmic term in equation (2.1–49), the horizontal deformation at distances very far from the applied load becomes indefinite. Stresses and strains, however, do not suffer from the presence of such singularity. The stresses read:

$$\sigma_x(x,z)=-\frac{2T}{\pi r^4}x^3 \tag{2.1–51}$$

$$\sigma_z(x,z)=-\frac{2T}{\pi r^4}xz^2 \tag{2.1–52}$$

$$\tau_{xz}(x,z)=-\frac{2T}{\pi r^4}x^2z \tag{2.1–53}$$

Strains are written as:

$$\varepsilon_x(x,z)=-\frac{Tx}{\pi\mu r^2}(1-\nu-\frac{z^2}{r^2}) \tag{2.1–54}$$

$$\varepsilon_z(x,z)=-\frac{Tx}{\pi\mu r^2}(\nu-\frac{z^2}{r^2}) \tag{2.1–55}$$

$$\varepsilon_{xz}(x,z)=-\frac{T}{\pi\mu r^4}x^2z \tag{2.1–56}$$

The problem of a three-dimensional half-space under the tangential concentrated force is known in the literature as the ‘problem of Boussinesq and Cerruti ‘ (Love 1944, Art.167). The final results of this problem are given as a comparison with those of the two-dimensional problem:

$$u_x(x,y,z)=\frac{T}{4\pi\mu}[\frac{1}{R}+\frac{x^2}{R^3}+(1-2\nu)\{\frac{1}{R+z}-\frac{x^2}{R(R+z)^2}\}] \tag{2.1–57}$$

$$u_y(x,y,z)=\frac{T}{4\pi\mu}[\frac{xy}{R^3}-(1-2\nu)\frac{xy}{R(z+R)^2} \tag{2.1–58}$$

$$u_z(x,y,z)=\frac{T}{4\pi\mu}[\frac{xz}{R^3}+(1-2\nu)\frac{x}{R(z+R)}] \tag{2.1–59}$$

Where $R=\sqrt{x^2+y^2+z^2}$ is the distance from an arbitrary point in the half-space to the point of application of the load. It can be seen that the deformation of a three-dimensional half-space does not include any singularities.

Johnson (1985) gives closed-form formulas for the stresses in three-dimensional half-space under a tangential concentrated force:

$$\frac{2\pi\sigma_x}{T}=-\frac{3x^3}{R^5}+(1-2\nu)\times\{\frac{x}{R^3}-\frac{3x}{R(R+z)^2}+\frac{x^3}{R^3(R+z)^2}+\frac{2x^3}{R^2(R+z)^3}\} \tag{2.1–60}$$

$$\frac{2\pi\sigma_y}{T}=-\frac{3xy^2}{R^5}+(1-2\nu)\times\{\frac{x}{R^3}-\frac{x}{R(R+z)^2}+\frac{xy^2}{R^3(R+z)^2}+\frac{2xy^2}{R^2(R+z)^3}\} \tag{2.1–61}$$

$$\frac{2\pi\tau_{xy}}{T}=-\frac{3x^2y}{R^5}+(1-2\nu)\{-\frac{y}{R(R+z)^2}+\frac{x^2y}{R^3(R+z)^2}+\frac{2x^2y}{R^2(R+z)^3}\} \tag{2.1–62}$$

$$\frac{2\pi\sigma_z}{T}=-\frac{3xz^2}{R^5} \tag{2.1–63}$$

$$\frac{2\pi\tau_{yz}}{T}=-\frac{3xyz}{R^5} \tag{2.1–64}$$

$$\frac{2\pi\tau_{xz}}{T}=-\frac{3x^2z}{R^5} \tag{2.1–65}$$

2.1.6 Mindlin's solution

Mindlin (1936) provided a series of closed-form solutions for the displacement field in an elastic half-space excited by static horizontal and vertical forces below the surface. The Mindlin solution plays an important role in the theory of static piles. Early solutions to the static soil-pile interaction problem implemented Mindlin's solution in their numerical algorithms. Figure 2-4 shows the notations used in Mindlin's equations.

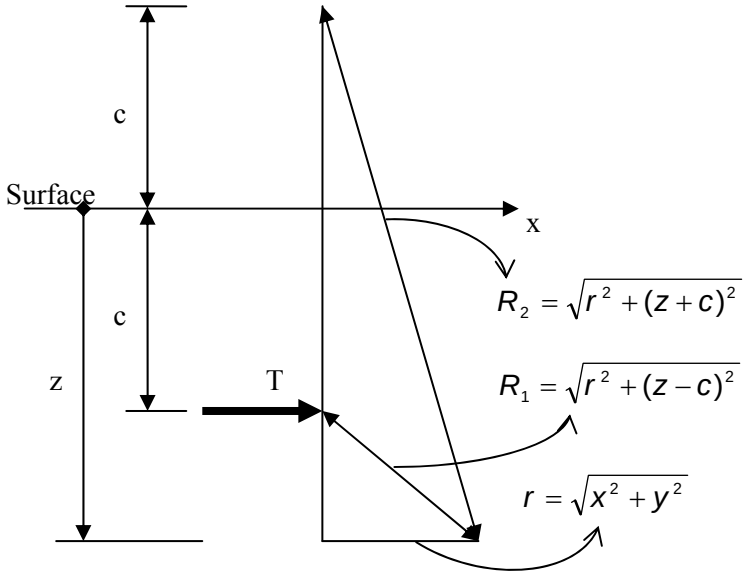

Figure 2-4 Geometry of an elastic half-space loaded horizontally under surface

The inline displacement components in the half-space are given as follows (Mindlin 1936):

$$u_x = \frac{T}{16\pi\mu(1-\nu)}\left[\frac{3-4\nu}{R_1} + \frac{1}{R_2} + \frac{x^2}{R_1^3} + \frac{(3-4\nu)x^2}{R_2^3} + \right.$$
$$\left. + \frac{2cz}{R_2^3}\left(1 - \frac{3x^2}{R_2^2}\right) + \frac{4(1-\nu)(1-2\nu)}{R_2 + z + c} \times \left(1 - \frac{x^2}{R_2(R_2 + z + c)}\right)\right] \quad (2.1\text{–}66)$$

$$u_y = \frac{Txy}{16\pi\mu(1-\nu)}\left[\frac{1}{R_1^3} + \frac{3-4\nu}{R_2^3} - \frac{6cz}{R_2^5} - \frac{4(1-\nu)(1-2\nu)}{R_2(R_2 + z + c)^2}\right] \quad (2.1\text{–}67)$$

$$u_z = \frac{Tx}{16\pi\mu(1-\nu)}\left[\frac{z-c}{R_1^3} + \frac{(3-4\nu)(z-c)}{R_2^3} - \frac{6cz(z+c)}{R_2^5} + \frac{4(1-\nu)(1-2\nu)}{R_2(R_2 + z + c)}\right] \quad (2.1\text{–}68)$$

The application of Mindlin's solution in the analysis of laterally loaded piles is discussed in section 2.3.3.

2.2 Beam on elastic foundation

The interaction between the soil and a flexible pile often results in a formulation analogous to the beam on elastic foundation. One of the earliest methods of investigating the interaction between the flexible pile and the soil was to consider the pile as an Euler- Bernouli beam and the soil as linear springs. It is not intended to duplicate the very well developed beam on

elastic foundation theory in this thesis. Only those parts of the theory that can be used as the basis for the rest of the study are formulated and developed to some extent.

2.2.1 Winkler's hypothesis

The beam on elastic foundation theory rests on the assumption that the reaction of the foundation on the beam at any point is proportional to the deflection of the beam at that point. This assumption was first made by Winkler (1867) in his study on railroads. Winkler's hypothesis was accepted and used by a number of authors (Zimmermann 1888; Timoshenko 1934). Hetenyi (1946) is frequently credited for full development of the theory, after his very famous book on this topic. Winkler's hypothesis can be mathematically expressed as:

$$q = -k_s y \tag{2.2–1}$$

Where 'q' is the reaction of the foundation on the beam, *'y'* is the deflection of the beam and k_s is called the modulus of the foundation (or the foundation modulus). Since 'q' has dimensions of force per unit length, the foundation modulus will have dimensions of stress. The negative sign indicates that the reaction is in the opposite direction to the deflection.

Throughout this thesis, piles are considered to be vertically aligned with the *'z'* axis and loaded in *'x'* direction. Therefore the notation *'X(z)'* is used here in place of *'y'*. Thus for the purpose of this thesis, we may rewrite the Winkler's hypothesis as:

$$q_x = -k_s X(z) \tag{2.2–2}$$

Employing Winkler's hypothesis and the Euler-Bernouli beam theory, the flexure equation of a flexible pile reads:

$$E_p I_p \frac{d^4 X(z)}{dz^4} + k_s X(z) = 0 \tag{2.2–3}$$

The general solution to equation (2.2–3) for an infinitely long pile can be written as:

$$X(z) = e^{-\beta z}(A\cos\beta z + B\sin\beta z) \tag{2.2–4}$$

Where $\beta = \sqrt[4]{k_s / 4E_p I_p}$ and *'A'* and *'B'* are constants that should be determined from the boundary conditions of the problem.

Under the action of a lateral force T_0 and a bending moment M_0 on its head, the pile experiences lateral displacement δ_0 and rotation θ_0. Rotation, bending moment and shear force at any point along the pile are related via the following relationships:

$$X'(z) = \frac{dX(z)}{dz} = -\beta e^{-\beta z}[A(\cos\beta z + \sin\beta z) - B(\cos\beta z - \sin\beta z)] \quad (2.2\text{–}5)$$

$$M(z) = -E_p I_p \frac{d^2X(z)}{dz^2} = -2E_p I_p \beta^2 e^{-\beta z}(A\sin\beta z - B\cos\beta z) \quad (2.2\text{–}6)$$

$$V(z) = E_p I_p \frac{d^3X(z)}{dz^3} = 2E_p I_p \beta^3 e^{-\beta z}[A(\cos\beta z - \sin\beta z) + B(\cos\beta z + \sin\beta z)] \quad (2.2\text{–}7)$$

Here *M(z)* and *V(z)* are bending moment and shear force at any arbitrary cross-section of the pile, respectively. Pile head rotation, bending moment and shear force are derived by setting *z=0* in expressions (2.2–5),(2.2–6) and (2.2–7), respectively:

$$\theta_0 = X'(0) = -\beta(A - B) \quad (2.2\text{–}8)$$

$$M_0 = M(0) = 2E_p I_p \beta^2 B \quad (2.2\text{–}9)$$

$$V_0 = V(0) = 2E_p I_p \beta^3 (A + B) \quad (2.2\text{–}10)$$

If no restraint is applied at the pile head (i.e. free-head pile), the general load deflection and rotation relationships can be written as:

$$\delta = \frac{1}{2E_p I_p \beta^3}(T_0 - \beta M_0) \quad (2.2\text{–}11)$$

$$\theta = \frac{-1}{2E_p I_p \beta^2}(T_0 - 2\beta M_0) \quad (2.2\text{–}12)$$

One may also write the pile head bending moment and rotation as a function of lateral displacement and rotation. Such a relationship can be expressed in matrix format.

$$\begin{Bmatrix} T_0 \\ M_0 \end{Bmatrix} = \begin{bmatrix} K_{xx} & K_{x\theta} \\ K_{x\theta} & K_{\theta\theta} \end{bmatrix} \begin{Bmatrix} \delta_0 \\ \theta_0 \end{Bmatrix} \quad (2.2\text{–}13)$$

The matrix ‘K’ is the lateral stiffness matrix whose elements are determined as:

$$K_{xx} = 4E_p I_p \beta^3 = \sqrt[4]{4E_p I_p K_s^3} \tag{2.2–14}$$

$$K_{\theta x} = 2E_p I_p \beta^2 = \sqrt{E_p I_p k_s} \tag{2.2–15}$$

$$K_{\theta\theta} = 2E_p I_p \beta = \sqrt[4]{4(E_p I_p)^3 k_s} \tag{2.2–16}$$

Piles with limited length are of importance to this thesis. The FEA study in chapter 3 implements formulations for limited length pile. A solution to flexure equation (2.2–3) can be provided for a pile with limited length *'L'* as follows:

$$X(z) = A\cos\beta z\cos\beta z + B\cos\beta z\sin\beta z + C\sin\beta z\cos\beta z + D\sin\beta z\sin\beta z \tag{2.2–17}$$

Factors *'A'* to *'D'* are determined based on the fixity of the pile tip. Figure 2-5 aims to compare an infinitely long pile, a pile clamped in a rigid soil layer (bedrock) and a floating pile. Relevant boundary conditions and stiffness components are also shown in this figure.

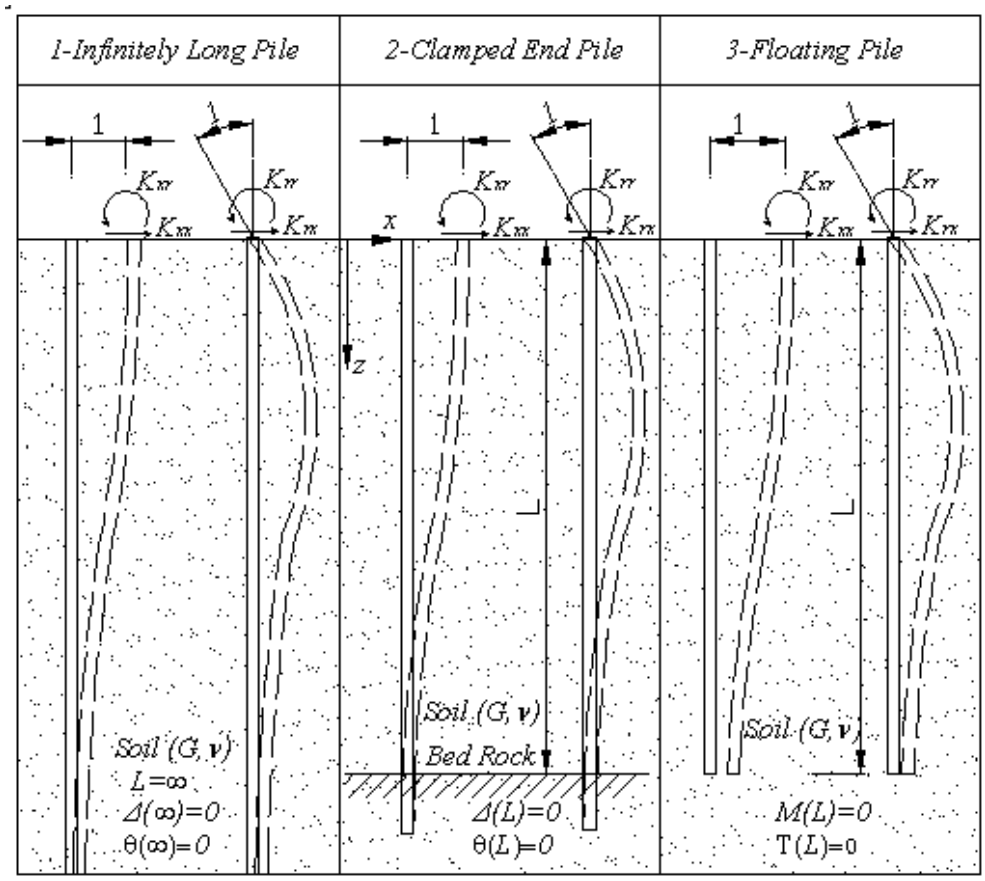

Figure 2-5 Boundary conditions for different pile types

Table 2-1 summarizes the relationships for the stiffness components. It should be noted that the stiffness of a free-head pile can be obtained by setting *'M_0=0'* in the equation (2.2–13) and then eliminating the top rotation between the two equations.

$$\begin{Bmatrix} T_0 \\ 0 \end{Bmatrix} = \begin{bmatrix} K_{xx} & K_{x\theta} \\ K_{x\theta} & K_{\theta\theta} \end{bmatrix} \begin{Bmatrix} \delta_0 \\ \theta_0 \end{Bmatrix} \Rightarrow \theta_0 = -\frac{K_{x\theta}}{K_{\theta\theta}}\delta_0 \Rightarrow T_0 = (K_{xx} - \frac{K_{x\theta}^2}{K_{\theta\theta}})\delta_0 \qquad (2.2\text{–}18)$$

This results in the following expression for the free-head pile stiffness:

$$K_h = K_{xx} - \frac{K_{x\theta}^2}{K_{\theta\theta}} \qquad (2.2\text{–}19)$$

The equation (2.1–19) and its algebraic expression are employed in chapter 3 to correlate the FEA results to Winkler spring stiffness.

Table 2-1 Summary stiffness coefficients for piles with different boundary conditions

Stiffness	**1 - Infinitely long**	**2 - Clamped end**	**2 - Floating**
K_{xx}	$4E_pI_p\beta^3$	$4E_pI_p\beta^3\frac{\sinh(2\beta L)+\sin(2\beta L)}{\cosh(2\beta L)+Cos(2\beta L)-2}$	$4E_pI_p\beta^3\frac{\sinh(2\beta L)+\sin(2\beta L)}{\cosh(2\beta L)+Cos(2\beta L)+2}$
$K_{\theta x}$	$-2E_pI_p\beta^2$	$-2E_pI_p\beta^2\frac{\cosh(2\beta L)-\cos(2\beta L)}{\cosh(2\beta L)+\cos(2\beta L)-2}$	$-2E_pI_p\beta^2\frac{\cosh(2\beta L)-\cos(2\beta L)}{\cosh(2\beta L)+\cos(2\beta L)+2}$
$K_{\theta\theta}$	$2E_pI_p\beta$	$2E_pI_p\beta\frac{\sinh(2\beta L)-\sin(2\beta L)}{\cosh(2\beta L)+\cos(2\beta L)-2}$	$2E_pI_p\beta\frac{\sinh(2\beta L)-\sin(2\beta L)}{\cosh(2\beta L)+\cos(2\beta L)+2}$
K_h	$2E_pI_p\beta^3$	$2E_pI_p\beta^3\frac{\sinh(2\beta L)+\sin(2\beta L)}{\cosh(2\beta L)+Cos(2\beta L)-2}$	$2E_pI_p\beta^3\frac{\sinh(2\beta L)+\sin(2\beta L)}{\cosh(2\beta L)+Cos(2\beta L)+2}$

2.2.2 Two parameter (Vlasov) model for beam on elastic foundation

One of the main criticisms of the Winkler model is that the soil is represented by a single parameter *'k_s'*. In the simplest form when the soil is considered as a perfectly elastic-

homogeneous body, it should at least be represented by two elastic parameters. To correct this shortcoming, Vlasov and Leont'ev (1966) proposed a two-parameter model for a beam on an elastic foundation, as an alternative to Winkler's (1867) single-parameter model. Using the Vlasov and Leont'ev model, Vallabhan and Das (1988; and 1991) proposed the following governing differential equation for the beam on an elastic foundation:

$$\frac{d}{dz^2}[E_p I_p \frac{d}{dz^2} X(z)] - k_1 \frac{d}{dz^2} X(z) + k_s X(z) = p \qquad (2.2\text{–}20)$$

In equation (2.2–20) *'k_s'* is the foundation modulus (Winkler spring stiffness or modulus of subgrade reaction), *'k_1'* is the shear foundation parameter and '*p*' is the externally applied distributed force on the beam. The notations of the above equation are changed to comply with the present thesis. The parameter *'k_1'* can be considered to be rotational stiffness while 'k_s' represents the translational stiffness of the soil. Although soil does not possess bending stiffness, shear stresses on the surface of the pile create a distributed bending moment relative to the pile axis. Figure 2-6 shows a small element of the beam under a general state of actions, i.e. a distributed force in the lateral *'x'* direction and a distributed bending moment in the transverse *'y'* direction. It should be noted that the axial direction is oriented in *'z'* direction. Static equilibrium of the beam element results in:

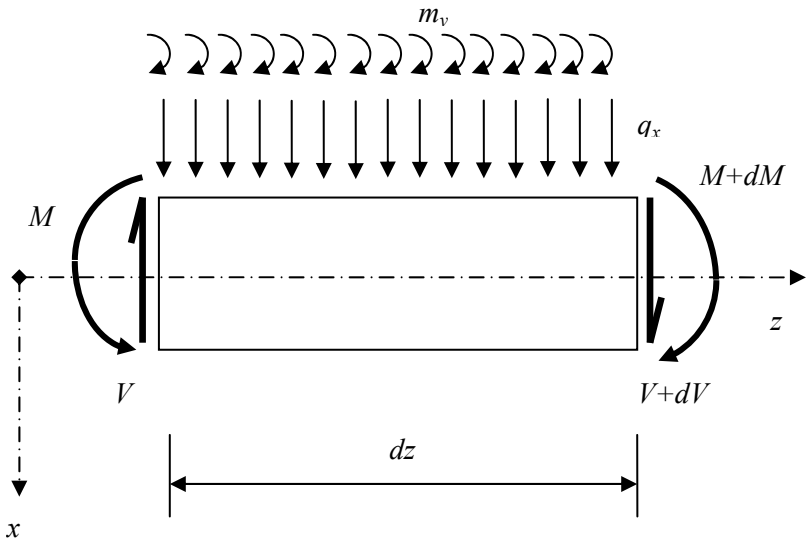

Figure 2-6 A beam element under lateral distributed force and bending moment

$$\frac{dV}{dz} = q_x \tag{2.2–21}$$

$$\frac{dM}{dz} = -m_y - V \tag{2.2–22}$$

If we differentiate the equation (2.2–22) with respect to *'z'* and then substitute for *'dV/dz'* from the equation (2.2–21), we conclude:

$$\frac{d^2M}{dz^2} = -\frac{d}{dz}m_y + q_x \tag{2.2–23}$$

Here we accept the assumption that the distributed bending moment is proportional to the rotation. The distributed bending moment is written as:

$$m_y = k_\theta \frac{d}{dz}X(z) \tag{2.2–24}$$

In the above equation, *'X(z)'* is the lateral deflection and k_θ is the proportionality factor which can be interpreted as the rotational spring constant. Combining equations (2.2–23) and (2.2–24) and substituting into the flexure equation leads to:

$$E_p I_p \frac{d^4}{dz^4}X(z) - k_\theta \frac{d^2}{dz^2}X(z) + k_s X(z) = 0 \tag{2.2–25}$$

It can be seen that the equation (2.2–25) is analogous to the equation (2.2–17). Solution of the differential equation (2.2–25) can be considered as exponential function:

$$X(z) = e^{Dz} \tag{2.2–26}$$

In the above equation '*D*' is a complex number. Substituting the equation (2.2–26) in the equation (2.2–25) results in:

$$E_p I_p D^4 - k_\theta D^2 + k_s = 0 \tag{2.2–27}$$

Rather than solving the above fourth order equation, it is convenient to introduce an equivalent beam on a Winkler support with an equivalent Winkler spring stiffness *'k_{se}'*, such that the Winkler beam has the same deflection as the Vlasov beam. The flexure equation for the equivalent beam reads:

$$E_p I_p \frac{d^4}{dz^4} X(z) + k_{se} X(z) = 0 \tag{2.2–28}$$

Substituting equation (2.2–26) into equation (2.2–28) yields:

$$E_p I_p D^4 + k_{se} = 0 \tag{2.2–29}$$

Solving for *'D^2'* reads:

$$\begin{cases} E_p I_p D^4 = -k_{se} \\ D^2 = \pm i \sqrt{\dfrac{k_{se}}{E_p I_p}} \end{cases} \tag{2.2–30}$$

Substituting this into equation (2.2–27) gives:

$$\mp i k_\theta \sqrt{\frac{k_{se}}{E_p I_p}} = k_{se} - k_s \tag{2.2–31}$$

Squaring both sides of the above equation leads to the following second order algebraic equation for *'k_{se}'*:

$$k_{se}^2 - (2k_s - \frac{k_\theta^2}{E_p I_p}) k_{se} + k_s^2 = 0 \tag{2.2–32}$$

Equation (2.2–32) is a second order algebraic equation from which the equivalent Winkler spring stiffness is derived as:

$$k_{se} = k_s - \frac{k_\theta^2}{2E_p I_p}[1 + \sqrt{1 - \frac{4E_p I_p k_s}{k_\theta^2}}] \cong k_s - i k_\theta \sqrt{\frac{k_s}{E_p I_p}} \tag{2.2–33}$$

An approximation is made in evaluation of the term in brackets by ignoring 1 against the term $4E_p I_p k_s / k_\theta^2$ whose value is much greater than the unity. The presence of the imaginary number '$i = \sqrt{-1}$' in the equation is not justifiable for a static model. In a dynamic analysis, however, the imaginary part plays an important role. In a dynamic analysis, as will be shown in chapter 4, k_s and k_θ are both complex-valued.

2.2.3 Variable soil modulus

So far, we have formulated the beam on elastic foundation for a laterally loaded infinitely long pile with constant soil modulus. Soil modulus, however, is unlikely to remain constant even in uniform soil layers. A solution involving constant soil modulus may be applicable only for piles in heavily overconsolidated soils. Normally consolidated clays and sands show zero stiffness at the ground line and vary rather linearly with depth (Reese and Van Impe 2001). Parabolic variations of modulus with depth are often considered for layered soils (Novak and El Sharnouby 1983).

In this section, we will establish an approximate solution to a beam on Winkler springs with variable spring stiffness. The following general relationship for lateral spring stiffness is considered:

$$k_s = k_p z^n \tag{2.2–34}$$

'k_p' and 'n' are site-specific constants. 'n' can vary from zero for constant spring stiffness, ½ for parabolic to 1 for linearly varying spring stiffness. Figure 2-7 shows spring stiffness vs. depth. It should be noted that the factor 'k_p' has dimensions of force divided by length to the power of '$(n+2)$'. In the SI system, its dimensions may be written as N/m^{n+2}.

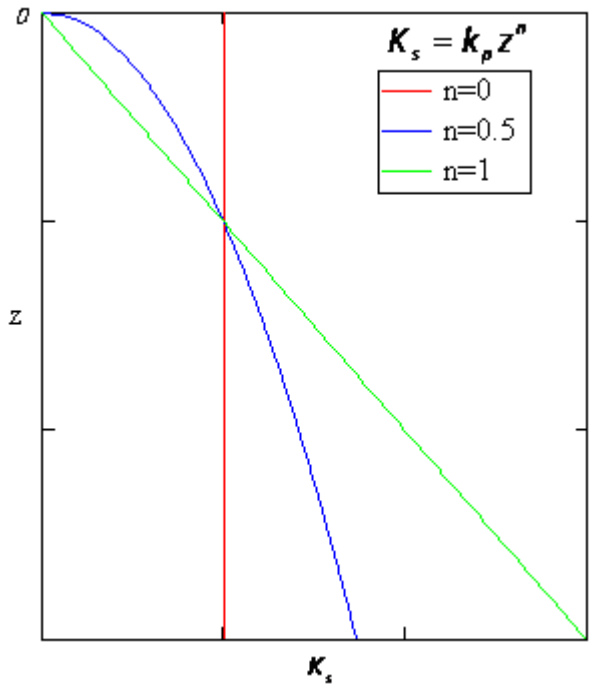

Figure 2-7 Constant, parabolic and linear spring stiffness with depth

The governing differential equation for the beam on elastic foundation with variable spring stiffness becomes:

$$E_p I_p \frac{d^4 X(z)}{dz^4} + k_p z^n X(z) = 0 \qquad (2.2\text{–}35)$$

To solve the above differential equation for '*n>0*' we define the following variables:

$$\alpha^{4+n} = \frac{k_p}{4E_p I_p}, \qquad \alpha z = s \qquad (2.2\text{–}36)$$

Substituting (2.2–36) into (2.2–35) results in a dimensionless differential equation:

$$\frac{d^4 X(s)}{ds^4} + 4s^n X(s) = 0 \qquad (2.2\text{–}37)$$

The end conditions of the problem, i.e. lateral load and bending moment on pile head, are also written in non-dimensional form as:

$$T_0 = E_p I_p \frac{d^3 X(0)}{dz^3} = \alpha^3 E_p I_p \frac{d^3 X(0)}{ds^3} \Rightarrow \frac{d^3 X(0)}{ds^3} = \frac{T_0}{\alpha^3 E_p I_p} = t_0 \qquad (2.2\text{–}38)$$

$$M_0 = E_p I_p \frac{d^2 X(0)}{dz^2} = \alpha^2 E_p I_p \frac{d^2 X(0)}{ds^2} \Rightarrow \frac{d^2 X(0)}{ds^2} = \frac{M_0}{\alpha^2 E_p I_p} = m_0 \qquad (2.2\text{–}39)$$

The equation (2.2–37) is a nonlinear fourth order differential equation for which an exact solution cannot be readily found. The author could not find a closed-form solution either in terms of transcendental functions or in the form of infinite series that can satisfy the above equation. It is customary to solve these types of equations with numerical methods. Rees and Van Impe (2001, Sec.2.2.2) thoroughly discuss the application of the finite difference method in solution of the pile equation. Presently, many commercial spreadsheets exist that implement numerical methods to solve differential equations of this kind, with very good accuracy. One of these spreadsheets is MathCAD (Maxfield 2009), which offers a number of different numerical algorithms in its built-in solvers for general ordinary differential equations.

To solve equation (2.2–37), we first consider the following linear differential equation:

$$\frac{d^4Y(s)}{ds^4} + 4Y(s) = 0 \qquad (2.2\text{–}40)$$

The above equation and its main function *Y(s)* have no physical meaning; just for reference we will call it the conjugate pile, as it represents an imaginary pile with depth variables 's' and '$\beta = 1$'. The solution of the equation (2.2–40) can be established for an infinitely long pile as:

$$Y(s) = \frac{1}{2}e^{-s}[(t_0 - m_0)\cos(s) + m_0 \sin(s)] \qquad (2.2\text{–}41)$$

The numerical solution for the differential equation (2.2–37) for the case of *n=1* and for two end conditions of (t_0*=1,* m_0*=0)* and (t_0*=0,* m_0*=1)* are represented graphically in Figure 2-8.

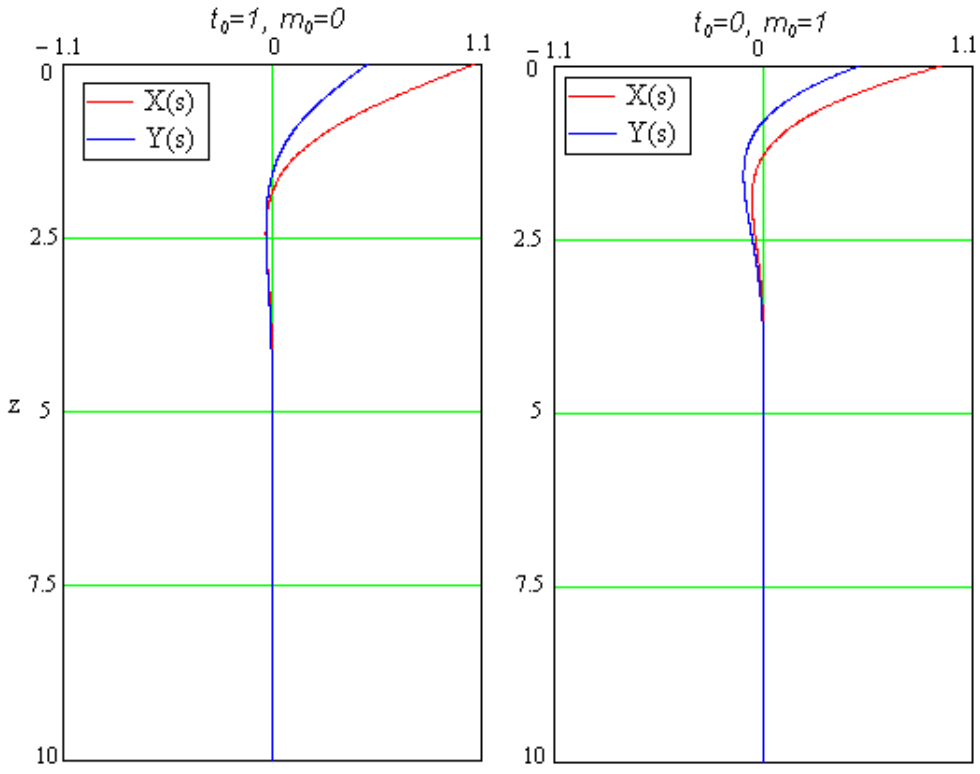

Figure 2-8 Graphical representation of numerical solution to (2.2-42)

Noting that *d/ds=(1/*α*)d/dz* and using curve fitting techniques, the non-dimensional load-deflection relationship for the pile (*n=1*) can be approximately written as:

$$\begin{cases} \delta = \dfrac{2.115}{2} t_0 + \dfrac{1.86}{2} m_0 = 1.0575 t_0 + 0.93 m_0 \\ \dfrac{\theta}{\alpha} = -\dfrac{1.86}{2} t_0 - 1.321 m_0 = -0.93 t_0 - 1.321 m_0 \end{cases} \tag{2.2–42}$$

Inverting the equation (2.2–42), one may write:

$$\begin{cases} t_0 = 2.48\delta + 1.75\theta/\alpha \\ m_0 = -1.75\delta - 1.99\theta/\alpha \end{cases} \tag{2.2–43}$$

By substituting for α, t_0 and m_0 from the equations (2.2–36), (2.2–38) and (2.2–39) and after some algebra, the stiffness components can be found (for *n=1*) as:

$$K_{xx}^{(1)} = 2.48\alpha^3 E_p I_p = 1.08\sqrt[5]{(E_p I_p)^2 k_p^3} \tag{2.2–44}$$

Note that a superscript is used for the stiffness coefficient to indicate that the equation (2.2–44) corresponds to *n=1*. The rotational stiffness is derived in a similar manner:

$$K_{\theta\theta}^{(1)} = -1.99\alpha E_p I_p = 1.51\sqrt[5]{(E_p I_p)^4 k_p} \tag{2.2–45}$$

And finally the coupled translational-rotational stiffness:

$$K_{\theta x}^{(1)} = 1.75\alpha^2 E_p I_p = -\sqrt[5]{(E_p I_p)^3 k_p^2} \tag{2.2–46}$$

The corresponding matrix equation can be written as:

$$\begin{Bmatrix} T_0 \\ M_0 \end{Bmatrix} = \begin{bmatrix} K_{xx}^{(1)} & K_{xr}^{(1)} \\ K_{xr}^{(1)} & K_{rr}^{(1)} \end{bmatrix} \begin{Bmatrix} \delta \\ \theta \end{Bmatrix} \tag{2.2–47}$$

For parabolic soil stiffness (i.e. for *n=0.5*), the parameter 'k_p' has units of $N/mm^{2.5}$ and we will have:

$$\begin{cases} \delta = \dfrac{1.599}{2} t_0 + \dfrac{1.476}{2} m_0 = 0.8 t_0 + 0.74 m_0 \\ \dfrac{\theta}{\alpha} = -\dfrac{1.476}{2} t_0 - 1.173 m_0 = -0.74 t_0 - 1.17 m_0 \end{cases} \tag{2.2–48}$$

$$\begin{cases} t_0 = 3.00\delta + 1.89\theta/\alpha \\ m_0 = -1.89\delta - 2.05\theta/\alpha \end{cases} \quad (2.2\text{–}49)$$

$$K_{xx}^{(0.5)} = 3.00\alpha^3 E_p I_p = 1.19\sqrt[3]{(E_p I_p) k_p^2} \quad (2.2\text{–}50)$$

$$K_{\theta\theta}^{(05)} = -2.05\alpha E_p I_p = 1.51\sqrt[9]{(E_p I_p)^7 k_p^2} \quad (2.2\text{–}51)$$

$$K_{\theta x}^{(0.5)} = 1.89\alpha^2 E_p I_p = -1.02\sqrt[9]{(E_p I_p)^5 k_p^4} \quad (2.2\text{–}52)$$

The stiffness of free-head pile (i.e. *M=0*) can be derived using the equation (2.2–19).

2.2.4 Biot's continuum solution for a beam on elastic foundation

Biot (1922) approached the beam on elastic foundation problem by solving elastostatic equations for a beam on the surface of 2D half-plane and 3D half-space. After deriving the maximum bending moment in the beam from the exact elastic theory, Biot equated it to the maximum bending moment from the beam on a Winkler spring and calculated the relationships for the foundation modulus *'k_s'*. Biot argued that although the exact elastic model and the beam on the Winkler support model both give an accurate bending moment, the deflection of the beam on the Winkler support is not exactly the same as that of the accurate elastic theory. This is a clear example of the shortcomings of a single parameter beam on elastic foundation model in predicting the exact behavior. Table 2-2 summarizes the results of Biot's paper in terms of maximum bending moment, maximum beam deflection and the foundation modulus. It should be noted that the original paper did not include maximum beam deflections and the formulas given in the table are derived by the author of this thesis using the original solution.

Table 2-2 Summary of Biot's solution for beam on soil surface

Theory	Maximum bending moment	Maximum beam deflection	Foundation modulus
Winkler	$M_{\max} = 0.353P(\frac{E_p I_p}{k})^{1/4}$	$\delta_{\max} = 0.645\frac{P}{E_p I_p}(\frac{E_p I_p}{k})^{0.25}$	N/A
2D continuum solution	$M_{\max} = 0.243PD(\frac{E_p I_p}{E_s D})^{1/}$	$\delta_{\max} = 1.596\frac{P}{E_s D}$	$0.71E_s[\frac{E_s(D/2)^4}{E_p I_p}]^{\frac{1}{3}}$ $= 0.71(1+\nu)\mu[\frac{(1+\nu)\mu D^4}{E_p I_p}$
3D continuum solution	$M_{\max} = 0.347PD(\frac{E_p I_p}{E_s D})^{1/}$	$\delta_{\max} = 0.796\frac{PD^3}{E_p I_p}(\frac{E_p I_p}{E_s D^4})^{0.817}$	$\frac{1.23E_s}{1-\nu^2}[\frac{E_s(D/2)^4}{(1-\nu^2)E_p I_p}]^{\frac{1}{9}}$ $=\frac{1.95\mu}{(1-\nu)^{10/9}}(\frac{\mu D^4}{E_p I_p})^{\frac{1}{9}}$

In the above table *'P'* is the concentrated load, *'D'* holds for beam width and '$E_p I_p$' holds for its flexibility factor.

2.2.5 Vesic's formulation of subgrade modulus

Vesic (1961) extended Biot's (1922) solution by deriving expressions for bending moment, deflection, rotation, shear force and contact pressure at any point of the beam under a concentrated load as well as a concentrated moment. The expressions are derived in terms of five different integrals with infinite limits. The integrals are then approximated using damped wave-type curves which are also similar to deflected curves obtained from the Winkler's beam model. The approximations are made with the aid of a factor $\lambda' = \pi/4x_0$, where *'x_0'* is the abscissa of the first zero of the integral. Vesic then equated this factor with the well-known beam on elastic foundation factor of '$\beta = \sqrt{k/4E_p I_p}$' which lead to the following expression for the subgrade modulus:

$$K = 0.65\frac{E_s}{1-\nu^2}\left(\frac{E_s D^4}{E_p I_p}\right)^{\frac{1}{12}} \qquad (2.2\text{–}53)$$

Vesic supported his expression by full size test results. His results shows that the calculated deflections of the beam underestimate the true deflections, while the calculated bending moment overestimates the maximum measured bending moment.

The main weakness of Vesic's solution is that the factor λ' does not have any physical meaning and is a pure mathematical value used for the approximation of integrals. Equating it to a factor which has a clear physical meaning without any physical justification is not reasonable. It is also not clear how good his proposed value estimates the test results. Although the calculated bending moments and deflections are close to the measured values, it is not clear where the calculations overestimate and where they underestimate the test results. From this point of view, Biot's (1922) proposed values are preferred by the author for having a clear theoretical meaning.

2.3 Laterally loaded piles – static

In this section, piles under the static lateral load are reviewed. There are many aspects which are not referenced here. The review in this subsection is limited to the early elastic methods and a brief reference to more recent methods, including some nonlinear effects of the soil on the analysis. Topics like the load bearing capacity of piles are not discussed in this chapter as they are considered to be a digression from the topic.

2.3.1 Critical length of the pile

The first aspect of a pile that should be referenced is its critical length. The critical length of a pile is defined as the depth beyond which the pile behaves as if it is infinitely long. In other words, any increase in the length of the pile beyond the critical length will not affect the deflection at the pile head (for a constant load). In order to determine the critical length, it is necessary to equate the stiffness values of a pile with infinite length to those of a similar pile with limited length and solve the equation for the length of the pile. The values of stiffness are given in Table 2-1. It is seen that stiffness values for a pile with limited length can be expressed as the stiffness of an infinitely long pile multiplied by a factor which is a function of pile length. We call this factor the influence factor. Table 2-3 summarizes the influence factors for different pile tip conditions.

Table 2-3 Summary of influence factors for limited length pile

Influence factor	**1 - Clamped tip**	**2 - Floating**
$F_{xx} = \frac{K_{xx}}{K_{xx}^{\infty}}$	$\frac{\sinh(2\beta L) + \sin(2\beta L)}{\cosh(2\beta L) + Cos(2\beta L) - 2}$	$\frac{\sinh(2\beta L) + \sin(2\beta L)}{\cosh(2\beta L) + Cos(2\beta L) + 2}$
$F_{\theta x} = \frac{K_{\theta x}}{K_{\theta x}^{\infty}}$	$\frac{\cosh(2\beta L) - \cos(2\beta L)}{\cosh(2\beta L) + \cos(2\beta L) - 2}$	$\frac{\cosh(2\beta L) - \cos(2\beta L)}{\cosh(2\beta L) + \cos(2\beta L) + 2}$
$F_{\theta\theta} = \frac{K_{\theta\theta}}{K_{\theta\theta}^{\infty}}$	$\frac{\sinh(2\beta L) - \sin(2\beta L)}{\cosh(2\beta L) + \cos(2\beta L) - 2}$	$\frac{\sinh(2\beta L) - \sin(2\beta L)}{\cosh(2\beta L) + \cos(2\beta L) + 2}$
$F_h = \frac{K_h}{K_h^{\infty}}$	$\frac{\sinh(2\beta L) + \sin(2\beta L)}{\cosh(2\beta L) + Cos(2\beta L) - 2}$	$\frac{\sinh(2\beta L) + \sin(2\beta L)}{\cosh(2\beta L) + Cos(2\beta L) + 2}$

The influence factors are displayed in Figure 2-9. It can be seen that influence factors for clamped end piles are greater than 1.0, while those for floating piles are less than 1.0. It is also seen that both sets of influence factors rapidly converge to the 1.0 for βL values greater than 3.0. From these findings, the critical length can be expressed as:

$$L_c = \frac{3}{\beta} \cong 4\sqrt[4]{\frac{E_p I_p}{k_s}} \qquad (2.3\text{–}1)$$

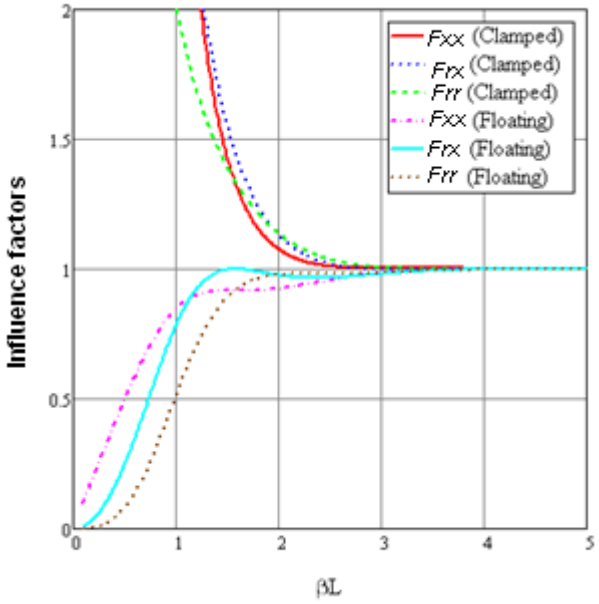

Figure 2-9 Influence factor for piles with limited length

The value of critical depth depends on the value of stiffness of Winkler springs. Some existing relationships for Winkler spring stiffness are discussed in section 2.2. Table 2-4 includes some formulas for Winkler spring stiffness and the resulting critical length. It also includes the results of an FEA study conducted by Randolph (1981), for comparison. The critical length given by Randolph (1981) agrees well with the critical length derived based on Biot's (1922) expression for Winkler spring stiffness.

Table 2-4 Winkler spring stiffness and critical length of pile (constant soil modulus)

Originator [1]	**Spring stiffness 'k_s'**	**Critical length ratio 'L_c/D'**
Biot (1922) [2][3]	$\mu \frac{6.458}{1-\nu} \sqrt[9]{\frac{1}{1-\nu}\frac{\mu I_s}{E_p I_p}}$	$\frac{L_c}{D} = 1.181[(1-\nu)\frac{E_p I_p}{\mu I_s}]^{0.28}$
Glick (1948)[4]	$\mu \frac{44.8(1-\nu)}{(3-4\nu)[2\ln(2L/D)-0.433]}$	$\frac{(L_c/D)^4}{2\ln(2L_c/D)-0.453} = 0.281(\frac{3-4\nu}{1-\nu}\frac{E_p I_p}{\mu I_s})$
Vesic (1961) [2]	$\mu \frac{3.54}{1-\nu} \sqrt[12]{(1+\nu)\frac{\mu I_s}{E_p I_p}}$	$\frac{L_c}{D} = 1.373\frac{(1-\nu)^{0.25}}{(1+\nu)^{0.02}}[\frac{E_p I_p}{\mu I_s}]^{0.27}$
Randolph (1981)[5]	(---)	$\frac{L_c}{D} = [\frac{1}{1+3/4\nu}\frac{E_p I_p}{\mu I_s}]^{0.29}$

Notes:

(1) Original formulas are modified to match the notations used in this thesis.

(2) Twice the original value is used for piles based on recommendations by Bowles (1997).

(3) The original formula includes a factor 'C'. For the purpose of this text the value of *'C=1.13'* is adapted. The original paper used the exponent 0.11 which is changed to its equivalent 1/9 in this paper.

(4) The critical length should be calculated from the given equation in the last column by trial and error.

(5) The Randolph (1981) formula is derived from a parametric finite element study.

The above relationships hold for homogeneous, linearly elastic soils. These types of soils are very rare. Most soils show some increase in their modulus with depth. Some relationships are given for a soil modulus that increases linearly with depth. Randolph (1981) proposed the following relationship for the critical length of the piles in linearly varying soils (notations are modified):

$$(l/D)_c^{Randolph} = 1.16(\frac{E_p I_p}{\kappa(1+3\nu/4)DI_s})^{0.22} \qquad (2.3\text{–}2)$$

Velez et al. (1982) provided a similar formula for the active length of the pile in linearly varying soils:

$$(l/D)_c^{Veles\&Gazetas} = 1.75\left(\frac{E_p I_p}{\kappa(1+3\nu/4)DI_s}\right)^{0.21} \quad (2.3\text{–}3)$$

In the equation (2.3–3) 'κ' is the rate of change of the soil modulus with depth.

2.3.2 Piles in variable soils

Randolph (1981) proposed load-deflection relationships for a laterally loaded pile in linearly varying soil. Velez et al. (1982) provided similar formulas. If the soil shear modulus is negligible at ground surface, a simple linear relationship can be considered for soil shear modulus ($\mu = mz$). The factor 'm' in this relationship holds for the rate of gain of shear modulus with depth 'z'. To include the effect of Poisson's ratio, an effective rate of gain and an effective shear modulus are introduced (Randolph 1981):

$$m^* = m(1+0.75\nu) \quad (2.3\text{–}4)$$

$$G^* = \mu(1+0.75\nu) \quad (2.3\text{–}5)$$

Stiffness factors for a laterally loaded pile were extracted from the work of these authors and are summarized in Table 2-5.

Table 2-5 Stiffness factors for a pile in linearly varying soil

Stiffness	**Randolph (1981)**	**Velez et al. (1982)**
K_{xx}	$1.13m^*D^2\left(\frac{2E_pI_p}{m^*DI_s}\right)^{\frac{1}{3}}$	$0.6m^*D^2\left(\frac{2E_pI_p}{m^*DI_s}\right)^{0.35}$
K_{rx}	$-0.3m^*D^3\left(\frac{2E_pI_p}{m^*DI_s}\right)^{\frac{5}{9}}$	$-0.17m^*D^3\left(\frac{2E_pI_p}{m^*DI_s}\right)^{0.6}$
K_{rr}	$0.135m^*D^4\left(\frac{2E_pI_p}{m^*DI_s}\right)^{\frac{7}{9}}$	$0.14m^*D^4\left(\frac{2E_pI_p}{m^*DI_s}\right)^{0.8}$

If the soil shear modulus at the ground surface is not negligible, a more general relationship is required to describe it:

$$G^* = G_0^* + mz \quad (2.3\text{–}6)$$

In the equation (2.3–6) the factor G_0^* is the soil effective shear modulus at the ground surface. Randolph (1981) defined a characteristic shear modulus (G_c) which is as the value of the shear modulus over the critical length of the pile. He also defined relative homogeneity factor (ρ_c) as the ratio of the value of shear modulus at ¼ of critical length to that at depth of ½ of critical length. Figure **2-10** shows the definitions of these two parameters.

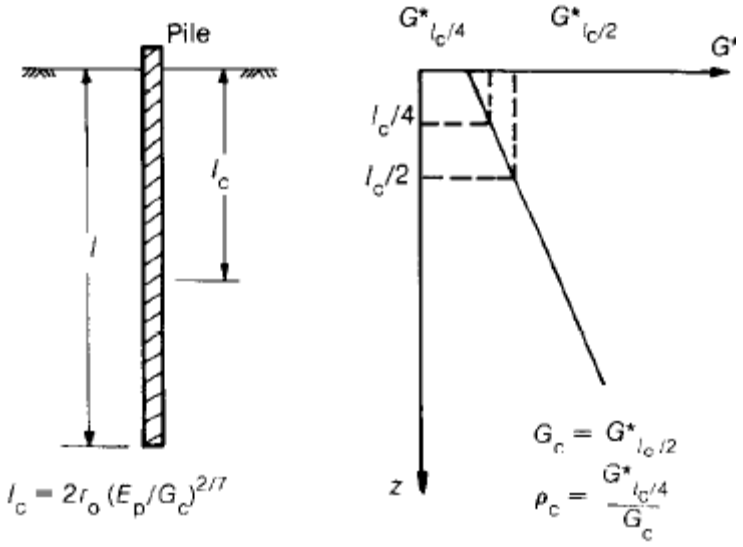

Figure 2-10- Definition of Gc and ρ_c (Randolph 1981)

With this definition, Randolph (1981) proposed the following relationship for critical length:

$$L_c = D(\frac{E_p}{G_c})^{2/7} \tag{2.3–7}$$

The following relationships for pile stiffness factors are concluded from Randolph's (1981) original paper after some algebraic manipulation:

$$K_{xx} = \sqrt{\rho_c^3} G_c (\frac{G_c}{E_p})^{1/7} \frac{200}{108\sqrt{\rho_c} - 45} L_c \tag{2.3–8}$$

$$K_{rx} = -\rho_c G_c (\frac{G_c}{E_p})^{1/7} \frac{25}{75\sqrt{\rho_c} - 30} L_c^2 \tag{2.3–9}$$

$$K_{rr} = \rho_c G_c (\frac{G_c}{E_p})^{1/7} \frac{15}{96\sqrt{\rho_c} - 40} L_c^3 \tag{2.3–10}$$

Free head pile stiffness can be determined using equation (2.2–19):

$$K_h = \rho_c G_c \left(\frac{G_c}{E_p}\right)^{1/7} \frac{6.4\sqrt{\rho_c} - 2.67}{3.46\sqrt{\rho_c} - 1.44} L_c \qquad (2.3\text{–}11)$$

It should be noted that in Randolph's (1981) method, the characteristic shear modulus (G_c) depends on the critical length of the pile and the critical length is defined in terms of the characteristic shear modulus. Randolph's (1981) proposed an iterative procedure to determine the critical length and the characteristic shear modulus in practical problems. In the present thesis, we combine the equations (2.3–16) and (2.3–17) to reach a characteristic equation from which the critical length can be found numerically:

$$G_c = G_0^* + m^* \frac{L_c}{2} \qquad (2.3\text{–}12)$$

$$0.5 m^* D (L_c / D)^{4.5} + G_0^* (L_c / D)^{3.5} - E_p = 0 \qquad (2.3\text{–}13)$$

2.3.3 Methods involving Mindlin's solution

Major improvements to the soil-pile interaction analysis are made by implementing Mindlin's (1936) solution. Douglas and Davis (1964) integrated Mindlin's solution to calculate deformations for a buried stiff plate. Butterfield and Banerjee (1971a) solved the problem of an axially loaded pile and group of piles by using numerical integration on boundary integral equations. They presented their results as graphs that showed the load displacement curve for single piles as well as the load distribution on piles in a group. Butterfield and Banerjee (1971b) also studied the interaction of piles with the pile cap in a group.

Poulos (1971a) developed a method to solve the problem of a laterally loaded pile. He integrated Mindlin's (1936) solution for deformations in soil over a small pile element. He then wrote the flexure equation for the pile in finite difference format and equated soil displacement with pile deflection. Having solved the finite difference equations, Poulos proposed general load-deformation formulas for single piles. His solution included non-dimensional parameters which were presented graphically. In his analysis, the pile was modeled as a thin, rectangular strip, such that the effect of the third dimension was ignored and the integration was made in a vertical plane. He also ignored the effect of shear stresses on the pile surface. Poulos (1971b) expanded this method to a group of piles. The results were presented graphically, showing the distribution of horizontal load along piles at different locations in the group. It was also possible to make a load-deflection prediction for the pile group using tabulated factors.

Banerjee and Davies (1978) described the solution for a laterally loaded pile in soil with a modulus that increased linearly with depth. Poulos and Davis (1980) have collected these solutions and their applications in their brilliant book, and have presented a consistent theoretical approach to the prediction of pile deformation and load capacity, provided a parametric presentation applicable to a wide range of cases, demonstrated methods for implementing theoretical solutions for design purposes, and reviewed their applicability to practical problems.

2.3.4 A reference to the p-y method

Due to its adoption by number of important codes of practice (e.g. API-RP-2A 2007), the p-y method is widely used for analysing laterally loaded piles. This chapter reviews the historical origins of this method.

Howe (1955) described the use of the finite difference method (FDM) in the analysis of laterally loaded piles. Reese and Matlock (1956) used FDM to create non-dimensional curves in order to estimate the ground line deflection and maximum pile bending moment for a given lateral load. Later Matlock and Reese (1960) expanded their original curves to include variable soils with a modulus that varied with depth. Since their original approach was based on elastic soil properties, they considered a modulus of elasticity that varied with depth:

$$E_s = n_h z^n \tag{2.3–14}$$

They also defined a relative stiffness factor as per the equation (2.3–15):

$$T = \left(\frac{E_p I_p}{n_h}\right)^{\frac{1}{n+4}} \tag{2.3–15}$$

Using the above definition, the Pile deflection, slope, bending moment, shear force and soil reaction are written as per the equations (2.3–16) to (2.3–20), respectively:

$$y = \left(\frac{V_0 T^3}{E_p I_p}\right) A_y + \left(\frac{M_0 T^2}{E_p I_p}\right) B_y \tag{2.3–16}$$

$$S = \left(\frac{V_0 T^2}{E_p I_p}\right) A_s + \left(\frac{M_0 T}{E_p I_p}\right) B_s \tag{2.3–17}$$

$$M = (V_0 T) A_m + (M_0) B_m \tag{2.3–18}$$

$$V = (V_0) A_v + (\frac{M_0}{T}) B_v \tag{2.3–19}$$

$$p = (\frac{V_0}{T}) A_p + (\frac{M_0}{T^2}) B_p \tag{2.3–20}$$

In the above set of equations *'y'* and *'S'*, are deflection and slope of the pile and *'M'*, *'V'* and *'p'* are the bending moment, shear force and soil resistance per unit length of the pile, respectively. The factors '*A'* and '*B'* are tabulated values which are given for non-dimensional depth parameter *'Z=z/T'*. For deflection and slope at the ground line one may write:

$$y_g = 2.43 \frac{V_0 T^3}{E_p I_p} + 1.62 \frac{M_0 T^2}{E_p I_p} \tag{2.3–21}$$

$$S_g = 1.62 \frac{V_0 T^2}{E_p I_p} + 1.75 \frac{M_0 T}{E_p I_p} \tag{2.3–22}$$

The initial use of FDM on laterally loaded piles (McClelland and Focht 1958) involved the use of springs *'p'* and lateral displacement *'y'*. It became common for practitioners to call this method *'p-y'* as a reference to its main aspects.

The current elaboration of *p-y* curves is different from the early approaches. The effect of the ultimate lateral resistance of the soil plays an important role in the current formulations. The American Petroleum Institute (2007) adapted a method based on the research of Matlock (1970) on p-y curves for soft clay, Reese and Cox (1975) for stiff clay, O'Neill and Murchison (1983) for sand and Georgiadis (1983) for layered soils. The relationship for the ultimate lateral resistance of soft clay is given as:

$$\begin{cases} p_u = 3c + \gamma X + J \dfrac{cX}{D}, & X < X_R \\ p_u = 9c, & X \geq X_R \end{cases} \tag{2.3–23}$$

Where

c = undrained shear strength for undisturbed clay soil samples

D = pile diameter

γ = effective unit weight of soil

J = dimensionless empirical constant with values ranging from 0.25 to 0.5, having been determined by field testing

X = depth below soil surface

X_R = depth below soil surface to bottom of reduced resistance zone.

For constant soil strength with depth, the two equations of (2.3–23) are solved simultaneously to give:

$$X_R = \frac{6D}{\frac{\gamma D}{c} + J} \tag{2.3–24}$$

API-RP-2A (2007) recommends a nonlinear p-y curve for soft clays as given in Table 2-6:

Table 2-6 Static p-y curve for soft clays (API-RP-2A 2007)

p/p_u	y/y_c
0.00	0.0
0.23	0.1
0.33	0.3
0.50	1.0
0.72	3.0
1.00	8.0
1.00	∞

In the above table, $y_c = 2.5\varepsilon_c D$ where ε_c is the strain which occurs at one-half the maximum stress on laboratory unconsolidated undrained compression tests of undisturbed soil samples. The p-y curve for cyclic loading is given in Table 2-7. The p-y curve for cyclic loading is similar to that of static loading up to the relative deflection of $y/y_c = 3.0$. After this limit, the static curve continues to show some strength up to $y/y_c = 8.0$ before failure, while the cyclic curve fails at the relative stiffness of $y/y_c = 3.0$.

Table 2-7 Cyclic p-y curve for soft clays (API-RP-2A 2007)

$X>X_R$		$X<X_R$	
p/p_u	y/y_c	p/p_u	y/y_c
0.00	0.0	0.00	0.0
0.23	0.1	0.23	0.1
0.33	0.3	0.33	0.3
0.50	1.0	0.50	1.0
0.72	3.0	0.72	3.0
0.72	∞	0.72 *X/XR*	*15.0*
		0.72 *X/XR*	∞

The ultimate lateral resistance of sand is given in (API-RP-2A 2007) as:

$$\begin{cases} p_{us} = (C_1 H + C_2 D)\gamma H \\ p_{ud} = C_3 D\gamma H \end{cases} \quad (2.3–25)$$

Where

p_u = ultimate resistance (force per unit length) of soil on foundation (*s*= shallow, *d*=deep)

γ = effective unit weight of soil

H = depth

ϕ' = angle of internal friction of sand

C1, C2, C3 = coefficients determined from Figure 2-11

D = average pile diameter from the surface to the depth under consideration.

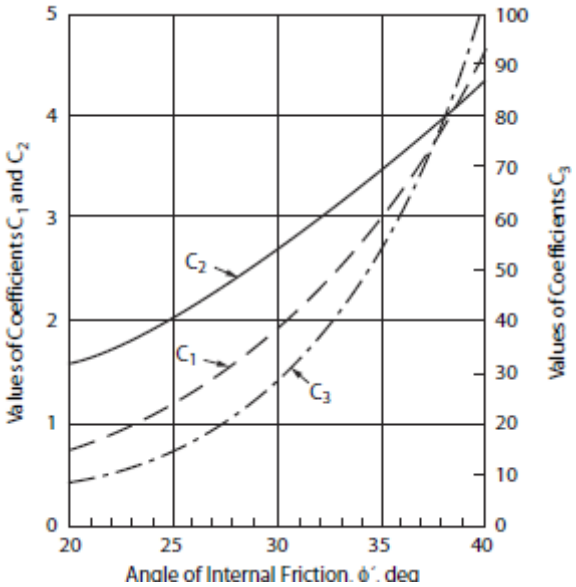

Figure 2-11 Coefficients C_1,C_2 and C_3 as a function of the angle of internal friction of sand (API-RP-2A 2007)

The load deformation relationship for sand is also nonlinear and related to its ultimate lateral resistance. API-RP-2A (2007) recommends the following relationship in the absence of more definitive information:

$$p = A \times p_u \times \tanh(\frac{\kappa \times z}{A \times p_u} y) \tag{2.3–26}$$

Here *'A'* is a factor to account for cyclic or static loading and is given as:

$$A = \begin{cases} 0.9, & for \quad cyclic \quad loading \\ (3.0 - 0.8\frac{z}{D}) \geq 0.9, & for \quad static \quad loading \end{cases} \tag{2.3–27}$$

The factor 'κ' is the initial modulus of the subgrade reaction determined as a function of the internal angle of friction 'ϕ' ' and is given in Figure 2-12.

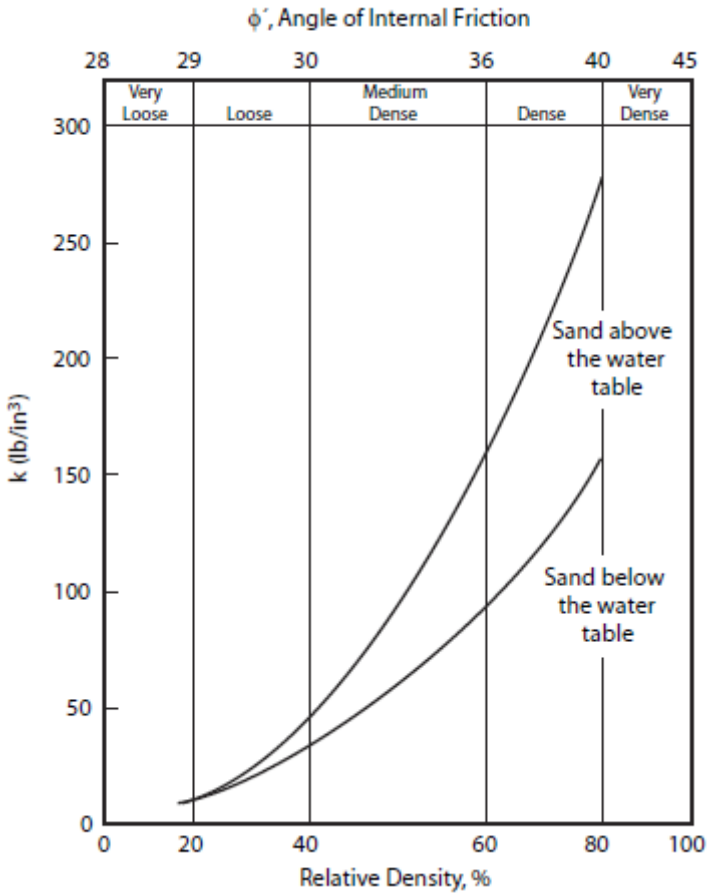

Figure 2-12 Initial modulus of the subgrade reaction for sands as a function of the angle of internal friction of sand (API-RP-2A 2007).

2.4 Laterally loaded piles – dynamic

In this section we review the dynamics of a laterally loaded pile, focusing on the solutions involving continuum mechanics. The number of such solutions is very limited; therefore it is convenient to conduct the review by the name of the researchers. It should be noted that numerical methods are only briefly touched upon, while empirical methods are not referred to, as these are considered as digressions from the topic.

2.4.1 Baranov's solution

Baranov (1967) provided an elastic solution for a cylindrical rigid embedded foundation, assuming that the soil is composed of infinite number of independent infinitesimally thin horizontal layers that extend to infinity (as described by Novak 1974). Since the foundation is assumed to be rigid, it undergoes a rigid body movement and a rigid body rotation which are independent from each other. A great deal of simplification is achieved by making the

assumption that lateral movement of the foundation imposes only horizontal deformations while its rotation imposes vertical deformations in the soil. Here we briefly discuss Baranov's approach. It is assumed that full connectivity is maintained between the soil and the foundation. This assumption establishes the boundary conditions of the problem. The solution is made for a steady-state vibration with frequency 'ω'. The lateral movement of the foundation at any arbitrary point *'u_1'* can be written as:

$$\begin{cases} u(r_0,\theta,t) = e^{i\omega t} u_1 \cos(\theta) \\ v(r_0,\theta,t) = -e^{i\omega t} u_1 \sin(\theta) \end{cases} \qquad (2.4\text{–}1)$$

Note that the equation (2.4–1) is a special case of the equations (2.1–46) and (2.1–47). The plane strain elastodynamic equations (2.1–38) and (2.1–39) are separated using Lamb (1904) transformations which are expressed in equations (2.1–41) and (2.1–42). Application of Lamb's transformation leads to the equations (2.1–43) and (2.1–44). These equations, which are in the form of partial differential equations, are solved by employing the separation of variables technique. Time is easily separated by using a harmonic function in steady-state conditions. Deformation and potential functions are written as:

$$\begin{cases} u(r,\theta,t) = \bar{u}(r,\theta)e^{i\omega t} \quad , \quad v(r,\theta,t) = \bar{v}(r,\theta)e^{i\omega t} \\ \varphi(r,\theta,t) = \bar{\varphi}(r,\theta)e^{i\omega t} \quad , \quad \psi(r,\theta,t) = \bar{\psi}(r,\theta)e^{i\omega t} \end{cases} \qquad (2.4\text{–}2)$$

Substituting equation (2.4–2) into equations (2.1–43) and (2.1–44) results in:

$$\begin{cases} (\nabla^2 + h^2)\bar{\varphi} = 0 \\ (\nabla^2 + k^2)\bar{\psi} = 0 \end{cases} \qquad (2.4\text{–}3)$$

Where

$$\begin{cases} h = \dfrac{\omega}{V_p} \\ k = \dfrac{\omega}{V_s} \end{cases} \qquad (2.4\text{–}4)$$

The differential equations (2.4–3) have two parameters r,θ that must be separated. We start with 'θ' knowing that the solution for deformations should be periodic with 'θ'. Fourier series expansion (e.g. see Pipes and Harvill 1970) is employed to describe the variation in displacement potential functions with variable 'θ'. After writing the Fourier expansion for potential functions and substituting into equation (2.4–3), they transform to the Bessel

differential equations with respect to the variable *'r'*. Solving these equations, Baranov reached the following solutions for the potential functions:

$$\begin{cases} \overline{\varphi} = \sum_{n=0}^{\infty} (A_n \cos n\theta + B_n \sin n\theta)[E_n H_n^{(1)}(hr) + F_n H_n^{(2)}(hr)] \\ \overline{\psi} = \sum_{n=0}^{\infty} (C_n \cos n\theta + D_n \sin n\theta)[G_n H_n^{(1)}(kr) + L_n H_n^{(2)}(kr)] \end{cases} \quad (2.4\text{–}5)$$

Where *'A_n'* to 'L_n' are constants to be determined using boundary conditions and $H_n^{(1)}$ and $H_n^{(2)}$ are Hankel functions of the first and the second kinds, respectively. In order to satisfy the principle of radiation, it is necessary to have zero deformation at very far distances from the foundation. Asymptotic expansions of the Hankel functions of the first and the second kind (Abramowitz and Stegun 1972 9.2.3 and 9.2.4) show that they both vanish at far distances from the pile, therefore the radiation boundary condition is satisfied. These expansions are given in the equations (2.4–6) and (2.4–7):

$$\lim_{r \to \infty} \quad e^{i\omega t} H_n^{(1)}(hr) \cong \sqrt{\frac{2}{\pi x}} \exp[i(\omega t + rh - (2n+1)\frac{\pi}{4})] \to 0 \quad (2.4\text{–}6)$$

$$\lim_{r \to \infty} \quad e^{i\omega t} H_n^{(2)}(hr) \cong \sqrt{\frac{2}{\pi x}} \exp[i(\omega t - rh + (2n+1)\frac{\pi}{4})] \to 0 \quad (2.4\text{–}7)$$

Equation (2.4–6) represents a wave travelling in the negative *'r'* direction. This can be proved by determining the phase velocity for the waves described by this equation. The phase is the argument of the exponential term, i.e. $\omega t + rh - (2n+1)\pi/4$. To determine the phase velocity, the expression for the phase is set to a constant to represent all points on a wave with the same phase. Differentiating this equation leads to the phase velocity of the waves. Equations (2.4–8) and (2.4–9) show the procedure. Equation (2.4–9) expresses the phase velocity which is negative and indicates transmission of waves in a negative radial direction.

$$\omega t + rh - (2n+1)\frac{\pi}{4} = const \quad (2.4\text{–}8)$$

$$\frac{dr}{dt} = -\frac{\omega}{h} \quad (2.4\text{–}9)$$

Equation (2.4–7), on the other hand, represents a wave travelling in the positive *'r'* direction. Baranov argues that the waves radiated from the pile should only travel in the positive *'r'* direction as there are no boundaries to reflect them. Therefore, Baranov chooses the Hankel function of the second kind as the valid answer to the problem and ignores the other (i.e. he proposes: $E_n = G_n = 0$). This choice obviously does not have an impact on the final result because Hankel functions of the first and the second kinds are complex conjugates of each other. It should also be noted that the function representing the progressive waves depends on the form of the time harmonic function which is adapted to separate the time variable. Baranov's decision to use '$e^{i\omega t}$' as the time harmonic function results in the presence of a Hankel function of the second kind in the progressive wave expression. One could equally use '$e^{-i\omega t}$' as the time harmonic function and have the Hankel function of the first kind in the progressive wave expression. After the necessary discussion on the right choice of Hankel function, Baranov goes back to the determination of the constants of the solutions. Since the factors *'F_n'* to *'L_n'* are multiplied to other unknown factors, they are arbitrarily set to unity. Symmetry of the deformations with the *x-z* plane requires that:

$$\begin{cases} \bar{u}(r,\theta) = \bar{u}(r,-\theta) \\ \bar{v}(r,\theta) = -\bar{v}(r,-\theta) \end{cases} \tag{2.4–10}$$

Equation (2.4–10) implies that the sine terms from the expression of $\bar{\varphi}$ and cosine terms from the expression of $\bar{\psi}$ in the equation (2.4–5) should be eliminated. This simplifies equation (2.4–5) to:

$$\begin{cases} \bar{\varphi} = \sum_{n=0}^{\infty} A_n \cos(n\theta) H_n^{(2)}(hr) \\ \bar{\psi} = \sum_{n=0}^{\infty} D_n \sin(n\theta) H_n^{(2)}(kr) \end{cases} \tag{2.4–11}$$

Substituting equations (2.4–11) into equations (2.4–1) results in:

$$\begin{cases} A_0 = A_2 = A_3 = \ldots = 0 \\ D_0 = D_2 = D_3 = \ldots = 0 \end{cases} \tag{2.4–12}$$

The only nonzero factors 'A_1' and 'D_1' are derived from the following set of algebraic equations:

$$\begin{cases} A_1 \dfrac{d}{dr} H_1^{(2)}(hr_0) + D_1 \dfrac{1}{r_0} H_1^{(2)}(kr_0) = u_1 \\ A_1 \dfrac{1}{r_0} H_1^{(2)}(hr_0) + D_1 \dfrac{d}{dr} H_1^{(2)}(kr_0) = u_1 \end{cases} \tag{2.4–13}$$

Now that the potential functions $\varphi = e^{i\omega t} A_1 \cos\theta H_1^{(2)}(hr)$ and $\psi = e^{i\omega t} D_1 \sin\theta H_1^{(2)}(kr)$ are determined, the stress components on the soil-pile interface can be written as:

$$\begin{cases} \sigma_r = -\lambda h^2 \varphi + 2\mu[\dfrac{\partial^2 \varphi}{\partial r^2} + \dfrac{\partial}{\partial r}(\dfrac{1}{r}\dfrac{\partial \psi}{\partial \theta})] \\ \tau_{r\theta} = -\mu k^2 \psi - 2\mu[\dfrac{\partial^2 \psi}{\partial r^2} - \dfrac{\partial}{\partial r}(\dfrac{1}{r}\dfrac{\partial \varphi}{\partial \theta})] \end{cases} \tag{2.4–14}$$

The result of these stresses on the foundation is derived as:

$$q = \int_0^{2\pi} (-\sigma_r \cos\theta + \tau_{r\theta} \sin\theta) r_0 d\theta = c_2 u_1 e^{i\omega t} \tag{2.4–15}$$

Baranov derives the factor *'c_2'* as:

$$c_2 = 2\pi\mu k r_0 \frac{\dfrac{1}{\eta} H_2^{(2)}(kr_0) H_1^2(hr_0) + H_2^{(2)}(hr_0) H_1^{(2)}(kr_0)}{H_0^{(2)}(kr_0) H_2^2(hr_0) + H_0^{(2)}(hr_0) H_2^{(2)}(kr_0)} \tag{2.4–16}$$

Where

$$\eta = \frac{h}{k} = \sqrt{\frac{1-2\nu}{2(1-\nu)}} \tag{2.4–17}$$

He then argues that the factor *'c_2'* is a complex function of soil shear modulus, the dimensionless factor *'kr_0'* and Poisson's ratio:

$$c_2(kr_0, \nu) = \mu[c_{21}(kr_0, \nu) + i c_{22}(kr_0, \nu)] \tag{2.4–18}$$

The dimensionless factor *'kr_0'* is called dimensionless frequency and is denoted as *'a_0'* in the Western literature. Baranov interprets the imaginary part of equation (2.4–18) as the damping force, while the real part is a combination of stiffness and inertia forces. Since expressions of factors *'c_{21}'* and *'c_{22}'* are not simple in general form, Baranov considers a special case. He argues that the factor 'η' varies from 0 to 0.707 when the Poisson's ratio of the soil varies from 0.5 to 0, respectively. Considering that most saturated soils have

Poisson's ratios close to 0.5, he chooses '$\eta = 0$' to expand equation (2.4–18) and finally propose the following relationships:

$$c_{21} = \pi(1 + 2\frac{J_0(kr_0)J_2(kr_0) + Y_0(kr_0)Y_2(kr_0)}{J_0(kr_0)^2 + Y_0(kr_0)^2}](kr_0)^2 , \qquad c_{22} = \frac{8}{J_0(kr_0)^2 + Y_0(kr_0)^2} \tag{2.4–19}$$

In the above equation *'J_n'* and *'Y_n'* hold for Bessel functions of the first and the second kind, respectively.

After solving for the lateral movement of the foundation, Baranov approaches a solution for the rotation of the foundation. Assuming that the foundation has a rigid rotation of 'φ' in the *x-z* plane, the deformation components at the side surface of the foundation read:

$$u(r_0, \theta, z, t) = 0, \quad v(r_0, \theta, z, t) = 0 \quad , \quad w(r_0, \theta, z, t) = e^{i\omega t}\varphi r_0 \cos\vartheta \tag{2.4–20}$$

Based on the nature of the deformations near the foundation, Baranov assumes that the horizontal deformations at every point within the soil media are zero. He also assumes that the vertical deformation is not variable with depth. The author of this thesis believes that these assumptions were unnecessary. It is enough to substitute the derived horizontal deformations in the three-dimensional elastodynamic equations and observe that these equations can be satisfied only if:

$$\frac{\partial}{\partial z} w(r, \theta, z, t) = 0 \tag{2.4–21}$$

Substituting equation (2.4–21) into equation (2.1–30) results in the following equation:

$$\frac{\mu}{r}\frac{\partial}{\partial r}(r\frac{\partial w}{\partial r}) + \frac{\mu}{r^2}\frac{\partial^2 w}{\partial \theta^2} = \rho\frac{\partial^2 w}{\partial t^2} \tag{2.4–22}$$

To solve the above differential equation, the method of separation of variables is employed:

$$w = e^{i\omega t} R(r)\Phi(\theta) \tag{2.4–23}$$

Substituting equation (2.4–23) into equation (2.4–22) results in the following two ordinary differential equations:

$$rR' + r^2 R'' + (k^2 r^2 - n^2)R = 0 \tag{2.4–24}$$

$$\Phi'' + n^2\Phi = 0 \tag{2.4–25}$$

The factor *'n'* in the above equation is an arbitrary constant that separates the two functions. The solutions to equation (2.4–24) can be expressed as Hankel functions, while those for equation (2.4–25) are sine and cosine functions. In general there may be an infinite number of values for *'n'* that satisfy the above equations, therefore the general solution is the sum of all possible solutions:

$$w = e^{i\omega t}\sum_{n=0}^{\infty}(A_n\cos n\theta + B_n\sin n\theta)[C_n H_n^{(1)}(kr) + D_n H_n^{(2)}(kr)] \qquad (2.4\text{–}26)$$

Symmetry about the *x-z* plane implies that: $w(\theta) = w(-\theta)$. It concludes that the sine term should vanish from the above equation (i.e. $B_n=0$). As before, the Hankel function of the second kind represents the propagating wave and we should have *'*$C_n=0$*'* to avoid waves travelling in negative radial directions. After substituting this result into equation (2.4–26) it is seen that the factors *'*A_n*'* and 'D_n*'* are multiplied together, therefore it is arbitrary to take one of them equal to the unity (e.g. $A_n=1$). The solution simplifies to:

$$w = e^{i\omega t}\sum_{n=0}^{\infty}D_n H_n^{(2)}(kr)\cos n\theta \qquad (2.4\text{–}27)$$

Substituting equation (2.4–27) into equation (2.1–48) results in:

$$D_0 = D_2 = D_3 = \ldots = 0, \qquad D_1 = \frac{\varphi r_0}{H_1^{(2)}(kr_0)} \qquad (2.4\text{–}28)$$

Stress components resulting from the vertical deformations in the soil on the foundation surface are derived as:

$$\sigma_r = \sigma_z = \tau_{r\theta} = \ldots = 0 \qquad (2.4\text{–}29)$$

$$\tau_{rz} = \mu\frac{\varphi r_0 e^{i\omega t}}{H_1^{(2)}(kr_0)}[-\frac{1}{r}H_1^{(2)}(kr) + kH_0^{(2)}(kr)]\cos\theta \qquad (2.4\text{–}30)$$

The shear stress expressed by the equation (2.4–30) has a resultant distributed bending moment when integrated over a horizontal cross-section of pile. The differential distributed bending moment on an infinitesimal length element of the foundation *'dz'* reads:

$$dm_y = -dz\int_0^{2\pi}\tau_{rz}.1.r_0 d\theta r_0\cos\theta = dz\pi\mu r_0^2\varphi[1 - kr_0\frac{H_0^{(2)}(kr_0)}{H_1^{(2)}(kr_0)}]e^{i\omega t} \qquad (2.4\text{–}31)$$

It should be noted that the distributed bending moment is a complex valued quantity:

$$dm_y = c_3(kr_0)\varphi r_0^2 e^{i\omega t}dz = \mu r_0^2 \varphi e^{i\omega t}(c_{32} + ic_{32})dz \qquad (2.4\text{–}32)$$

For the case of $\nu = 0.5$, Baranov presents simple formulas for real and imaginary parts:

$$c_{32} = \pi(1 - kr_0 \frac{J_0(kr_0)J_1(kr_0) + Y_0(kr_0)Y_1(kr_0)}{J_1(kr_0)^2 + Y_1(kr_0)^2}) \quad , \quad c_{32} = \frac{2}{J_1(kr_0)^2 + Y_1(kr_0)^2} \qquad (2.4\text{–}33)$$

The vertical vibrations of the foundation are also discussed by Baranov. He argues that because of the symmetry, horizontal deformation components in the soil caused by a vertical movement of the foundation are zero. He also concluded that the vertical deformation component in the soil is independent to directional variable θ. Using these assumptions Baranov proposes a solution for the vertical deformation component in the soil imposed by the vertical movement of the foundation.

Here we may argue that this assumption is by no means valid for an embedded foundation with a finite length. The reason is that the base of the foundation imposes certain boundary conditions on the soil media. Baranov's assumption is valid only if the embedded foundation is infinitely long. This, by definition, turns the foundation into a pile. Therefore, Baranov's solution for vertical vibrations is more valid for a rigid pile than for an embedded rigid foundation. Long piles, on the other hand are not rigid. Flexibility of long piles plays a very important role in their behaviour and their interaction with the soil. The flexibility of pile makes its lateral deflection dependent upon depth. Therefore, the earlier assumption of the non-variability of horizontal deflections with depth as a cause of the soil being in plane strain is invalidated.

2.4.2 Novak's contribution to the dynamic pile problem

Novak formulated stiffness and damping of piles in a series of articles. In his first paper (Novak 1974) he partially employed Baranov's (1967) solution to estimate impedance and damping of single piles under lateral vibration. In his approach he ignored the effect of shear stresses. As mentioned in the previous section, shear stresses result in a distributed bending moment on the pile, as described by equation (2.4–32). Novak chose to use only lateral soil resistance in his model and ignore the distributed bending moment caused by the vertical shear stress. The lateral soil resistance is expressed by equation (2.4–15). This approach resulted in a generalized beam on Winkler support. Novak expressed the flexure equation of the pile as:

$$m_p \frac{\partial^2 X(z,t)}{\partial t^2} + c_p \frac{\partial X(z,t)}{\partial t} + \mu(c_{21} + ic_{22})X(z,t) + E_p I_p \frac{\partial^4 X(z,t)}{\partial z^4} = 0 \qquad (2.4\text{–}34)$$

The notation in the above equation and the rest of the equations in this section are modified from the Novak's original papers to match the notations of the present thesis. For a steady-state analysis, Novak wrote:

$$E_p I_p \frac{d^4 X(z)}{dz^4} + [\mu c_{21} - m_p \omega^2 + i(c_p \omega + \mu c_{22})]X(z) = 0 \qquad (2.4\text{–}35)$$

He proposed the following solution for the above equation for a pile with limited length *'l'*:

$$X(z) = C_1 \cosh(\lambda \frac{z}{l}) + C_2 \sinh(\lambda \frac{z}{l}) + C_3 \cos(\lambda \frac{z}{l}) + C_4 \cos(\lambda \frac{z}{l}) \qquad (2.4\text{–}36)$$

Where

$$\lambda = l \sqrt{\frac{1}{E_p I_p}[m_p \omega^2 - \mu c_{21} - i(c_p \omega + \mu c_{22})]} \qquad (2.4\text{–}37)$$

The factors *'C_1'* to *'C_4'* are integration constants that should be determined from pile end conditions. In the rest of his paper, Novak formulated the pile stiffness and damping coefficients and provided tabular values for dimensionless factors which form the stiffness coefficients of a pile in a homogeneous soil layer. He also investigated the effect of a static axial load on stiffness. Novak provided the full procedure and examples for the application of his method.

Novak and Aboul-Ella (1978) extended the theory towards the prediction of pile stiffness and damping in layered soil. Novak and Sheta (1982; 1991) discussed the shortcomings of the plane strain theory that result in zero stiffness for very low vibration frequencies. This feature of the plane strain model is in contradiction with the general sense that a dynamic theory should approach static values for small frequencies, as stated by other researchers (Blaney, Kausel and Roesset 1976; Novak and Nogami 1977; Kaynia and Kausel 1980; Takemiya and Yamda 1981). In an attempt to correct this drawback, Novak and Sheta (1982) suggest using a constant stiffness calculated at '*a_0=0.3'* for all dimensionless frequencies less than 0.3. However, they neither proposed a closed-form value for the static stiffness nor reasons for using the chosen stiffness as the representative stiffness under static condition.

Novak and El Sharnouby (1983) extended their approach for variable soil profiles and included material damping of the soil and the pile.

Novak has made an undeniably great contribution to the analysis of dynamically loaded pile foundations. A computer program DYNA3 (Novak, Sheta, El-Hifnawy, El-Marsafawi and Ramadan 1991) was written based on his research into the calculation of the dynamic response of foundations. The profit from this program together with his family's contribution provides for the Milos Novak Memorial Award,[1] which is normally awarded annually to an engineer who wishes to pursue graduate studies in geotechnical engineering at the University of Western Ontario, Canada.

2.4.3 Nogami's contribution to solving the dynamic pile problem

Nogami and Novak (1977) proposed a solution to the problem of laterally vibrating piles. They considered a limited thickness, homogeneous, isotropic, viscoelastic soil layer overlaying rigid bedrock. They assumed that vertical displacements associated with horizontal vibrations are negligibly small.

To implement viscoelasticity of the soil, they introduced the complex valued Lamé's constants:

$$\begin{cases} \lambda' = \lambda + iD_v\lambda \\ \mu' = \mu + iD_s\mu \end{cases} \tag{2.4–38}$$

Where *'D_v'* and *'D_s'* are called hysteretic damping ratios associated with volumetric and shear strain, respectively. In the footnote of their paper, however, Nogami and Novak explained that these factors are in fact tangent loss angles and equal twice the damping ratios.

In order to solve the elastodynamic equations, they adapted Lamb's (1904) transformations employing potential functions φ, ψ as per equations (2.1–41) and (2.1–42). The difference between their approach and Novak's (1974) initial approach was that the potential functions were considered variable with depth. After substituting the potential functions in the elastodynamic equations, the following equations were obtained:

$$\begin{cases} \{1 + i\frac{1}{\eta^2}[(\eta^2 - 2)D_v + D_s]\}\nabla^2\varphi + [(\frac{\omega}{V_p})^2 + \frac{1}{\eta^2}(1 + iD_s)\frac{\partial^2}{\partial z^2}]\varphi = 0 \\ (1 + iD_s)\nabla^2\psi + [(\frac{\omega}{V_p})^2 + (1 + iD_s)\frac{\partial^2}{\partial z^2}]\psi = 0 \end{cases} \tag{2.4–39}$$

[1] http://www.eng.uwo.ca/gradstudies/internal_scholarships.htm#novak

The separation of variable technique was implemented to solve the above equations:

$$\varphi = R(r)\Theta(\theta)Z(z) \tag{2.4–40}$$

Substituting equation (2.4–40) into equation (2.4–39) resulted in:

$$\{1+i\frac{1}{\eta^2}[(\eta^2-2)D_v+2D_s]\}(\frac{1}{R}\frac{\partial^2 R}{\partial r^2}+\frac{1}{r}\frac{1}{R}\frac{\partial R}{\partial r}+\frac{1}{r^2}\frac{1}{\Theta}\frac{\partial^2\Theta}{\partial\theta^2}+\frac{1}{\eta^2}(1+iD_s)\frac{1}{Z}\frac{\partial^2 Z}{\partial z^2}+(\frac{\omega}{V_p})^2=0 \tag{2.4–41}$$

In the above equation, functions of single variables are separated. Since their sum equals zero, each part must be a constant. Nogami and Novak introduced two independent constants *'m'* and *'h'* and one dependent constant *'q'*:

$$\frac{1}{R}\frac{\partial^2 R}{\partial r^2}+\frac{1}{r}\frac{1}{R}\frac{\partial R}{\partial r}-\frac{1}{r^2}m^2=q^2 \tag{2.4–42}$$

$$\frac{1}{Z}\frac{\partial^2 Z}{\partial z^2}=-h^2 \tag{2.4–43}$$

$$\frac{1}{\Theta}\frac{\partial^2\Theta}{\partial\theta^2}=-m^2 \tag{2.4–44}$$

$$q^2=\frac{(1+iD_s)h^2-(\omega/v_s)^2}{\eta^2+i[(\eta^2-2)D_v+2D_s]} \tag{2.4–45}$$

Assuming that the factors *'m'* and *'h'* are real-valued, Nogami and Novak proposed the following solutions:

$$\begin{cases} R=A_1K_m(qr)+B_1I_m(qr) \\ Z=A_2\sin(hz)+B_2\cos(hz) \\ \Theta=A_3\sin(m\theta)+B_3\cos(m\theta) \end{cases} \tag{2.4–46}$$

Where $'I_m'$ and $'K_m'$ are modified Bessel functions of the first and second kinds of order *'m'*. *'A'* and *'B'* are integration constants. With a similar approach for the second potential function 'ψ', Nogami and Novak proposed the following expressions:

$$\varphi=[A_1K_m(qr)+B_1I_m(qr)][A_2\sin(hz)+B_2\cos(hz)][A_3\sin(m\theta)+B_3\cos(m\theta)] \tag{2.4–47}$$

$$\psi=[A_4K_m(sr)+B_4I_m(sr)][A_5\sin(hz)+B_5\cos(hz)][A_6\sin(m\theta)+B_6\cos(m\theta)] \tag{2.4–48}$$

$$s^2 = \frac{(1+iD_s)h^2 - (\omega/V_s)^2}{1+iD_s} \tag{2.4–49}$$

They then argued that to have displacements vanish at infinity, the coefficients of the modified Bessel functions of the first kind should be zero. In order to have zero displacement on the bedrock it is necessary to have:

$$h = \frac{\pi}{2H}(2n-1), \qquad n = 1,2,...\infty \tag{2.4–50}$$

Where *'H'* is the thickness of the layer. It should be noted that Nogami and Novak put the origin of the coordinate system on the bedrock and not on the ground level. Here we can spot a major flaw in Nogami and Novak's solution. The fact that the parameter *'h'* is real-valued results in an undamped vibration in a vertical direction, i.e. waves through the media are not damped with depth if the soil hysteretic damping is ignored. In fact their solution becomes real-valued if the soil damping is ignored. This means that there would not be a geometric damping for the vibrating pile.

Nogami and Novak proposed the following expressions for the displacement components:

$$\begin{cases} u = \cos\theta \sum_{n=1}^{\infty} \sin(h_n z)\{-A_n[\frac{1}{r}K_1(q_n r) + q_n K_0(q_n r)] + B_n \frac{1}{r}K_1(s_n r) \\ v = \sin\theta \sum_{n=1}^{\infty} \sin(h_n z)\{-A_n \frac{1}{r}K_1(q_n r) + B_n[\frac{1}{r}K_1(s_n r) + s_n K_0(s_n r)] \end{cases} \tag{2.4–51}$$

At this stage, Nogami and Novak stated that ignoring vertical displacements resulted in nonzero vertical stresses at the ground surface. They also claimed that they had compared the results with the static solutions and found good agreements, and concluded that the error was negligible.

In order to implement the boundary conditions at the pile surface, Nogami and Novak employed a modal analysis approach, claiming that the deflected curve of the pile could be expressed as the infinite sum of modes:

$$X(z) = \sum_{n=1}^{\infty} X_n \sin(h_n z) \tag{2.4–52}$$

Here the factors *'X_n'* are depth independent modal amplitudes. It is evident that the above equation does not satisfy the boundary conditions of the pile. Equation (2.4–52) results in nonzero slope at the bedrock which contradicts the original assumption of the pile being

clamped at its tip. On the other hand, the slope at the pile head (i.e. at $z=H$) becomes zero, meaning that the rotation at pile head is restrained. Therefore equation (2.4–52) is only valid for a pile with a hinged tip and restrained head and not for general pile boundary conditions.

Nogami and Novak continued the rest of their solution by determining the soil reaction on the pile as a distributed force, ignoring the effect of vertical shear stress. This solution, regardless of its serious weaknesses, is important from the point of view that the resonance frequencies of the soil layer are included.

In a subsequent paper, Novak and Nogami (1977) studied the soil-pile interaction using their solution. Ignoring the fact that the modal expression used in the evaluation of their integration constants has serious limitations, they provided closed-form solutions for stiffness and damping for different end conditions of the pile.

Nogami and Konagai (1986) proposed a simple model for a vertically vibrating pile. Their proposed model was composed of three Kelvin-Voigt models which could successfully simulate the behaviour of piles in a plane strain soil as described by Novak, Nogami and Aboul-Ella (1978). The Kelvin-Voigt model consists of a spring and a dashpot connected in parallel. Nogami and Konagai (1988) developed a Winkler-type model for laterally vibrating piles. Their model was based on the solution given by Nogami and Novak (1977) with some simplifications to the main formulations. Figure 2-13 shows their proposed model which was composed of a mass and three Kelvin-Voigt models.

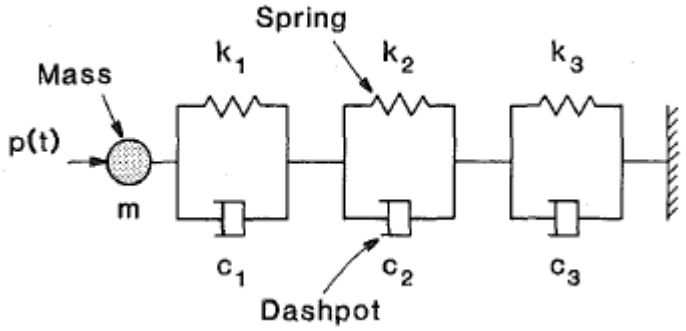

Figure 2-13 Winkler model for lateral pile shaft response (after Nogami and Konagai 1988)

The parameters of the model are:

$$m_s = \xi_m(\nu)\rho\pi r_0^2 \tag{2.4–53}$$

$$k_s = \xi_k(\nu)\mu\begin{cases}3.518, & n=1\\3.581, & n=2\\5.529, & n=3\end{cases} \tag{2.4–54}$$

$$c_s = \xi_k(\nu)\frac{\mu r_0}{V_s}\begin{cases}113.097, & n=1\\25.133, & n=2\\9.362, & n=3\end{cases} \tag{2.4–55}$$

Where $\xi_m(\nu)$ and $\xi_k(\nu)$ are given as tabulated values for different Poisson's ratios (note that the same factor is used for stiffness and damping). The author of this thesis fit curves to the tabulated values and correlated the following polynomial expressions:

$$\xi_m(\nu) = 12.78\nu^3 - 5.3747\nu^{22} + 1.0314\nu + 1.213 \tag{2.4–56}$$

$$\xi_k(\nu) = \begin{cases}179.36\nu^3 - 175.95\nu^2 + 57.319\nu - 6.1385, & \nu \geq 0.25\\0, & \nu < 0.25\end{cases} \tag{2.4–57}$$

2.4.4 Kaynia's solution for layered soil

Kaynia (1982) proposed a solution to the general problem of the group of piles in elastic layered soil. His final solution for soil displacement components was in the form of integral equations which demanded numerical evaluation. He proposed graphs for non-dimensional stiffness and damping of piles in 2×2, 3×3 and 4×4 groups. Kaynia's solution cannot be considered to be a closed-form solution as it requires numerical evaluation. However, it is referred to in the literature as an accurate solution to the lateral vibration of pile. His conclusions as summarized in his PhD thesis are as follows (Kaynia 1982):

1) Dynamic pile group behaviour is highly frequency-dependent. This is due to the characteristics of the wave generated by the piles and the interface between these waves and the different piles in the group.
2) For close spacing, the characteristics of group stiffness are similar to those in footings. For large spacing, however, the group behaviour is dominated by the interactions between the piles.
3) Interaction effects are stronger for softer soil media.
4) Radiation damping generally increases with foundation size.
5) Pile groups subjected to seismic excitations essentially follow the low-frequency components of the ground motion, while filtering to a large extent its intermediate

and high frequency components. The rotational component, on the other hand, is negligible for typical dimensions of the foundation.

6) The distribution of applied dynamic loads on the pile cap is different from that of static loads. For certain frequency intervals, the poles closest to the centre take the largest portion of the load. Also, large dynamic amplification factors are expected for the forces in these piles.
7) Pile groups are less influenced by conditions near the ground surface than single piles are. Therefore, techniques using the results of single pile nonlinear analyses, field tests on single piles, and empirical group reduction factors to derive group stiffness are less accurate than expected.

The mathematical approach is concisely described in Kaynia and Kausel (1991).

The only weakness in Kaynia's approach that may be referred to is that he did not attempt to satisfy ground surface zero traction boundary conditions. He ignored the effect of friction between the pile surface and the soil, and he did not include compatibility conditions between the adjacent layers at their interfaces (e.g. Dobry, Oweis and Urzua 1976).

2.4.5 Gazetas and Dobry – simplified radiation damping of piles

The fundamental continuum solutions given so far by Baranov (1967), Novak (1974), Nogami and Novak (1977), Novak and Nogami (1977), Kaynia and Kausel (1980) and Kaynia (1982) all include geometrical (radiation) damping of the pile as the imaginary part of the solutions. Although being mathematically rigorous, this method of expressing the damping lacks the physical meaning and the simplicity that makes the concept understandable for practicing engineers. Several attempts have been made in the literature to address the concept of radiation damping via a simple physical model. Berger et al. (1977) proposed a one-dimensional wave propagation model to address the concept of radiating energy from a vibrating pile to infinity. They assumed that the waves are radiated from the pile within two narrow zones similar to a propagated wave in long rods (Figure 2-14 (a),(b)), and that P-waves are propagated in the zone in line with pile motion while the SH-waves are transferred through the perpendicular zone. The width of both zones is taken to be equal to the pile diameter. The analogy is made with a viscous damper (dashpot) being able to absorb all the energy radiated in two directions. The following coefficient is derived for a dashpot with this quality:

$$c_r = 4r_0 \rho V_s (1 + \frac{V_p}{V_s}) \tag{2.4–58}$$

Where *'c_r'* stands for the radiation damping coefficient of the system. Pressure and shear wave velocities (V_p and V_s) are related via Poisson's ratio:

$$V_p = V_s \sqrt{\frac{2(1-\nu)}{1-2\nu}} \tag{2.4–59}$$

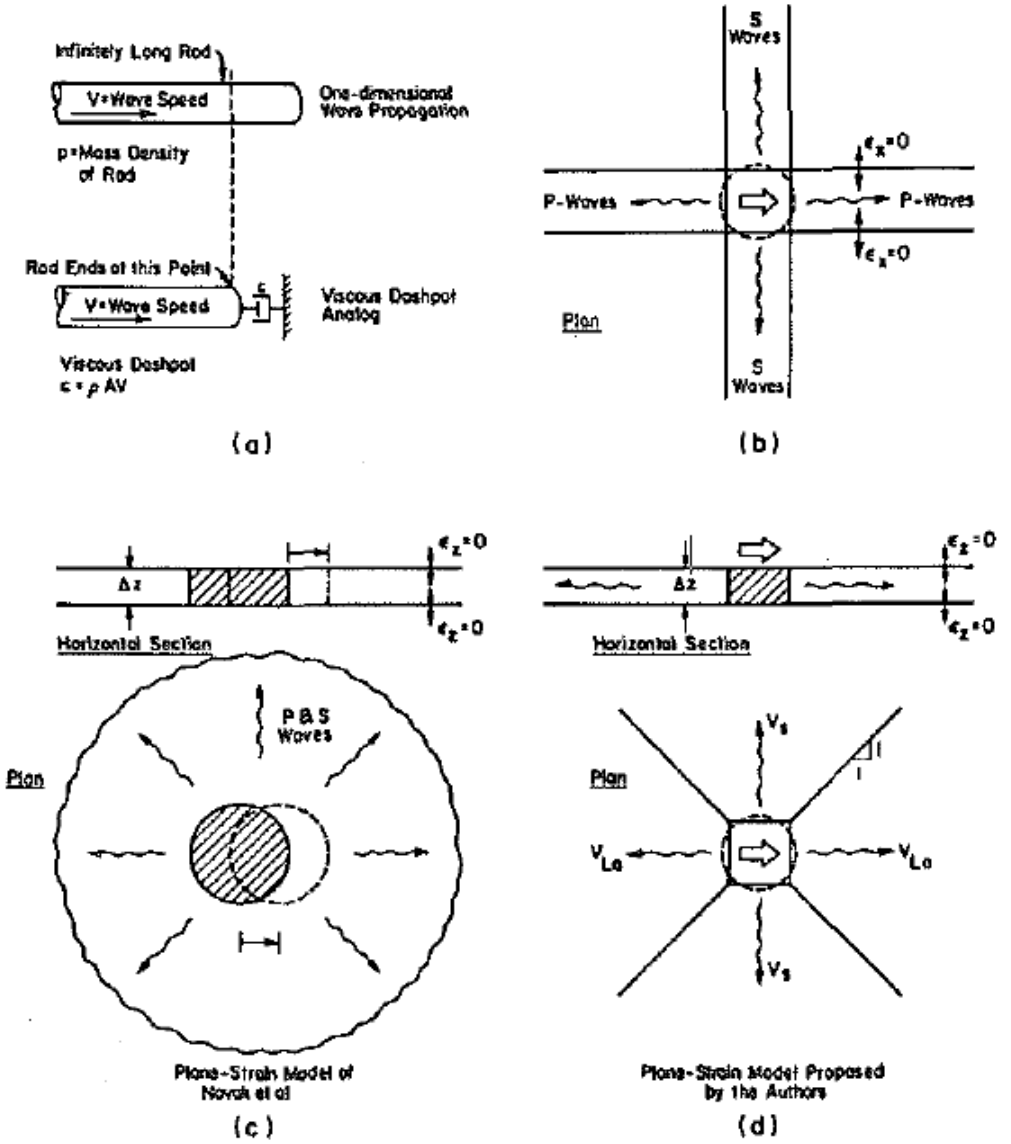

Figure 2-14 Radiation model (a), (b) (Berger et al. (1977)) (c),(d) (Gazetas and Dobry (1984))

There are two obvious drawbacks to this theory, as explained by Gazetas and Dobry (1984):

1) The dashpot coefficient is frequency-independent.
2) The dashpot coefficient becomes extremely large for soils with Poisson's ratios close to 0.5, as results from equation (2.4–59).

O'Rourke and Dobry (1979) proposed accepting Berger's analogy but using it with another velocity than 'V_p'. They proposed three candidates for the velocity:

$$V_c = V_s\sqrt{\frac{2}{1-\nu}} \qquad (2.4\text{–}60)$$

V_c is derived from the boundary conditions of $\varepsilon_z = 0, \sigma_x = 0$ (see Figure 2-14 (c),(d)). The second possibility is to use rod velocity *'V_L'* which is defined by the boundary conditions of $\sigma_z = \sigma_x = 0$:

$$V_L = V_s\sqrt{2(1+\nu)} \qquad (2.4\text{–}61)$$

The third possibility is to use Lysmer's analogue 'wave velocity – V_{La}':

$$V_L = \frac{3.4V_s}{\pi(1-\nu)} \qquad (2.4\text{–}62)$$

An alternative approximate plane-strain model, which does not have the limitations of Berger's model, has been developed by Gazetas and Dobry (1984). Rather than two narrow zones, Gazetas and Dobry assumed that compression-extension waves propagate in the two quarter-planes along the direction of loading, while shear waves are generated in the two quarter-planes perpendicular to the direction of loading. Figure 2-14 (d) illustrates the basic elements of the model for the case of a square pile cross-section. Only horizontal soil deformations are allowed within each quarter-plane, and all straight lines originally normal to the corresponding direction of wave-propagation remain normal during the oscillation. Each of the four quarter-planes is assumed to vibrate independently of the three others. If the pile cross-section is circular, it is replaced by a square section having the same perimeter $2\pi r_0$. By assuming that S-waves propagate with velocity *'V_s'* and compression-extension waves propagate with velocity *'V_{La}'*, and by adding up the energies radiated away in the four quarter planes, Gazetas and Dobry derived the following expression for the radiation damping coefficient:

$$\frac{c_4}{4r_0\rho V_s} = \{1 + [\frac{3.4V_s}{\pi(1-\nu)}]^{5/4}\}(\frac{\pi}{4})^{3/4} a_0^{-1/4} \qquad (2.4\text{–}63)$$

Gazetas and Dobry found very good agreement between the above formula and the results of the plane strain model derived by Novak (1974). They suspected, however, that the above equation would probably overestimate the value of the radiation damping coefficient in shallow depths. They explained that this might be due to the stress-free ground surface which facilitates the generation of surface-type waves in addition to plane strain body waves. Therefore they proposed using wave propagation velocity of *'V_s'* in all four regions for depths of less than 2.5 pile diameters. This led to the following expression for damping ratio for the top soil region:

$$\frac{c_4}{4r_0\rho V_s} = 2(\frac{\pi}{4})^{3/4} a_0^{-1/4}, \quad z \le z_4 = 2.5D \qquad (2.4\text{–}64)$$

The above equation is used in the literature for its simplicity (e.g. Gazetas, Fan and Kaynia 1992). An apparent drawback of equation (2.4–64) is that its value becomes infinitely large for very small frequencies. This is a typical feature of any plane strain model to show very small stiffness and large damping at low frequencies. Novak and Sheta (1991) explain this by referring to the fact that plane strain models are unable to transfer waves in vertical directions and that at lower frequencies these kinds of waves are more common. For high frequencies, however, waves propagate more horizontally and the plane strain model is therefore more accurate for this range of frequencies.

2.4.6 Nonlinear effects in pile dynamics

Nogami et al. (1992) provided a nonlinear dynamic analysis methodology which implemented soil nonlinearity and included separation and slippage on the pile surface. They divided the soil into two parts, a near field which was highly plastic and a far field which was linearly elastic. They considered the size of the near field region to be from 1.5 to 3 times the pile radius away from the pile surface. The near field model included an interface element allowing for separation and slippage, a consistent mass matrix and a stiffness matrix. The consistent mass matrix is given as:

$$m_n = \frac{\pi\rho r_0^2}{6}(\frac{r_1}{r_0} - 1)\begin{bmatrix} \frac{r_1}{r_0} + 3 & 3\frac{r_1}{r_0} + 1 \\ 3\frac{r_1}{r_0} + 1 & \frac{r_1}{r_0} + 1 \end{bmatrix} \qquad (2.4\text{–}65)$$

No explanation was given in their paper as to how the consistency mass matrix was derived. They only said that the displacements within the near field were assumed to vary linearly with the radial distance from the pile. The degree of freedom of the pile element was designated as 1 and that for the far field element was designated as 2. The members in the consistency mass matrix relates to the corresponding degrees of freedom. The near field stiffness is given as:

$$k(\omega) = k_n - \omega^2 m_{n,1} - \frac{k_n^2 + 2\omega^3 k_n m_{n,12} + \omega^4 m_{n,12}}{k_n + k_f - \omega^2 (m_{n,2} + m_f)} \tag{2.4–66}$$

Where $m_{n,ij}$ are *ij-th* members of the consistency mass matrix and *'m_f'* is the far field mass defined in equation (2.4–53). The factor *'k_f'* is defined as:

$$k_f = (\sum_{s=1}^{3} \frac{1}{k_s + i\omega c_s})^{-1} \tag{2.4–67}$$

Where *'k_s'* and *'c_s'* are far field stiffness and damping defined as three Kelvin-Voigt models in equations (2.4–54) and (2.4–55), respectively. The near field stiffness is defined as:

$$k_n = \frac{k(0) k_f(0)}{k_f(0) - k(0)} \tag{2.4–68}$$

$k_f(0)$ is the static far field stiffness and is given as:

$$k_f(0) = [\frac{1}{k_{\max}(0)} - \frac{3-4\nu}{8\pi\mu(1-\nu)} \ln \frac{r_1}{r_0}]^{-1} \tag{2.4–69}$$

Where *'k_{max}'* is the stiffness in the linear elastic range and is determined by a conventional cyclic *p-y* curve. The significance of the proposed model is that it can rationally reproduce the coupling between the nonlinear soil behaviour and dynamic conditions.

El Naggar and Novak (1994; 1995) adopted a similar method to Nogami et al. (1992) to include the effect of nonlinearities in the analysis. They introduced an inner field which was defined by a spring. The spring stiffness was derived by Novak and Sheta (1980) as:

$$k_{nl}(0) = \frac{8G_m(1-\nu)(3-4\nu)[(r_0/r_1)^2 + 1]}{(r_0/r_1)^2 + (3-4\nu)^2[(r_0/r_1)^2 + 1]\ln(r_1/r_0) - 1} \tag{2.4–70}$$

'r_0' and *'r_1'* are the inner and outer radii of the inner field, respectively. *'G_m'* is the modified shear modulus calculated according to the strain level, assuming that Poisson's ratio is constant, as:

$$G_m = G_{\max}(1-\eta) \tag{2.4–71}$$

G_{max} is the initial shear modulus of the soil layer and η is the mobilization ratio defined as:

$$\eta = p / p_u \tag{2.4–72}$$

Where *'p'* is the lateral soil resistance on the pile and *'p_u'* is its ultimate value given by API-RP-2A(WSD) (API-RP-2A 2007) (see section 2.3.4).

The far field model is considered as a single Kelvin-Voigt model using the solution given by Novak et al. (1978). They also included the effect of discontinuity between the pile and the soil in the form of slippage and separation in their model.

It is interesting that El-Naggar and Novak (1994) and Nogami et al. (1992) used the same reference for their far field model, yet they came out with two different results. The Nogami et al. (1992) model, being earlier to that of El-Naggar and Novak (1994), seems to be more rigorous. The latter did not consider a consistency mass between the far field and the inner field, therefore their model neglects the transmission of inertia forces from the pile towards the infinity. They also expanded their model to cover groups of piles. El-Naggar and Novak (1994) validated their model by back analysis of field tests as well as comparison with a more in-depth method (Nogami 1980). They reported that their results complied with field test data and more rigorous methods.

2.5 Axially loaded piles – dynamic

A pile under the action of a vibrating axial load is considered in this section. The problem was approached by Novak (1974) using the plane strain model (Baranov 1967; Novak and Beredugo 1972). The vertical (distributed) soil reaction on the pile at depth 'z' is written as:

$$\mu(S_{w1} + iS_{w2})w(z,t) \tag{2.5–1}$$

Where

$$\begin{cases} S_{w1} = 2a_0 \dfrac{J_1(a_0)J_0(a_0)+Y_1(a_0)Y_0(a_0)}{J_1^2(a_0)+Y_1^2(a_0)} \\ S_{w1} = \dfrac{4}{J_1^2(a_0)+Y_1^2(a_0)} \end{cases} \tag{2.5–2}$$

With the soil reactions defined by equation (2.5–1), the differential equation for damped axial vibration of the pile becomes:

$$m_p \frac{\partial^2}{\partial t^2} w(z,t) + c_p \frac{\partial}{\partial t} w(z,t) - E_p A_p \frac{\partial^2}{\partial z^2} w(z,t) + \mu(S_{w1} + iS_{w2}) w(z,t) = 0 \tag{2.5–3}$$

Assuming harmonic vibration in steady-state conditions (i.e. $w(z,t) = w(z)e^{i\omega t}$), the equation (2.5–3) reduces to an ordinary differential equation:

$$[-m_p\omega^2 + ic_p\omega + \mu(S_{w1} + iS_{w2})]w(z) - E_p A_p \frac{\partial^2}{\partial z^2} w(z) = 0 \tag{2.5–4}$$

A solution to equation (2.5–4) is easy to obtain. Novak (1974) compared his solution with the rigorous solution and concluded that there was good agreement. However, the agreement was only good for very high frequencies. It is now known that the plane strain model only gives reasonable results for high frequencies. The error is considerable for low frequencies.

Nogami and Novak (1976) tried to improve upon the plane strain model by providing a new solution for a vertically vibrating pile. They considered a vertical end-bearing pile under an axially vibrating load in a homogeneous viscoelastic soil layer overlaying rigid bedrock. Neglecting horizontal displacement, they wrote the equation for the vertical motion *w(r,z,t)* of the soil as:

$$(\lambda'+2\mu') \frac{\partial^2}{\partial z^2} w(r,z,t) + \mu' \left(\frac{1}{r}\frac{\partial}{\partial r} + \frac{\partial^2}{\partial r^2}\right) w(r,z,t) = \rho \frac{\partial^2}{\partial t^2} w(r,z,t) \tag{2.5–5}$$

Where λ' and μ' hold for complex valued Lamé's constants. It should be noted that equation (2.5–5) is the third of the elastodynamic equations, pertaining to the equilibrium in vertical directions. Nogami and Novak did not explain why they ignored the other two equations. For instance, the first elastodynamic equation leads to the following condition:

$$\left(\frac{\lambda'+2\mu'}{\mu'} - 1\right) \frac{\partial^2}{\partial r \partial z} w(r,z,t) = 0 \tag{2.5–6}$$

This equation indicates that the vertical deformation in the soil should be invariable with either depth or distance from the pile or both. This, of course, is an unphysical conclusion which results from ignoring horizontal displacements. Ignoring equation (2.5–6), on the other hand, leads to a solution that does not satisfy the equilibrium in a radial direction.

Nogami and Novak (1976) continued their solution by employing the method of separation of variables and concluded the following solution for soil deformations:

$$w(r,z,t) = e^{i\omega t}\sum_{n=1}^{\infty} A_n K_0(q_n r)\sin(h_n z) \qquad (2.5\text{–}7)$$

Where *'K_0'* denotes the modified Bessel function of the second kind of order zero and:

$$\begin{cases} \eta = \dfrac{V_p}{V_s} = \sqrt{\dfrac{\lambda+2\mu}{\mu}} = \sqrt{\dfrac{2(1-\nu)}{1-2\nu}} \\ h_n = (2n-1)\dfrac{\pi}{2H}, \quad n = 1,2,3...\infty \\ q_n^2 = \dfrac{\{\eta^2 + i[D_v(\eta^2-2)+2D_s]\}h_n^2 - (\omega/V_s)^2}{1+iD_s} \end{cases} \qquad (2.5\text{–}8)$$

The factors *'D_v'* and *'D_s'* are defined in section 2.4.3 and *'H'* is the thickness of the soil layer. It should be noted that the origin of the factor 'z' is located at the bedrock, therefore the ground surface is at *'$z=H$'* and the value of *'$w(r,z)$'* is at its maximum at the ground surface.

At resonance, the amplitude of the undamped vibrations in the soil should grow indefinitely. It calls for '$q_n = 0$' for *'$D_v=D_s=0$'* which results in undamped natural frequencies of the soil layer:

$$\omega_n = \sqrt{\frac{2(1-\nu)}{1-2\nu}}\,\frac{V_s}{2H}(2n-1)\pi, \quad n = 1,2,3...\infty \qquad (2.5\text{–}9)$$

This result is not in agreement with the first free vibration frequency of a homogeneous soil layer as reported by Dobry et al. (1976):

$$\omega_1 = \frac{V_s}{2H}\pi \qquad (2.5\text{–}10)$$

Any difference between the resonance frequencies of a vibrating pile and a vibrating soil layer should only be due to the presence of the pile. However, equation (2.5–9) does not have any terms including any properties of the pile. Therefore this difference is not justifiable and may be considered as a sign of error in the theory.

The soil vertical reaction at the pile skin is calculated as:

$$p(z,t) = -2\pi r \mu_0 (1 + iD_s) e^{i\omega t} \sum_{n=1}^{\infty} A_n q_n K_1(q_n r_0) \sin(h_n z) \qquad (2.5\text{–}11)$$

Nogami and Novak considered the effect of concentrated load *'P'* as a distributed load on the pile skin which is expressed in Fourier series:

$$P(z,t) = \frac{2P}{H} e^{i\omega t} \sum_{n=1}^{\infty} (-1)^{n-1} \sin(h_n z) \qquad (2.5\text{–}12)$$

Equation (2.5–12) has its maximum value at the ground surface and zero value at the pile tip. This raises doubts about physical meaning of the force *'P(z,t)'* which is defined by this equation. Moreover, the infinite series in the equation (2.5–12) is not convergent. This mathematical deficiency and the incompatible free vibration frequency which is calculated for the soil layer raise doubts about the soundness of this solution. Concluding their solution, Nogami and Novak (1976) calculated the stresses in the pile and found zero stresses in the pile head.

The author of this thesis believes that Nogami and Novak's approach was erroneous. In section 4.2 we propose another method of analysis which is based on the Laplace transform and leads to physically meaningful expressions and fully satisfies the boundary conditions. However, equation (2.5–7) is still the core of this solution, therefore some degree of approximation is still included.

For another attempt to solve the problem of an axially vibrating pile we refer to Nogami and Konagai (1986) who provided the methodology for time domain dynamic analysis of an axially loaded pile. They used three Kelvin-Voigt models to simulate a plane strain soil. Surprisingly, the stiffness and damping values of the three Kelvin-Voigt models are exactly the same as they used two years later (Nogami and Konagai 1988) for the time domain analysis of laterally loaded piles (section 2.4.3) and the extension towards the inclusion of nonlinearities (Nogami, Konagai and Chen 1992).

2.6 Numerical methods

The availability and popularity of high speed computers to practicing engineers and researchers has led to the development of different numerical methods in pile-soil-structure interaction. The present text is mainly involved with closed-form solutions for the elastic interaction between soil and pile, however numerical methods are used as a basis for the assessment of the developed solutions. A thorough study on the lateral stiffness of a statically loaded pile using the FE method is conducted in chapter 3of this thesis. Therefore the numerical methods appearing in the literature are briefly referenced in this section.

Finite element analysis is one of the most widely used numerical methods due to the availability of developed codes and software that can effectively model the soil-pile system. Kuhelmeyer (1979) was one of the first researchers to analyse a laterally loaded pile using the finite element method. He applied viscous damping in the boundaries to account for the radiation of waves in semi-infinite soil media.

Pak and Jenings (1987) formulated the interaction between a one-dimensional pile and three-dimensional elastic soil as a Fredholm integral equation of the second kind. The integral equation was then solved via an appropriate numerical method (Pak 1985) involving a series of approximate integral operators defined over a set of nodal points along the pile.

The above references to numerical methods for soil-pile interaction are by no means thorough. The development of these methods and the amount of research conducted in the past three decades is such a huge area that a complete reference demands a full chapter. This might be considered a digression from the topic, however, so such a review is not included in this thesis.

2.7 Application

Boominathan and Ayothiraman (2006) conducted full-scale dynamic lateral load tests on large number of piles in clay. Their report is well documented and is chosen here to demonstrate application of some of the topics discussed in this chapter. Table 2-8 is a summary of the soil properties in test sites which is extracted from the original paper. Due to the variability of the soil with depth, the best method of evaluating the stiffness of the piles is in situe testing. Methods described in the present chapter can be used for preliminary calculations. Boominathan and Ayothiraman (2006) have compared their measurements with the results of computer program PILAY (Novak and Aboul-Ella 1997). PILAY is a computer program developed by extending the Novak's solution (section 2.4.2) to layered soil.

Therefore another benefit of choosing Boominathan's and Ayothiraman's (2006) study is that the application of the theory described in section 2.4.2 is implicitly addressed.

Table 2-8- Summary soil properties of test sites (Boominathan and Ayothiraman 2006)

Site	Stratum	Thickness of layer: m	Description	N_{avg}	V_s: m/s	G_{max}: MN/m^2
Mathura I	I	3·0	Grey silty clay mixed with kankars	9	190·82	64·08
(MSQ unit site)	II	6·50	Yellowish silty clay mixed with kankars	12	210·24	84·86
	III	11·50	Silty sand in yellowish colour mixed with kankars	32	292·60	170·37
Mathura II	I	0·70	Filled up soil	–	–	–
(COGEN site)	II	6·80	Stiff brownish clayey silt	10·5	201·0	74·74
	III	3·00	Loose brownish grey sandy silt	3	131·77	32·12
	IV	3·50	Brownish grey sandy clayey silt	15·5	220·60	92·95
	V	1·0	Grey clayey silt with kankars	–	240·15	110·15
	VI	7·50	Dense to very dense grey brownish silty sand/ sandy silt with kankars	43	234·68	110·15
	VII	4·50	Very stiff brownish clayey silt with kankars and fine sand	28	250·44	124·19
Panipat	I	4·0	Stiff brown clayey silt, medium plastic (ML)	8	183·39	60·54
(IPP plant site)	II	0·5	Loose to medium dense light brown sandy silt with traces of gravel, low plasticity (CL)	8	183·39	60·54
	III	5·5	Loose to medium dense light brown silty fine sand (SM)	9	190·82	66·63
	IV	0·5	Loose light brown sandy silt with traces of gravel, low plasticity (CL)	6	166·45	50·70
	V	1·0	Loose to medium dense light brown silty fine sand (SM)	9	190·82	66·63
	VI	4·5	Medium dense light brown sandy silt, low plasticity (CL)	10·7	202·08	80·45
	VII	1·5	Dense light brown silty fine sand (SM)	33	295·65	174·82
	VIII	3·0	Very dense light brown silty sand (SM)	47·5	334·26	223·46
Haldia I	I	1·50	Filled up soil	–	–	–
(MSQ unit site)	II	0·80	Moderate stiff brownish grey silty clay	9	190·82	75·00
	III	2·80	Soft to medium stiff brownish grey silty clay	4	87·03	14·09
	IV	3·90	Soft bluish grey silty clay	1	102·89	19·69
	V	5·50	Medium dense bluish grey silty fine sand	17·7	241·03	106·31
	VI	5·50	Moderately stiff light grey silty clay	5·5	186·85	56·21
	VII	3·30	Moderately stiff to stiff greyish brown silty clay	22	147·82	45·67
	VIII	6·15	Medium dense to dense/very dense brownish yellow fine sand	31·3	289·49	175·15
Haldia II	I	1·5	Firm to stiff brownish clay	8	183·39	62·50
(HCU site)	II	5·7	Very soft to soft silty clay	3	131·77	29·64
	III	4·7	Loose to medium dense sandy silty clay	12	210·25	77·23
	IV	6·3	Soft to moderate stiff clay	3	131·77	30·20
	V	3·7	Stiff to very stiff sandy silty clay	13	215·99	91·52
	VI	12·1	Medium dense to very dense silty sand	20	249·74	112·35
	VII	1·9	Very stiff to hard silty clay	34	298·64	168·42
Hazira	I	0·60	Filled up soil	–	–	–
(PTA-3 site)	II	2·00	Medium dense black silty sand	16	231·65	101·42
	III	6·90	Soft to medium stiff clayey silt	7	175·32	51·64
	IV	3·00	Medium dense black silty sand	16·5	234·06	104·09
	V	4·00	Dense dark brown silty sand	52	344·62	237·53
	VI	1·50	Hard black clayey sand with silt and kankar	76·5	392·49	323·50
	VII	2·00	Very dense black silty sand	89	413·03	358·25

ML, silt with low plasticity; CL, clay with low plasticity; SM, silty sand.

The first step in back analysing the tests is to linearize the soil shear modulus. This is done via excel spreadsheet curve fitting techniques. Soil shear modulus is drawn vs. depth for each pile and linear trend lines are fit to each set of data. The results are depicted in Figure 2-15. It should be noted that the lines fitted to the data are the best fits and do not have physical meaning. The values of Poisson's ratio of the soil layers are not reported. A typical value of 0.3 is chosen for Poisson's ratio.

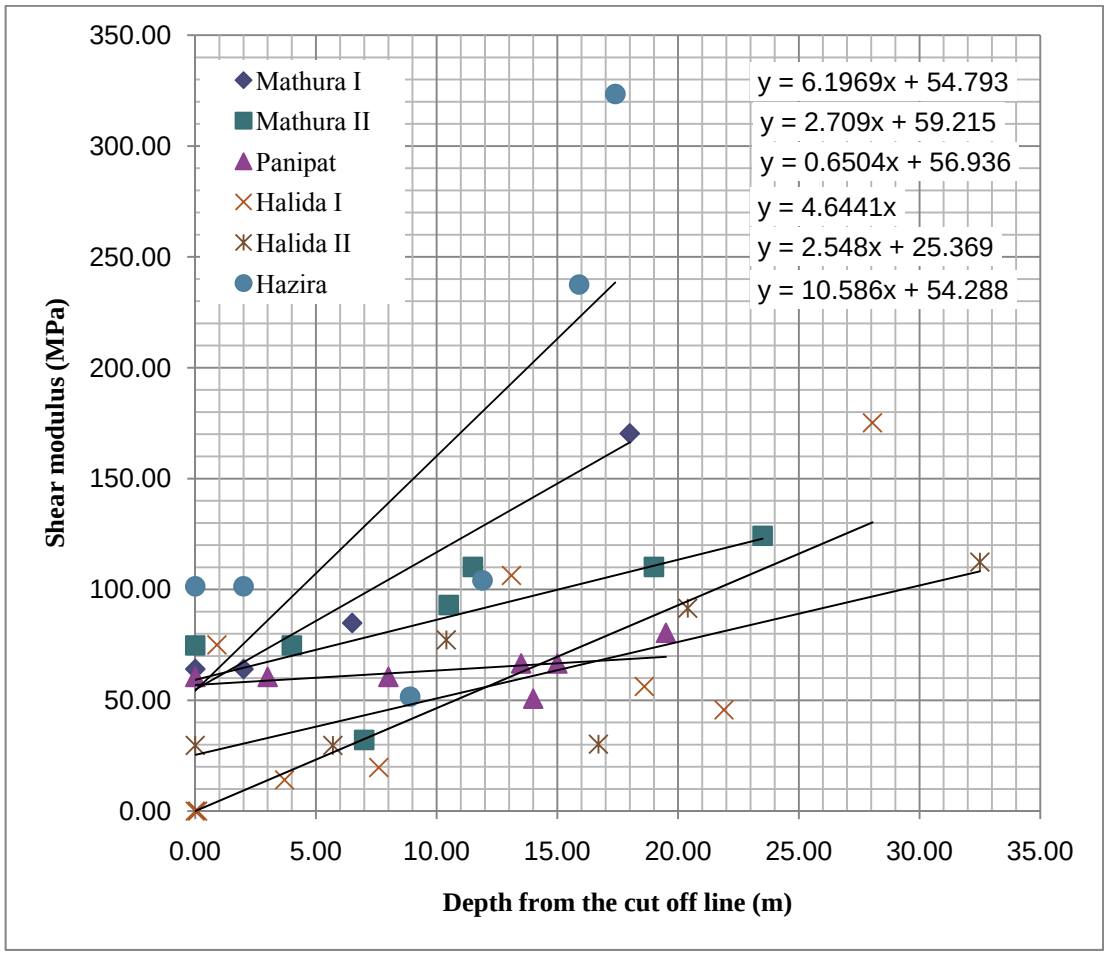

Figure 2-15 Linearization of the soil shear modulus with depth

The elastic modulus of concrete piles depends on the material grade of concrete. The piles were made from concrete with different grades given in the original paper. Concrete elastic modulus is calculated via a formula given in ACI 318 (2011) for ordinary weight concrete.

$$E_p = 4700\sqrt{f'_c} \qquad (2.7\text{–}1)$$

In the above formula, *f'c* is concrete nominal compressive strength in MPa. The modulus of elasticity E_p is also derived in MPa when the equation (2.5–12) is used.

The calculations are performed using Mathcad (Maxfield 2009) spreadsheet. There are many benefits using a Mathcad spreadsheet over excel, some of which are listed bellow:

- The formulas are clearly seen and checked in Mathcad
- The units are assigned and viewed so the potential for mistakes is minimized
- It is very easy to solve algebraic equation using built in functions (e.g. root function)
- It is easy to perform matrix operations and calculations in compact algebraic form

In the present section, it is aimed to solve equation (2.3–13). This task is performed using Mathcad root function.

Pile diameter

$$D := \begin{pmatrix} 500 \\ 450 \\ 500 \\ 500 \\ 400 \\ 451 \\ 500 \\ 451 \end{pmatrix} mm$$

Mathura I
Mathura II
Panipat
Halida I
Halida II-1
Halida II-2
Halida II-3
Hazira

Assumed value for soil Poisson's ratio

$$\nu := 0.3$$

Effective value of rate of gain of soil shear modulus (ν=0.3)

$$m_s := \left(1 + \frac{3}{4}\nu\right) \cdot \begin{pmatrix} 6.20 \\ 2.71 \\ 0.65 \\ 4.64 \\ 2.55 \\ 2.55 \\ 2.55 \\ 10.59 \end{pmatrix} \frac{MPa}{m}$$

Effective value of rate of gain of soil shear modulus (ν=0.3)

$$G_0 := \left(1 + \frac{3}{4}\nu\right) \cdot \begin{pmatrix} 54.79 \\ 59.20 \\ 56.94 \\ 0.00 \\ 25.37 \\ 25.37 \\ 25.37 \\ 54.29 \end{pmatrix} MPa$$

Pile material modulus of elasticity

$$E_p := \begin{pmatrix} 23500 \\ 23500 \\ 23500 \\ 23500 \\ 25743 \\ 25743 \\ 25743 \\ 27806 \end{pmatrix} MPa$$

Ratio of critical length to diameter (L_c/D)

$$xx_i := \text{root}\left(\frac{m_{s_i} \cdot D_i}{2} \cdot x^{4.5} + G_{0_i} \cdot x^{3.5} - E_{p_i}, x\right) \qquad xx = \begin{pmatrix} 5.13 \\ 5.139 \\ 5.252 \\ 8.658 \\ 6.582 \\ 6.555 \\ 6.53 \\ 5.285 \end{pmatrix}$$

Pile critical length

$$L_{c_i} := xx_i \cdot D_i \qquad L_c = \begin{pmatrix} 2.565 \\ 2.313 \\ 2.626 \\ 4.329 \\ 2.633 \\ 2.956 \\ 3.265 \\ 2.383 \end{pmatrix} \text{m}$$

Characteristic shear modulus

$$G_{c_i} := G_{0_i} + m_{s_i} \cdot \frac{L_{c_i}}{2} \qquad G_c = \begin{pmatrix} 77 \\ 76 \\ 71 \\ 12 \\ 35 \\ 36 \\ 36 \\ 82 \end{pmatrix} \cdot \text{MPa}$$

Homogeneity factor

$$\rho_{c_i} := \frac{G_{0_i} + m_{s_i} \cdot \frac{L_{c_i}}{4}}{G_{c_i}} \qquad \rho_c = \begin{pmatrix} 0.937 \\ 0.975 \\ 0.993 \\ 0.5 \\ 0.942 \\ 0.935 \\ 0.93 \\ 0.906 \end{pmatrix}$$

$$K_{h_i} := \rho_{c_i} \cdot G_{c_i} \cdot \left(\frac{G_{c_i}}{E_{p_i}} \right)^{\frac{1}{7}} \cdot L_{c_i} \cdot \left(\frac{6.47 \cdot \sqrt{\rho_{c_i}} - 2.67}{3.46 \cdot \sqrt{\rho_{c_i}} - 1.44} \right)$$

$$K_h = \begin{pmatrix} 1.534 \times 10^5 \\ 1.429 \times 10^5 \\ 1.515 \times 10^5 \\ 1.714 \times 10^4 \\ 6.399 \times 10^4 \\ 7.255 \times 10^4 \\ 8.086 \times 10^4 \\ 1.449 \times 10^5 \end{pmatrix} \cdot \frac{kN}{m}$$

Table 2-9 summarizes calculated values for stiffness of the pile and compares with the test values. It is seen that for piles in stiff clay (site Mathura I); the calculated values from the formulas of section 2.3.2 and computer program PILAY have close agreement with the test result. For other sites where loose sandy silt or soft clays exist, the agreement between he test results and the calculated values are not good. The reason is that for stiff clays, the soil is more likely to behave linearly elastic under small deformations, while for soft soils the plastic deformation governs. There are other factors that affect pile behaviour in practice that cannot be addressed via an elastic approach. The aim of the present calculations is to show the applicability of the method for preliminary studies. Therefore no further argument is made on the test results and other effective factors, like pile installation method, etc.

Table 2-9 Summary back analyzed stiffness values for full scale test piles

Site	Dia (mm)	(1)	Gr.[2] (MPa)	L_p[3] (m)	G_0 (MPa)	m	L_c (m)	Kh (kN/m × 10^4)		
								Calc.[4]	PILAY[5]	Test[6]
Mathura I	500	C	25	11	54.79	6.20	2.57	15.34	14.50	12.80-13.70
Mathura II	450	C	25	21.5	59.20	2.71	2.31	14.29	23[7]	6.00-16.70[7]
Panipat	500	C	25	19.5	56.94	0.65	2.63	15.15	31.5	26.5-29.4
Haldia I	500	C	25	28.58	0.00	4.64	4.33	1.71	4.2	1.47-2.45
Halida II	400	C	30	30	25.37	2.55	2.63	6.4	16.2	0.50-1.23
Halida II	451[8]	S	30	30	25.37	2.55	2.96	7.26	17.1	3.90-4.90
Halida II	500	C	30	30	25.37	2.55	3.27	8.09	18.4	2.90-5.00
Hazira	451[8]	S	35	17	54.29	10.59	2.38	14.49	8.9	0.69-1.77

(1) Shape: C= Circular, S= Square 400 × 400
(2) Concrete nominal compressive strength in MPa
(3) Pile length
(4) Calculated stiffness value based on section 2.3.2 procedure
(5) Resulted stiffness from the computer program PILAY (Novak and Aboul-Ella 1997)
(6) Test results as reported by Boominathan and Ayothiraman (2006)
(7) The reported values are suspicious for being erroneous (10^{-1} times of the true value)
(8) Equivalent diameter is calculated for a 400×400 square section

2.8 Summary chapter two

Early approaches to the laterally loaded pile problem was based on a beam on Winkler springs model. The stiffness of Winkler springs were determined by number of authors who has approached the problem via elasticity theory (Biot 1922; Vesic 1961).

Applicability of elastic Winkler spring model to practical pile design has clear limitations. Soil plasticity, nonlinear stress strain curve and variable soil properties with depth are main reasons why a beam on elastic springs may have restricted application in practical pile design.

Major improvement on pile design under lateral load is made when (p-y) method is introduced (Reese and Matlock 1956; Matlock and Reese 1960; Matlock 1970) and accepted by many codes and recommended practices (e.g. API-RP-2A 2007). In this method, the soil is modelled as lateral springs. The stiffness of the springs which is empirically determined for different soil types is variable with pile lateral deflection and depth and is expressed in terms of soil ultimate resistance factors rather than its elastic properties.

Loading on piles are rarely static. Wind, earthquake and sea waves (for offshore structures) are examples of dynamic lateral loads that may be imposed on piles. The vibration energy is radiated away from the pile into the soil in form of shear and pressure waves (SH-P). Since the soil is a semi-infinite body, this energy does not return to the system in each cycle and therefore it has a damping effect known as geometric damping.

Early approaches to dynamic pile problem was based on an infinitely long Euler-Bernouli beam embedded in semi infinite soil (Baranov 1967; Novak 1974). In this model, the soil is considered as infinite number of very thin horizontal layers in plane strain conditions. Soil reaction on pile is derived to be linearly dependent to deformation; therefore Winkler hypothesis is deemed valid for plane strain model. This model satisfactorily predicts pile response to high frequency vibrations but results in very small stiffness for low or zero frequencies. The latter is considered as the main shortcoming of the plane strain model.

Further improvement on dynamic pile problem is made by introducing a simplified 3D continuum solution (Nogami and Novak 1977; Novak and Nogami 1977). In this model the soil is considered as a semi infinite homogeneous linearly elastic material. Vertical deformations in the soil caused by pile lateral vibrations are ignored and only horizontal components of soil deformations are included. Therefore this model can be referred to as ‘planar deformation’. In this solution, the modal reaction of soil on the pile is proportional to the pile modal deformation. Therefore Winkler hypothesis is valid for each individual mode

of vibration. This solution is based on an end bearing pile, i.e. the pile tip is clamped into rigid bedrock. Since the presence of rigid bedrock plays major role in the solution process, the solution cannot be extended to infinitely long piles. The solution is in terms of real valued modified Bessel functions. Therefore (ignoring soil material damping); the solution does not include any geometrical damping. This can be considered as a major shortcoming of the solution.

Development of computers and their availability for research work changed the nature of approach to the problem of laterally vibrating piles in early 70's. Many researches approached formulations which required numerical evaluation where no closed form solutions were available. Early employment of Mindlin's solution (1936) in formulation of soil-pile interaction problem required application of finite difference method (Poulos 1971a; Poulos 1971b; Poulos 1973). Finite element method which has been used since late 70's and early 80's by number of researches (Kuhelmeyer 1979; Randolph 1981) to address the problem of laterally loaded piles became more and more popular. Some of researchers formulated the soil-pile interaction in layered soil and for group of piles in terms of integral equations which needed numerical evaluation (Kaynia and Kausel 1980; Kaynia 1982; Kaynia and Kausel 1991). Development of integral equation formulation combined with advanced numerical algorithms lead to development of boundary element method (e.g. Pak 1985; Pak and Jennings 1987; Rajapakse and Wang 1990; Pak and Guzina 1999). Combined finite element and boundary element method is probably the most general way of analysis of piles and pile groups (Xu and Poulos 2000).

Some researches proposed to combine effects of nonlinearity, plasticity and soil-pile separation and slippage with the radiation damping properties of the semi infinite soil in a dynamic analysis model (Nogami, Konagai and Chen 1992; El Naggar and Novak 1994).

CHAPTER THREE

3 FEA STUDY

3.1 Introduction

The development of fast computers and sophisticated software in the past few decades has enabled researchers and engineers to model virtually any type of soil-pile-structure interaction problem with great accuracy. The effects of nonlinearities and changes in soil properties can be properly modelled using the finite elements method. However, computer programs capable of performing these kinds of analyses are still expensive and obtaining accurate results is still time-consuming.

The beam on Winkler springs support is one of the earliest models for lateral pile analysis and is still attractive for its simplicity. Most of the commercial structural analysis programs are capable of modelling springs, either linear or nonlinear, at specified nodes, and some are also able to model mass and dashpots in a dynamic analysis. The problem with the Winkler spring model is that there is no unanimously accepted relationship for the spring stiffness, with different expressions being proposed in the literature for Winkler spring stiffness.

Biot (1922) solved the problem of an infinite beam on the surface of a half-space elastic media and made some proposition for spring stiffness (see Table 2-2).

Vesic (1961) proposed a relationship for the spring stiffness of a beam on an elastic foundation (see section 2.2.5). Bowles (1997) recommended using twice the value of Vesic's relationship due to the pile being embedded in the soil:

$$k_s = 2\times\frac{0.65E_s}{1-\nu^2}\left(\frac{E_s D^4}{E_p I_p}\right)^{\frac{1}{12}} = \mu\frac{2.754}{1-\nu}\left(\frac{(1+\nu)\mu D^4}{E_p I_p}\right)^{\frac{1}{12}} \qquad (3.1\text{–}1)$$

Bowles (1997) also cited a number of different formulas proposed in the literature based on empirical methods which range from 1.0 to 1.8 times E_s. Alternatively, Bowles presents methodologies for using bearing capacity formulas to estimate lateral spring stiffness.

In some of his contributions, Gazetas (Gazetas and Dobry 1984; Markis and Gazetas 1992,) considers a value of $1.2E_s$ for the spring stiffness.

Randolph (1981) conducted a finite element study on laterally loaded piles, using triangular-linear strain elements to model the soil. Randolph proposed expressions for deflection and

rotation at the top of a pile under the action of a lateral force and a bending moment. Using Randolph's results, free-head pile stiffness *'K_h'* can be derived as follows, after some algebraic manipulation:

$$(K_h)_{Randolph} = 2D\mu\sqrt[7]{(1+\frac{3}{4}\nu)^6}\sqrt[7]{\frac{E_p}{\mu}\frac{I_p}{\pi D^4/64}} \qquad (3.1\text{–}2)$$

Substituting the above value into the expression of *'K_h'* for infinitely long piles (Table 2-1) results in an expression for spring stiffness:

$$(k_s)_{Randolph} = 2.731\,\mu(1+\frac{3}{4}\nu)^{\frac{8}{7}}(\frac{\mu D^4}{E_p I_p})^{\frac{1}{7}} \qquad (3.1\text{–}3)$$

The values of the coefficient and power of the above equation are close to those given by Biot (1922) (Table 2-2).

Novak and El Sharnouby (1983) summarized the results of a dynamic continuum mechanics solution for pile dynamic stiffness into tabulated values. Their formulas are presented here with slight changes in notation:

$$K_{HH} = (\pi f_u/8)DE_p, \quad K_{MM} = (\pi f_\psi/32)D^3E_p, \quad K_{HM} = (\pi f_{c1}/16)D^2E_p \qquad (3.1\text{–}4)$$

Where K_{HH}, K_{MM} and K_{HM} are translational, rotational and coupled stiffness, respectively. f_u, f_ψ and f_{c1} are dimensionless tabulated parameters. Free-head pile stiffness can be derived from the following relationship (Pender, Carter and Pranjoto 2007):

$$K_h = \frac{K_{HH}K_{MM}-K_{HM}^2}{K_{MM}-eK_{HM}} = \frac{\pi}{8}(f_u - \frac{f_{c1}^2}{f_\psi})DE_p \qquad (3.1\text{–}5)$$

Where '$e=M/F_0$' is the ratio of bending moment to shear force on the pile top. One may calculate the spring stiffness from Novak and El Sharnouby's (1983) values as:

$$(k_s)_{Novak} \cong 0.114\mu(\frac{E_p}{G})(f_u - \frac{f_{c1}^2}{f_\psi})^{4/3}(\frac{D^4}{I_p})^{1/3} \qquad (3.1\text{–}6)$$

Poulos and Davis (1980) provided general continuum solutions for floating piles. Their solution for a pile under the action of a horizontal force (zero bending moment) at its top can be written as:

$$(K_h)_{Poulos} = \frac{E_s L}{I_{\rho H}} = 2(1+\nu)\mu \frac{L}{I_{\rho H}} \qquad (3.1\text{–}7)$$

'L' in the above equation holds for pile length. Values for '$I_{\rho H}$' are given in graphs for different values of '*L/D*'. Calculated spring stiffness from Poulos and Davis's work is:

$$(k_s)_{Poulos} \cong 4\mu \left(\frac{1+\nu}{I_{\rho H}} \frac{L}{D}\right)^{\frac{4}{3}} \left(\frac{\mu D^4}{E_p I_p}\right)^{\frac{1}{3}} \qquad (3.1\text{–}8)$$

This equation is similar to Biot's (1922) 2D formula (Table 2-2), as they both involve the power of (1/3) in their expressions. Although Poulos and Davis (1980) implemented the general Mindlin (1936) solution, their numerical integration considers the pile as a long (2D) strip of width *'D'* and length *'H'* (Poulos and Davis 1980, Sec. 8.3.1.1). This is indeed a 2D model and for this reason their solution is similar to Biot's (1922) 2D solution.

One may conclude the following from the above review on the stiffness of Winkler springs for laterally loaded piles:

- Winkler spring stiffness is proportional to the shear modulus of the soil;
- Winkler spring stiffness increases with increasing Poisson's ratio;
- A dimensionless factor involving pile flexibility $E_p I_p$ and a measure of soil flexibility appears in the stiffness expression.

In order to investigate the stiffness of Winkler springs for a laterally loaded pile, a finite element study is conducted as part of the present thesis. The results of this study will be used to verify the results of the continuum mechanics study which is the core of the present research.

3.2 Finite element study

A 3D finite element study is conducted in order to obtain the stiffness of Winkler springs on a laterally loaded pile. The soil is modeled with elastic-homogenous, three-dimensional cubic elements. The soil layer is 10m thick and extends 29.5m from each side of the pile. Examinations have shown that changing the far end restraint on the modeled soil does not significantly affect the calculated head stiffness of a pile. Therefore the extension of the modeled soil is deemed to satisfactorily represent soil stiffness properties.

3.2.1 Method statement

A horizontal load is applied in the y-direction; therefore the lateral deflection of the pile takes place in the y-z plane. Only one quarter of the space is modeled due to the symmetry with respect to the 'y-z' plane. It is evident that each quarter-space bounded by *'xz'* and *'yz'* planes, includes exactly the same number of brick elements and the same quarter-cylindrical cavity shape. This similarity is only from the stiffness point of view when attributed to pile elements and is not valid for stresses and strains in soil elements. To successfully replace the full-space model with a quarter-space model, appropriate restraints on artificial boundaries must be formed to correctly simulate the effect of the eliminated parts from the model. Artificial boundary surfaces formed by the *'xz'* and *'yz'* planes should be restrained for deformation in *'x'* direction. Having done this, the quarter-space model possesses one quarter the stiffness of the full model. In addition, a full model FE analysis is made and the force-deflection ratio at the top of the pile proved to be one quarter that of the quarter-space model.

The bottom surface of the modeled soil is restricted in movement to resemble the rigid bedrock. The presence of a pile shaft is modeled as a quarter-cylindrical cavity. By changing the diameter of this cavity, the effect of the pile shaft diameter on free-head pile stiffness is investigated. A 3m × 3m transition region is introduced to transfer from the very fine mesh on the pile shaft surface to a uniform mesh of 0.5m × 0.5m × 0.5m which extends to the rest of the model. A total of 71,060 three-dimensional elements are used in modeling the soil. The pile is considered to be a solid (non-tubular) circular cross-section with a typical Young's modulus of elasticity of 25,000 MPa. Classic Euler-Bernouli elements are used to model the pile. Since only a quarter of the soil is modeled, cross-sectional properties of the pile are multiplied by a factor of 0.25.

Full connectivity between the soil and the surface of the pile shaft is provided via a number of rigid, one-dimensional elements which connect the pile's centerline nodal points to the relevant points of the soil elements in both horizontal directions.

Even in a perfectly elastic model, some degree of vertical slippage between the soil and pile surface would be inevitable. In reality, this slippage might be affected by factors like pile surface conditions, soil type, large deformations, etc. Although modern finite element software is equipped with features like gap elements, links, etc., by which such effects can be included in the model, numerical values for the essential characteristics of such features are only justifiable for specific types of soil and pile surface conditions. It would be impractical and unrealistic to perform large numbers of FE analyses with a wide range of possible soil

mechanical characteristics with the abovementioned features included. For the aim of this study, a homogeneous elastic assumption is necessary for the material with simple connectivity between the pile and soil, enabling a large number of FE analyses. For this reason, a qualitative evaluation of the upper and lower limits of soil-pile connectivity conditions is necessary.

Full slippage between the pile and soil represents a lower limit to the present problem, as it leads to underestimation of pile lateral stiffness. A finite element model with such connectivity shows zero vertical deformation throughout all elemental nodal points. A fully connected model, on the other hand, results in an overestimation of pile lateral stiffness. The reality will be somewhere in between these two extremes.

The pile tip is restrained against movement and rotation in order to resemble an end-bearing pile with full penetration into bedrock. A horizontal force in 'y' direction is applied to the pile top and static analyses are performed. Figure 3-1 shows the configuration of the finite element model used for this study.

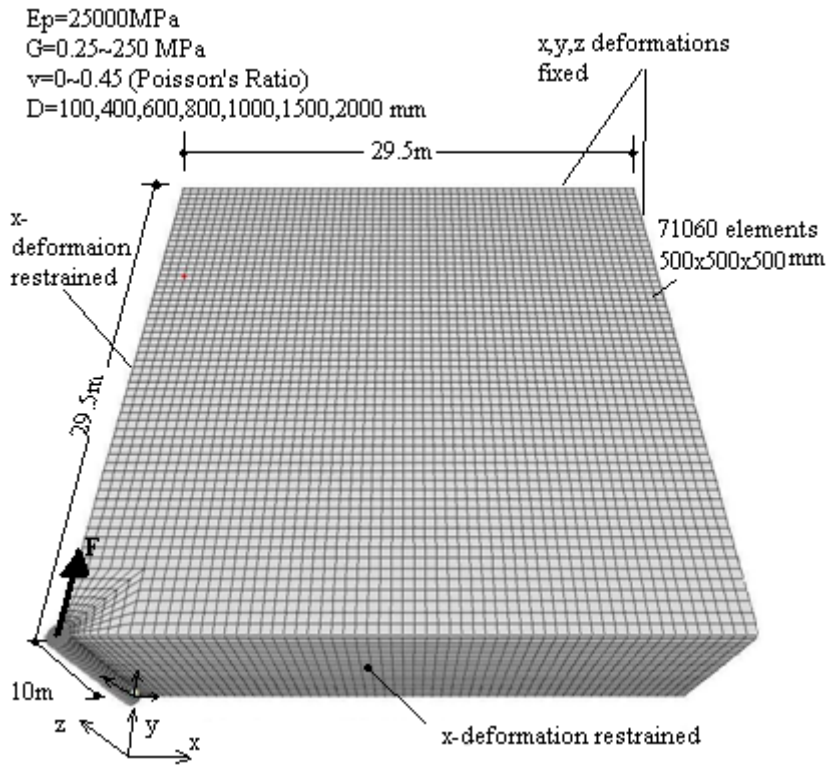

Figure 3-1 Quarter space FE model

A number of FE models with diameters of 400mm, 600mm, 800mm and 1000mm are created and analyzed. The shaft's second moment of inertia $\pi r_0^4/4$ is taken as equal to the pile's second moment of inertia I_p for simplicity. By changing the soil shear modulus and Poisson's ratio, variations of free-head pile stiffness are examined.

3.2.2 Presentation of the results

Table 3-1 summarizes the FE analyses of a pile with $r_0=0.5m$ radius. The Poisson's ratio and modulus ratio are varied and pile lateral stiffness 'k_{xx}' calculated by dividing the applied lateral load into the head deflection. Note that in this section, the notation *'G'* is used to denote the soil shear modulus.

Table 3-1 Free-head pile stiffness-3D FE values for $r_0=0.5m$, $E_p=25GPa$

E_p/G	K_h (kN/mm)				
	$\nu = 0$	$\nu = 0.2$	$\nu = 0.4$	$\nu = 0.45$	$\nu = 0.48$
100	999.00	1104.67	1265.02	1330.67	1404.49
250	446.08	489.96	555.79	581.99	610.50
500	245.10	267.97	302.14	315.48	329.54
1000	135.85	147.93	165.91	172.84	179.92
2500	63.12	68.41	76.28	79.28	82.22
5000	35.75	38.60	42.87	44.49	46.05
10,000	20.65	22.18	24.48	25.36	26.19
20,000	12.48	13.29	14.51	14.97	15.41
50,000	7.29	7.63	8.14	8.33	8.52
100,000	5.50	5.67	5.93	6.03	6.13

Table **3-2** summarizes another set of 3D FEA results for pile stiffness in which pile radius and modulus ratio are varied while Poisson's ratio is kept at zero.

Table 3-2 Free-head pile stiffness (kN/mm)-3D FE values for $\nu = 0$, E_p=25GPa

E_p/G	*Pile diameter (mm)*					
	100	**400**	**600**	**800**	**1500**	**2000**
100	129.21	360.62	535.91	719.81	1407.95	1932.37
250	54.24	164.72	247.72	334.62	658.00	906.21
500	28.41	91.83	138.96	187.95	369.58	513.22
1000	15.04	51.48	78.12	105.63	208.40	297.31
2500	6.62	24.07	36.55	49.44	100.31	157.83
5000	3.61	13.57	20.63	27.97	60.84	109.06
10,000	2.00	7.68	11.70	15.92	40.14	84.17
20,000	1.11	4.36	6.67	9.20	29.50	71.59
50,000	0.52	2.08	3.22	4.75	22.49	63.99
100,000	0.29	1.19	1.91	3.16	20.83	61.45

The third set of analyses is performed on piles similar to those in Table 3-2 but with a constant second moment of inertia for the pile. The values in this table are used only to investigate the effect of pile diameter on the spring stiffness when other factors are invariable. The reference value for the second moment of inertia is that of a pile with a 1m diameter (i.e. I_{Ref}=0.049087m^4). Note that in Table 3-3 only the values for a pile diameter of 1000mm are physically meaningful and set for reference.

Table 3-3 Free-head pile stiffness (kN/mm) – Values for $\nu = 0$ and $I_p=I_{Ref}$

Ep/G	*Pile diameter (mm)*						
	100	**400**	**600**	**800**	**1000**	**1500**	**2000**
100	446.33	627.35	724.38	817.66	**999.00**	1142.53	1379.79
250	217.08	299.85	343.05	384.02	**446.08**	525.35	630.12
500	126.03	171.60	194.96	216.91	**245.10**	291.61	347.01
1000	73.37	98.36	110.92	122.59	**135.85**	161.76	190.59
2500	35.95	47.33	52.87	57.93	**63.12**	74.51	86.48
5000	21.13	27.39	30.39	33.10	**35.75**	41.79	47.96
10,000	12.85	16.22	17.83	19.27	**20.65**	23.84	27.03
20,000	8.40	10.17	11.01	11.77	**12.48**	14.15	15.80
50,000	5.60	6.34	6.69	7.00	**7.29**	7.98	8.66
100,000	4.65	5.02	5.20	5.36	**5.50**	5.85	6.20

The fourth set of analyses is performed on a pile with 1m diameter, but the horizontal restraints to the soil element are released. All the other sets of analyses were performed with full connectivity between the pile and the soil elements in all directions; therefore they represent an upper bond for soil stiffness. The new set of analyses, on the other hand, represents a lower bond for the pile stiffness because of the full slippage between the pile and the soil surface. Table 3-4 summarizes the stiffness values obtained for this set of analyses.

Table 3-4 Free-head pile stiffness for r_0=0.5m, $\nu = 0$ – full slippage

E_p/G	K_h (kN/mm)
100	754.86
250	352.80
500	199.81
1000	113.91
2500	54.75
5000	31.69
10,000	18.65
20,000	11.48
50,000	6.89
100,000	5.30

3.2.3 Spring stiffness

Spring stiffness values are obtained from the FE values for Free-head pile stiffness by equating them to the relevant formula from Table 2-1:

$$K_h = 2E_p I_p \beta^3 \frac{\sinh(2\beta L) + \sin(2\beta L)}{\cosh(2\beta L) + Cos(2\beta L) - 2} \qquad (3.2\text{–}1)$$

The above equation is obtained for a pile with limited length resting on lateral springs representing the soil. Simple spreadsheet calculations with Excel give the values for spring stiffness. Table 3-5 includes the calculated spring stiffness values pertaining to the stiffness values in Table 3-1. Similarly, Table 3-6 to Table 3-8 include spring stiffness values pertaining to the stiffness values in Table 3-2 to Table 3-4, respectively.

Table 3-5 Calculated values of k_s/G corresponding to pile stiffness values in Table 3-1

Ep/G	k_s/G				
	$\nu = 0$	$\nu = 0.2$	$\nu = 0.4$	$\nu = 0.45$	$\nu = 0.48$
100	5.92	6.77	8.11	8.68	9.33
250	5.05	5.73	6.78	7.20	7.68
500	4.55	5.12	6.01	6.37	6.75
1000	4.12	4.63	5.40	5.70	6.02
2500	3.66	4.08	4.72	4.98	5.23
5000	3.41	3.78	4.35	4.57	4.78
10,000	3.27	3.60	4.11	4.31	4.50
20,000	3.20	3.51	3.99	4.18	4.35
50,000	3.15	3.45	3.91	4.09	4.26
100,000	3.14	3.43	3.89	4.07	4.23

Table 3-6 Calculated values of k_s/G corresponding to pile stiffness values in

Table **3-2**

Ep/G	k_s/G, $\nu = 0$					
	D=100mm	**D=400mm**	**D=600mm**	**D=800mm**	**D=1500mm**	**D=2000mm**
100	8.35	5.17	5.10	5.15	5.45	5.63
250	6.56	4.54	4.56	4.64	4.92	5.06
500	5.54	4.17	4.22	4.30	4.51	4.72
1000	4.74	3.85	3.91	3.99	4.17	4.52
2500	3.97	3.50	3.55	3.60	3.91	4.40
5000	3.54	3.26	3.31	3.33	3.82	4.36
10,000	3.21	3.05	3.08	3.12	3.77	4.34
20,000	2.95	2.86	2.88	3.00	3.75	4.33
50,000	2.67	2.63	2.72	2.92	3.29	4.33
100,000	2.49	2.48	2.65	2.89	3.73	4.32

Table 3-7 Calculated values of k_s/G corresponding to pile stiffness values in Table 3-3

E_p/G	k_s/G, $\nu = 0$, $I_p=I_{Ref}$					
	D=100mm	D=400mm	D=600mm	D=800mm	D=1500mm	D=2000mm
100	2.02	3.19	3.86	4.53	7.08	9.11
250	1.93	2.98	3.56	4.14	6.28	8.01
500	1.86	2.82	3.35	3.86	5.73	7.23
1000	1.79	2.67	3.14	3.59	5.22	6.50
2500	1.72	2.48	2.88	3.26	4.58	5.60
5000	1.69	2.39	2.75	3.08	4.20	5.05
10,000	1.67	2.34	2.67	2.97	3.97	4.70
20,000	1.66	2.32	2.63	2.92	3.85	4.51
50,000	1.66	2.30	2.61	2.89	3.77	4.39
100,000	1.65	2.30	2.60	2.88	3.75	4.36

Table 3-8 Calculated values of k_s/G corresponding to pile stiffness values in Table 3-4

Ep/G	k_s/G, $\nu = 0$, Full slippage
100	4.08
250	3.70
500	3.46
1000	3.25
2500	3.02
5000	2.90
10,000	2.84
20,000	2.81
50,000	2.79
100,000	2.79

The following hypothetical formula is assumed for the spring stiffness:

$$k_s = G S_{G/Ep} S_\nu S_D S_I \qquad (3.2\text{–}2)$$

In the above equation, the stiffness of lateral soil springs is proportional to soil shear modulus 'G' and is modified by some scale factors. Each scale factor is related to one of the main parameters and is derived by curve fitting on the FE data.

The Poisson's ratio scale factor 'S_ν' can be derived by curve fitting on the data in Table 3-1. It is assumed that the value of S_ν is 1 for a Poisson's ratio of 0. Dividing the data in columns two to six of Table 3-5 with the values in the first column, then subtracting from 1, results in the value of '$S_\nu - 1$'. Table **3-9** lists the relevant calculations.

Table 3-9 Ratio of the values in Table **3-5** to its first column for $\nu = 0$

ν	$S_\nu - 1$				
	0	**0.2**	**0.4**	**0.45**	**0.48**
$\nu/(1-\nu)$	**0**	**0.25**	**0.667**	**0.818**	**0.923**
E_p/G=100	0	0.105	0.266	0.332	0.406
E_p/G=250	0	0.098	0.246	0.305	0.369
E_p/G=500	0	0.093	0.233	0.287	0.345
E_p/G=1000	0	0.089	0.221	0.272	0.324
E_p/G=2500	0	0.084	0.209	0.256	0.303
E_p/G=5000	0	0.080	0.199	0.245	0.288
E_p/G=10,000	0	0.074	0.186	0.228	0.268
E_p/G=20,000	0	0.064	0.162	0.199	0.234
E_p/G=50,000	0	0.046	0.116	0.143	0.168
E_p/G=100,000	0	0.031	0.078	0.096	0.113

Curves pertaining to the data in Table **3-9** are illustrated in Figure 3-2.

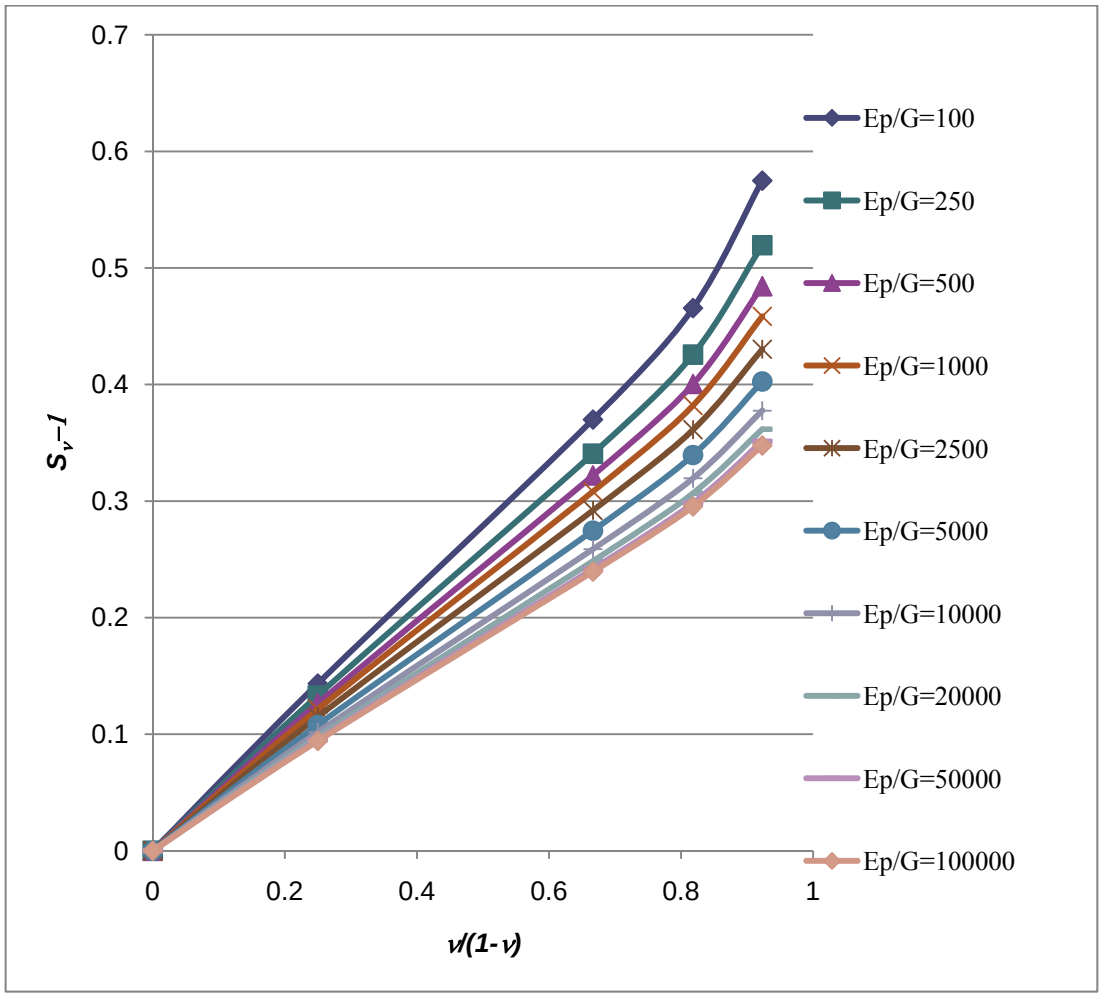

Figure 3-2 Curves for Poisson's ratio scaling factor (data in Table **3-9**)

The scaling factor 'S_v' is almost linear with the factor '$\nu/(1-\nu)$' but shows dependence on modulus ratio 'E_p/G'. In order to investigate this dependency, the factors in Table **3-9** are divided with the relevant value of $\nu/(1-\nu)$. For each row of the resulting values a multiplying factor 'm' is derived such that the resulting value is closest possible to the true value listed in Table **3-9**. Table 3-10 shows the difference between the values of $m\nu/(1-\nu)$ and the true values in Table **3-9**. Note that the factor 'm' is specified for each line in Table **3-9**, i.e. each multiplier 'm' corresponds to a unique value of modulus ratio 'E_p/G'. Minimization of the error is performed by using the inbuilt data analysis tool 'Solver' in an Excel work sheet. Curve fitting on the values of 'm' is shown in Figure 3-3.

Table 3-10 Difference between the value of $m\nu/(1-\nu)$ and values in Table **3-9**

m	$m\nu/(1-\nu)$				**Relative error**
	0.2	**0.4**	**0.45**	**0.48**	
0.578045	0.007323	0.041613	0.015835	-0.07199	0.72%
0.530384	-0.00493	0.037831	0.019549	-0.05761	0.52%
0.499752	-0.01206	0.034566	0.020995	-0.04754	0.40%
0.477065	-0.0178	0.032023	0.021794	-0.03939	0.34%
0.450716	-0.01944	0.028831	0.020865	-0.03299	0.27%
0.423178	-0.01966	0.027117	0.019858	-0.02971	0.24%
0.398205	-0.02122	0.025918	0.019604	-0.02651	0.22%
0.382214	-0.02252	0.025236	0.019567	-0.0244	0.21%
0.371702	-0.02321	0.024804	0.019495	-0.02316	0.21%
0.368096	-0.02341	0.024691	0.01945	-0.02278	0.21%

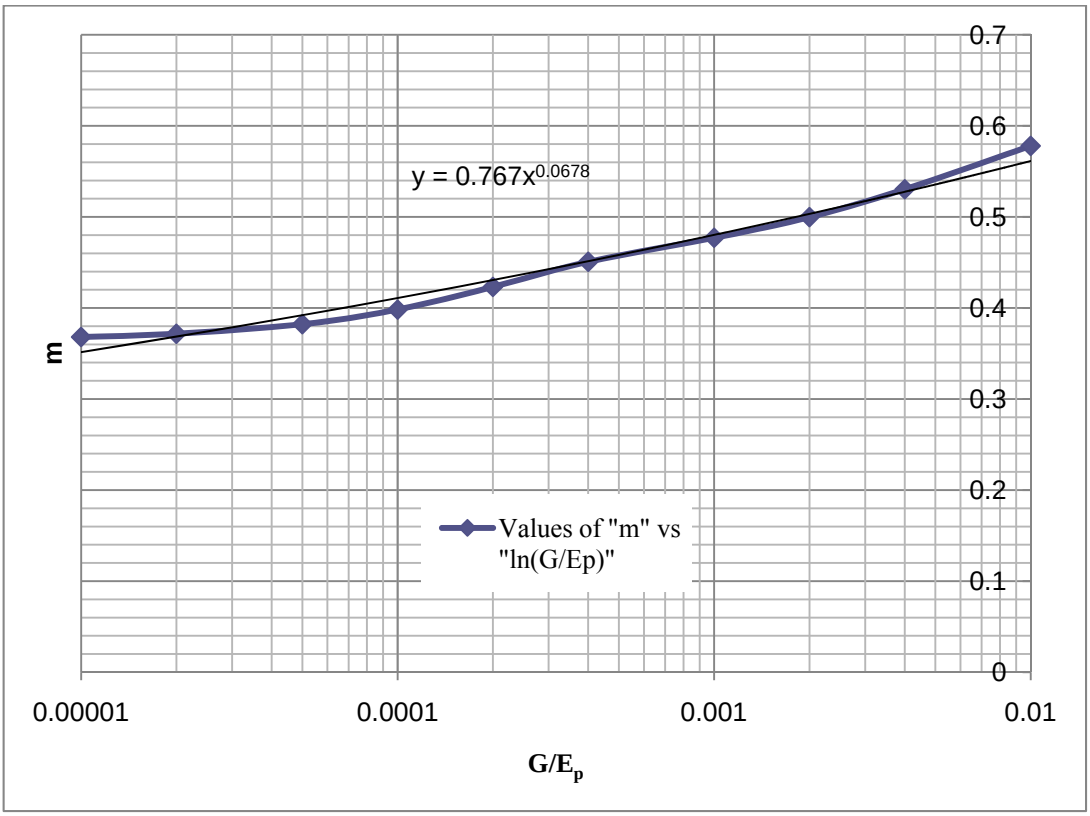

Figure 3-3 Values of 'm' vs. 'G/E_p' in logarithmic scale

Based on the correlation formula, the following equation is proposed for the Poisson's ratio scale factor:

$$S_\nu = 1 + \left(\frac{G}{50E_p}\right)^{0.0678} \frac{\nu}{1-\nu} \qquad (3.2\text{–}3)$$

Diameter scale factor 'S_D' can be investigated from the stiffness factors calculated from the values in Table 3-3. Dividing the values in the table by the reference values for $D=1000mm$ gives the diameter scale factor. This factor also shows some variations with the modulus ratio but the variations are negligible and for $D/D_{Ref} \geq 0.4$ a simple linear equation can be fit for the values. Table **3-11** summarizes the ratios of the values of 'k_s' pertaining to the stiffness values from Table 3-3, pertaining to those from the first column of Table 3-1. Figure 3-4 depicts variations of the diameter scale factor with the diameter ratio.

Table 3-11 Ratios of the values in Table **3-7** to those from the first column of Table **3-1**

Item	***D (mm)=***	***100***	***400***	***600***	***800***	***1500***	***2000***
	D/D_{ref}=	***0.1***	***0.4***	***0.6***	***0.8***	***1.5***	***2***
E_p/G	**100**	0.34	0.54	0.65	0.77	1.20	1.54
	250	0.38	0.59	0.70	0.82	1.24	1.58
	500	0.41	0.62	0.74	0.85	1.26	1.59
	1000	0.43	0.65	0.76	0.87	1.26	1.58
	2500	0.47	0.68	0.79	0.89	1.25	1.53
	5000	0.49	0.70	0.81	0.90	1.23	1.48
	10,000	0.51	0.72	0.82	0.91	1.21	1.44
	20,000	0.52	0.72	0.82	0.91	1.20	1.41
	50,000	0.53	0.73	0.83	0.92	1.20	1.40
	100,000	0.53	0.73	0.83	0.92	1.20	1.39

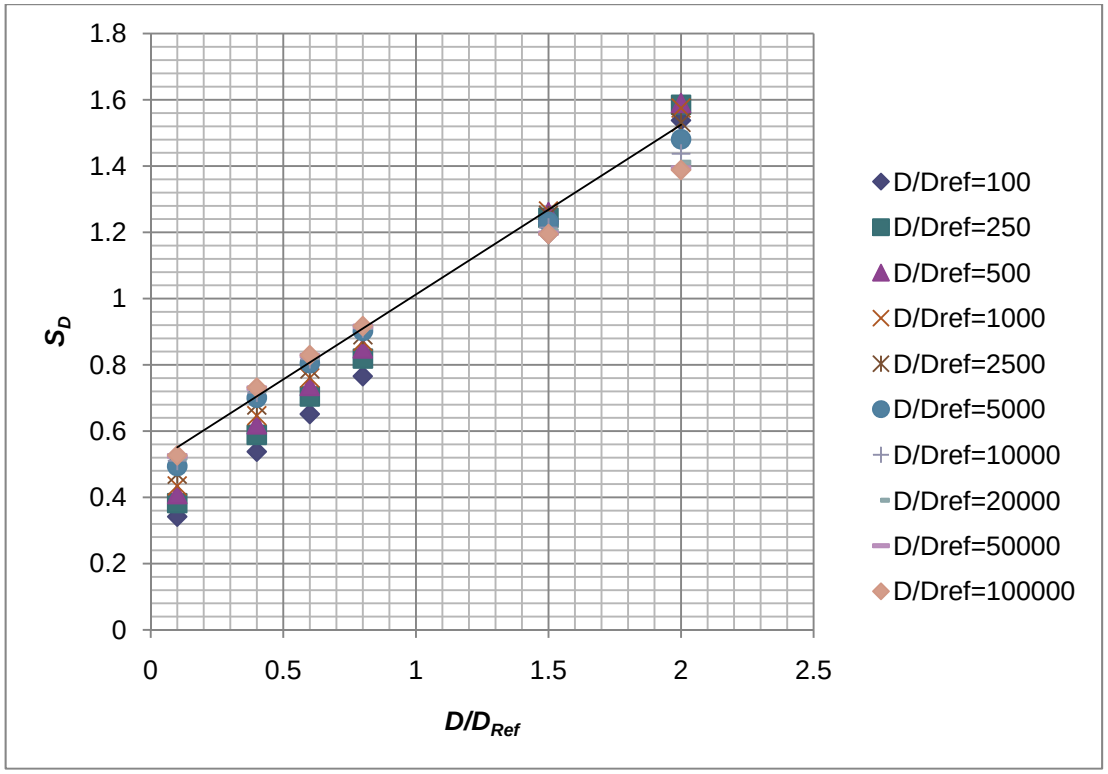

Figure 3-4 Variations in the scale factor S_D with the diameter ratio

Based on the above information the following equation is proposed for the diameter scale factor:

$$S_D = 0.5(1 + \frac{D}{D_{Ref}}) \qquad (3.2–4)$$

The moment of inertia scale factor is obtained by dividing the values in Table 3-6 into the corresponding values in Table 3-7. Table **3-12** includes the numerical values. Figure 3-5 depicts the scale factor *'S_I'* vs. I_{Ref}/I_p for different modulus ratios in log-log scale. Although the correlation with a straight line is poor for very high modulus ratios, it is possible to fit a general function as '$b(I_{Ref}/I_p)^n$' to the data, where '*b*' and 'n' are directly obtained by curve fitting. Table 3-13 includes the calculated values for '*b*' and '*n*'. The value of '*b*' can be taken as unity. Figure 3-6 shows variations of the factor 'n' with the modulus ratio. The correlation formula for this factor is also given in the same figure.

Table 3-12 Scale factor S_I as a ratio of the values from Table **3-6** to those from Table **3-7**

Diameter	**100**	**400**	**600**	**800**	**1000**	**1500**	**2000**
I_{Ref}/I_p	**10,000**	**39.1**	**7.7**	**2.4**	**1**	**0.20**	**0.06**
1	4.13	1.62	1.32	1.14	1.00	0.77	0.62
2	3.39	1.53	1.28	1.12	1.00	0.78	0.63
3	2.97	1.48	1.26	1.11	1.00	0.79	0.65
4	2.65	1.45	1.25	1.11	1.00	0.80	0.70
5	2.31	1.41	1.23	1.11	1.00	0.85	0.79
6	2.10	1.36	1.20	1.08	1.00	0.91	0.86
7	1.92	1.30	1.15	1.05	1.00	0.95	0.92
8	1.77	1.23	1.09	1.03	1.00	0.97	0.96
9	1.61	1.14	1.04	1.01	1.00	0.87	0.98
10	1.51	1.08	1.02	1.01	1.00	0.99	0.99

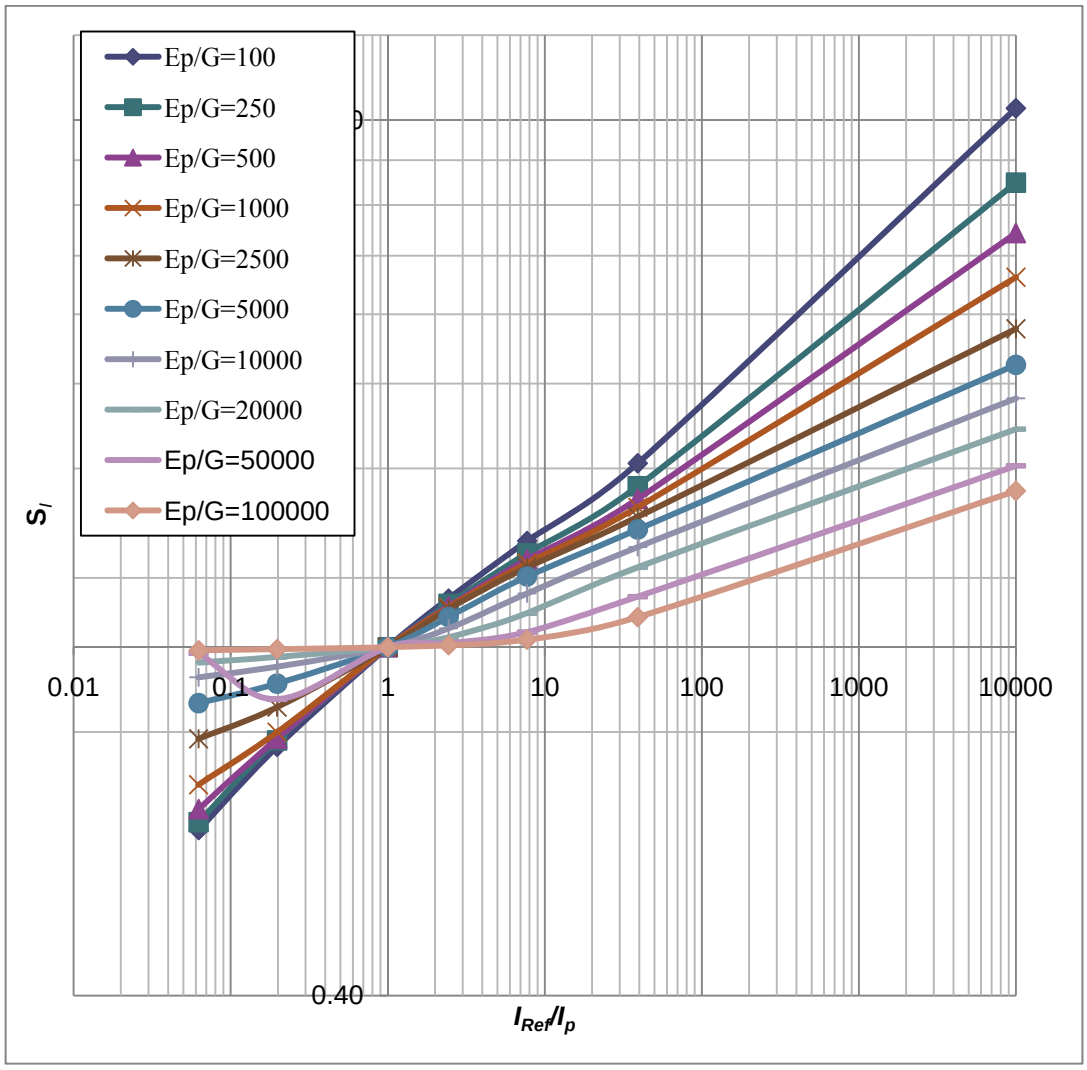

Figure 3-5 Moment of inertia scale factor for different modulus ratios

Table 3-13 Values of '*b*' and '*n*' of correlation function $S_I=b(I_{Ref}/I_p)^n$

G/Ep	b	n
0.01	0.9711	0.155
0.004	0.9638	0.1365
0.002	0.9636	0.1235
0.001	0.9751	0.1107
0.0004	1.0077	0.0909
0.0002	1.0296	0.0762
0.0001	1.0369	0.0636
0.00005	1.0329	0.0532
0.00002	0.9967	0.0464
0.00001	1.0146	0.0351

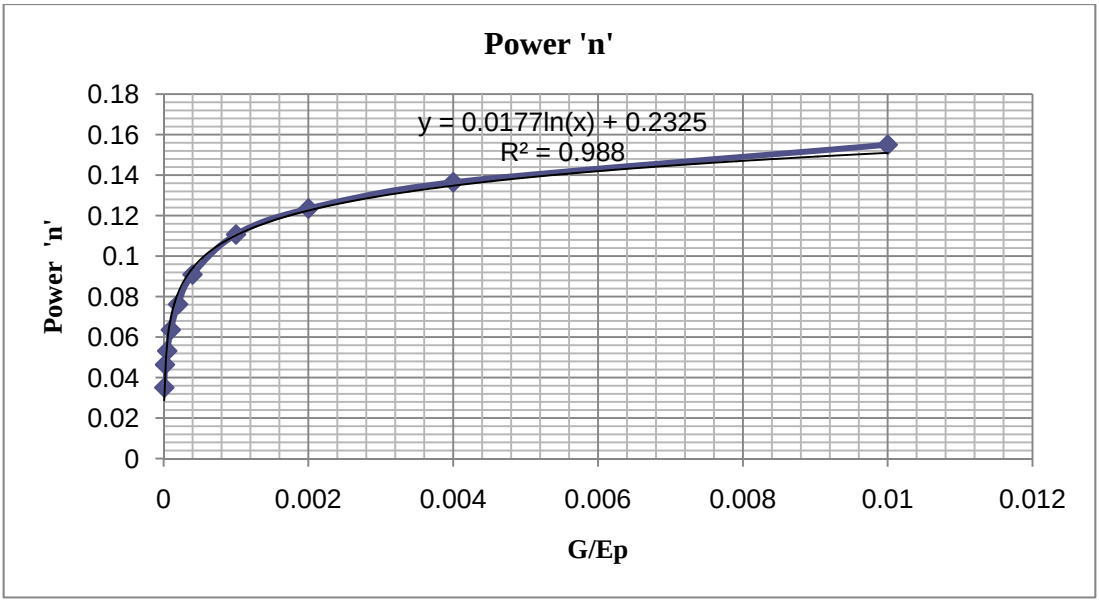

Figure 3-6 Power '*n*' vs. modulus ratio

$$S_I = \left(\frac{I_{\mathrm{Re}f}}{I_p}\right)^{0.0177\ln\left(\frac{G}{E_p}\right)+0.2325} \qquad (3.2\text{–}5)$$

So far, Poisson's ratio scale factor and the second moment of inertia scale factors show dependency on the modulus ratio, while the diameter scale factor is found to be independent of it. The main formula for the spring stiffness is yet to be investigated for two extreme cases of full connectivity and full slippage between the soil and the pile skin. This will be done by curve fitting on the values of the first columns of Table 3-5 and Table 3-8, as the values of these two columns correspond to $D=1m$ and $\nu = 0$, for which all the scale factors are 1. Table **3-14** includes the calculation results.

Table 3-14 Values of k_s/G for the cases of full slippage and no slippage

G/Ep	No slippage	Full slippage	Average
0.01000	5.92	4.08	5.00
0.00400	5.05	3.70	4.37
0.00200	4.55	3.46	4.00
0.00100	4.12	3.25	3.69
0.00040	3.66	3.02	3.34
0.00020	3.41	2.90	3.16
0.00010	3.27	2.84	3.06
0.00005	3.20	2.81	3.00
0.00002	3.15	2.79	2.97
0.00001	3.14	2.79	2.96

Figure 3-7 shows the basic scale factor for the spring stiffness vs. the modulus ratio.

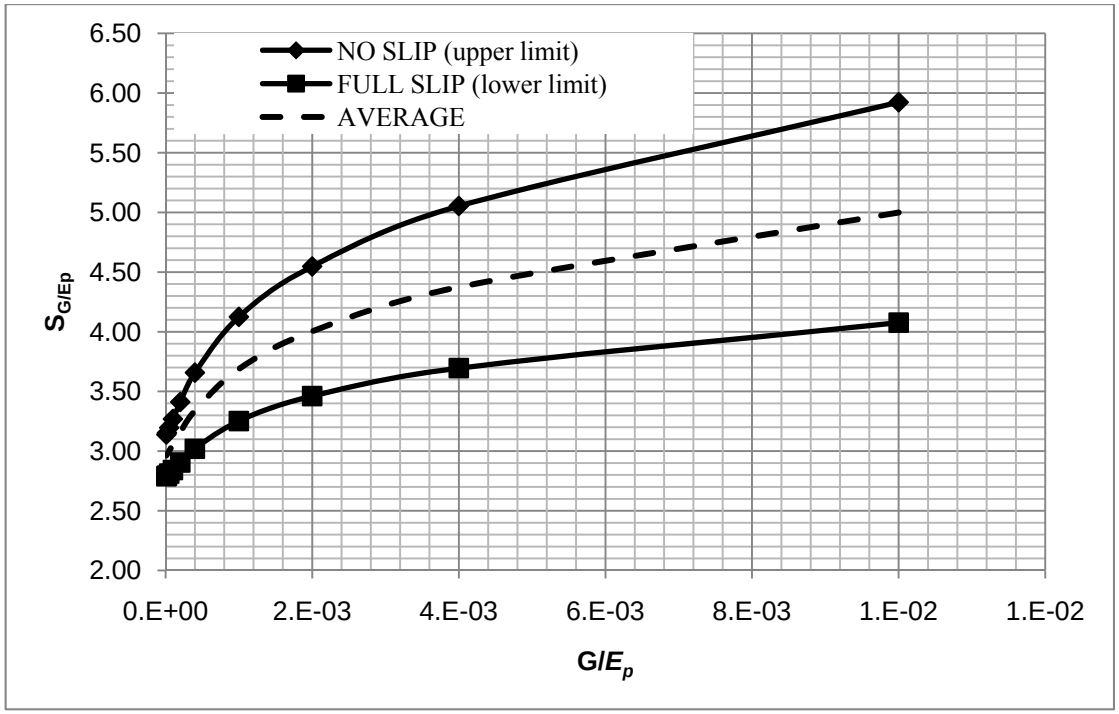

Figure 3-7 Modulus ratio scale factor vs. modulus ratio

The correlation functions for the three curves shown in Figure 3-7 are given as follows:

$$(S_{G/Ep})^{U} = 2.86 + 20.15\left(\frac{GI_s}{E_p I_p}\right)^{0.41} \quad (3.2\text{–}6)$$

$$(S_{G/Ep})^{L} = 2.65 + 9.10\left(\frac{GI_s}{E_p I_p}\right)^{0.40} \quad (3.2\text{–}7)$$

$$(S_{G/Ep})^{Ave} = 2.75 + 14.62\left(\frac{GI_s}{E_p I_p}\right)^{0.40} \quad (3.2\text{–}8)$$

The results of this study were published in a paper (Bahrami and Nikraz 2012). During the review cycle for this paper, the reviewers asked whether the constant values given in the above formulas were the result of numerical inaccuracies in the FE results. The authors of the paper believed that the values were significant and could not be considered to be errors.

At the time, the authors justified the presence of a constant factor by considering a hypothetical case of a very rigid pile in a very soft soil. For this case, the modulus ratio almost vanished, but there was still some lateral resistance to the pile. In Chapter 4, it will be shown that a constant value is a result of a continuum solution with a strong theoretical basis.

3.2.4 Comparison with published results by others

In this section a comparison is made between the FE analysis results and other published results for the stiffness of laterally loaded piles.

Mindlin (1936) developed an accurate solution for the deformations, stresses and strains caused by a force (both vertical and horizontal) under the surface of an elastic half-space. Many researchers (Douglas and Davis 1964; Spillers and Stoll 1964; Lenci, Maurice and Madigner 1968; Matthewson 1969; Poulos 1971a; Poulos 1973; Banerjee 1978; Banerjee and Davies 1978) have used Mindlin's solution to investigate pile load-deflection behaviour. All of these approaches are similar in principle and the differences come from details and assumptions regarding the pile behaviour.

Poulos and Davis (1980) provided diagrams for non-dimensional factors appearing in the pile top deflection equation:

$$u = \frac{T_0}{E_s L}\left(I_{\rho H} + \frac{e}{L} I_{\rho M}\right) \qquad (3.2\text{–}9)$$

Where L is the pile length, e is the ratio of top moment to the top horizontal force, $I_{\rho H}$ and $I_{\rho M}$ are non-dimensional influence factors. For a free head (i.e. *e=0)* the horizontal stiffness component K_h can be written as:

$$K_h = \frac{T_0}{u} = \frac{E_s L}{I_{\rho H}} = \frac{2D(1+\nu)G}{I_{\rho H}}\left(\frac{L}{D}\right) \qquad (3.2\text{–}10)$$

It is important to note that values of $I_{\rho H}$ are given for different slenderness ratios (i.e. *L/D*) by Poulos and Davis (1980). These values (for $\nu = 0.5$) are extracted from the original graphs and are listed in Table **3-15**.

Table 3-15 Pile stiffness for r_0=0.5m, L=10m, $\nu = 0.5$ (Poulos and Davis 1980)

E/G	***K_R***	$\frac{G}{E_p} = \frac{\pi}{128}\frac{1}{K_R(L/D)^4(1+\nu)}\frac{I_p}{I_s}$	***L/D=10***		***L/D=100***	
			$I_{\rho H}$	***K_h/G***	$I_{\rho H}$	***K_h/G***
5,704,113	10	1.75312E-07	3.62	7735	5.00	56,000
570,411	1	1.75312E-06	3.65	7671	5.10	54,902
57,041	0.1	1.75312E-05	3.71	7547	5.34	52,387
5704	0.01	0.000175312	4.31	6497	6.72	41,641
2852	0.005	0.000350624	5	5600	7.76	36,089
570	0.001	0.001753121	6.5	4308	9.28	30,186
29	0.00005	0.035062418	9.28	3017	12.41	22,556
6	0.00001	0.17531209	10	2800	15.52	18,044

Novak and El Sharnouby (1983) provided tabular data for different stiffness and damping components of a single pile based on three-dimensional continuum mechanic dynamic analysis. Their proposed formula for the lateral translational stiffness is as follows:

$$K_h = \frac{E_p I_p}{a^3} f_{u1} \qquad (3.2\text{–}11)$$

Numerical values of f_{u1} are given in tables for a homogenous soil profile as well as a parabolic soil profile. The modulus ratio E_p/G varies in the range of 250-10,000. Tables are given for Poisson's ratios of 0.2 and 0.4. Table **3-16** is extracted from the above reference.

Table 3-16 Pile stiffness for r_0=0.5m, $\nu = 0.5$ (Novak and El Sharnouby 1983)

ν	E_p/G	f_{u1}	K_{xx} (kN/mm)
0.2	10,000	0.0042	659.7345
	2500	0.0119	1869.248
	1000	0.0236	3707.079
	500	0.0395	6204.645
	250	0.0659	10351.55
0.4	10,000	0.0047	738.2743
	2500	0.0132	2073.451
	1000	0.0261	4099.778
	500	0.0436	6848.672
	250	0.0726	11403.98

Randolph (1981) conducted a parametric study on laterally loaded piles, using linear strain triangular elements. As a result, he proposed simple formulas similar to those for a beam on Winkler springs (Winkler 1867,; Hetenyi 1946):

$$u = 0.25\frac{T_0}{G^* a}\left(\frac{G^*}{E^*}\right)^{1/7} + 0.27\frac{M_0}{G^* a^2}\left(\frac{G^*}{E^*}\right)^{3/7} \quad (3.2\text{–}12)$$

$$\theta = 0.27\frac{T_0}{G^* a^2}\left(\frac{G^*}{E^*}\right)^{3/7} + 0.8\frac{M_0}{G^* a^3}\left(\frac{G^*}{E^*}\right)^{5/7} \quad (3.2\text{–}13)$$

Where $G^* = (1+3/4\nu)GI_s$ and $E^* = E_p I_p$. The translational components of the pile stiffness are obtained from equations (3.2–12) and (3.2–13):

$$k_h^{Randolph} = 4G^* a\left(\frac{E_p}{G^*}\right)^{1/7} = 4(1+3/4\nu)Ga\sqrt[7]{\frac{E_p}{G(1+3/4\nu)}} \quad (3.2\text{–}14)$$

Figure 3-8 shows the non-dimensional stiffness factor K_h/GD vs. modulus ratio. It is seen that there is considerable variability in the stiffness of the pile reported by different researchers. The results of the present study fall in the middle of these, closer to the results obtained by Poulos and Davis (1980) for *L/D=10*.

It is also noted that results from Randolph (1981) and Novak and El Sharnouby (1983) perfectly follow a straight line, while the results from Poulos and Davis (1980) and the present study deviate from a straight line. The reason might be explained by noting that the first two authors used 2D analyses while Poulos and Davis as well as the present study implement full 3D analyses.

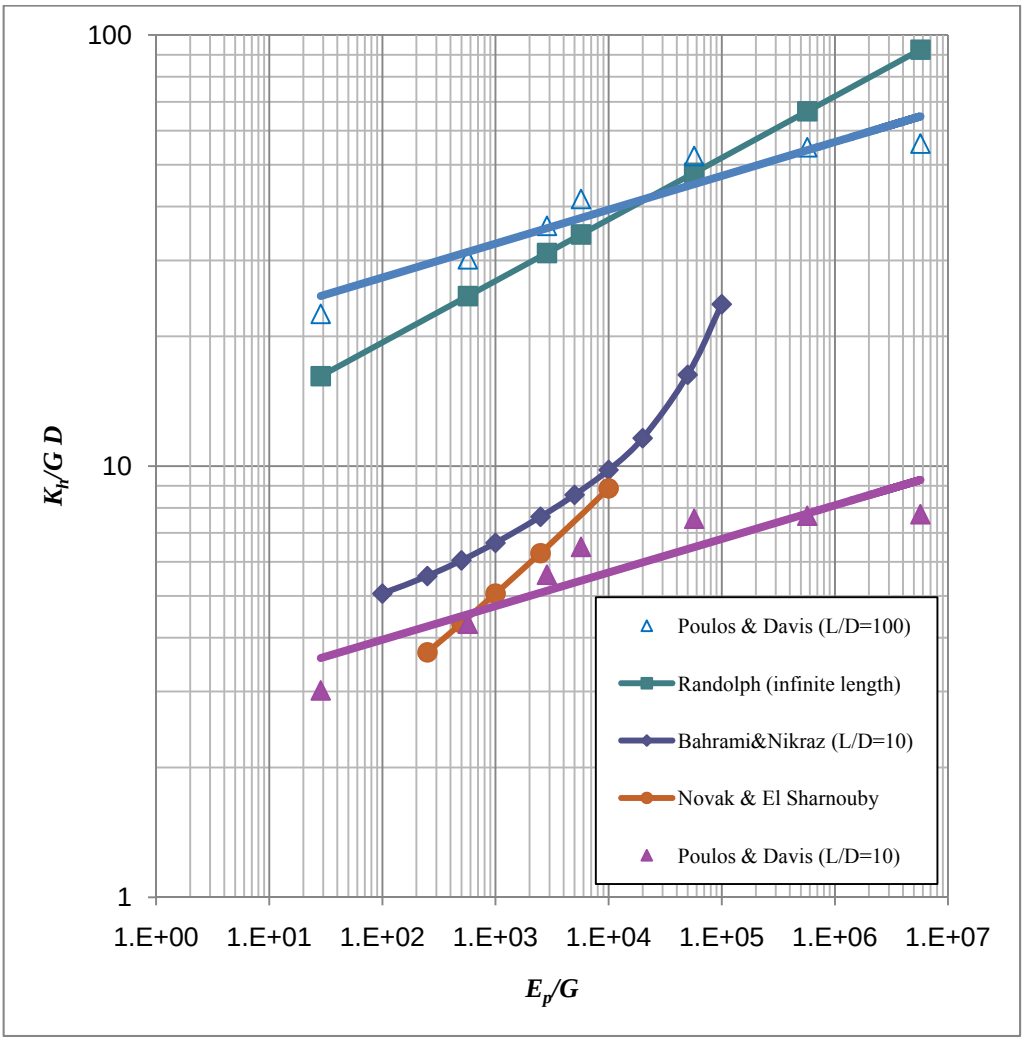

Figure 3-8 Non-dimensional stiffness ratio vs. pile modulus ratio by different authors

3.3 Application

In order to show the application of the results obtained in this chapter, test results reported by Boominathan and Ayothiraman (2006) and discussed in section 2.7, are considered. Pile in

site Mathura I is chosen as a typical example. Winkler spring stiffness for each layer is calculated using equations (3.2–3) to (3.2–8). Spring stiffness for lower limit (LL), mean value (MV) and upper limit (UL) are given in Table 3-7.

Table 3-17 Scaling factors for a test pile (Boominathan and Ayothiraman 2006)

Site	Dia (mm)	G_{max} (MPa)	Ep (GPa)	$S_{G/Ep}$			S_v	S_D	S_I	k_s (MPa)		
				LL	MV	UL				LL	MV	UL
Mathura I	500	64.08	23.5	3.51	4.13	4.65	1.22	0.750	1.43	293	345	389
		64.08		3.51	4.13	4.65	1.22	0.750	1.43	293	345	389
		84.86		3.61	4.29	4.87	1.23	0.750	1.45	407	484	549
		170.37		3.92	4.79	5.53	1.24	0.750	1.50	926	1131	1307

Analysis is performed via general purpose structural analysis software which is capable of modelling elastic materials, conventional Euler- Bernouli beam and linear springs. Three similar models of pile are created to represent lower limit, mean value and upper limit Winkler springs stiffness. The pile is modelled as beam elements, subdivided to comply with thickness of each soil layer. The elements are divided within each layer to increase the accuracy of the results. Element length within the first soil layer which is 2m deep is taken 200 mm. In the second layer the elements are 250mm long. Element lengths are increased in subsequent layers, knowing that the critical length of the pile is already passed (Table 2-9) and beyond that length the effect of the soil springs on the analysis result is minimal. Table 3-18 summarizes spring stiffness values as introduced to the model. Figure 3-9 shows details of the structural models corresponding to the lower limit (LL), mean value (MV) and upper limit Winkler springs stiffness values.

A horizontal load of 100 kN is applied to the pile top. The analysis gives the deflection at the point where the lateral load is applied. Head pile stiffness is obtained by dividing the load with the deflection. The results are given in Table 3-19. Also values from Table 2-9 are included in this table for comparison. It is seen that the lower limit and mean value spring stiffness under-estimates the stiffness of the pile, while the upper limit value has better compliance with the test results. It is also seen that the method introduced in Sec. 2.3.2 and computer program PILAY (1997) over estimate the test results. In this particular case, the results of the analysis have better agreement with the test results than other methods.

It should be noted that the aim of this section is only to demonstrate the applicability of the results of this chapter and does not cover all the practical issues that may be faced in a real design problem.

Table 3-18 spring stiffness values in the computer model

Soil layer description	Element length (mm)	Depth (from cut off line) (m)	Spring stiffness (N/mm)		
			LL	MV	UL
Grey silty clay mixed with kankars	200.00	0	29350	34539	38909
		0.2	58699	69079	77819
		0.4	58699	69079	77819
		0.6	58699	69079	77819
		0.8	58699	69079	77819
		1.0	58699	69079	77819
		1.2	58699	69079	77819
		1.4	58699	69079	77819
		1.6	58699	69079	77819
		1.8	58699	69079	77819
		2.0	80215	95017	107517
Yellowish silty clay mixed with kankars	250.00	2.25	101731	120955	137216
		2.5	101731	120955	137216
		2.75	101731	120955	137216
		3.00	101731	120955	137216
		3.25	101731	120955	137216
		3.50	101731	120955	137216
		3.75	101731	120955	137216
		4.00	101731	120955	137216
		4.25	101731	120955	137216
		4.50	282311	343270	395446
Silty sand in yellowish color mixed with kankars	500.00	5.00	462891	565584	653676
		5.50	462891	565584	653676
		6.00	462891	565584	653676
		6.50	462891	565584	653676
		7.00	462891	565584	653676
		7.50	462891	565584	653676
		8.00	462891	565584	653676
		8.50	462891	565584	653676
		9.00	462891	565584	653676
		9.50	462891	565584	653676
		10.00	462891	565584	653676
		10.50	462891	565584	653676
		11.00	231445	282792	326838

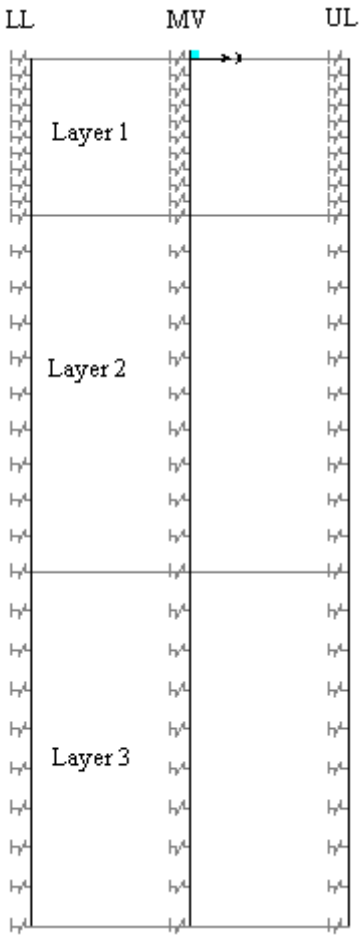

Figure 3-9 Pile models as beam on Winkler support

Table 3-19 Analysis results for lateral stiffness of test pile (tests conducted by Boominathan and Ayothiraman 2006)

Deflection (mm)*			**Stiffness (kN/m × 10^4)**					
LL	**MV**	**UL**	**Analysis result**			**Values from Table 2-9**		
			LL	**MV**	**UL**	**2.3.2**	**PILAY**	**Test**
1.1079	0.9837	0.9018	9.026	10.17	11.09	15.34	14.50	12.80-13.70

*- LL= Lower Limit

*- MV= Mean value

*- UL= Upper limit

3.4 Summary chapter three

In this chapter large numbers of finite element analyses are performed in order to obtain elastic Winkler spring stiffness. Elastic spring stiffness is assumed to be directly proportional to the soil shear modulus. The proportionality constant is considered as product of number of scaling factors, each reflecting the effect of a major physical or mechanical parameter. These scale factors are listed as follows:

- Poisson's ratio scale factor, S_ν
- Diameter scale factor, S_D
- Moment of inertia scale factor, S_I
- Modulus ratio scale factor, $S_{G/Ep}$

The value of these scale factors are obtained by curve fitting on the FEA resulted values. One of the most disputed factors is the diameter scale factor. Many researchers believe that the Winkler spring stiffness should not be dependent on the diameter, similar to a beam on the surface of an elastic half space. Some researchers proposed diameter dependent relationships for spring stiffness (Carter 1984; Pender, Carter and Pranjoto 2007), others provide evidence to contradict this idea (Ashford and Juirnarongrit 2003). The results of this study support the idea that the Winkler spring stiffness depends on the diameter (Bahrami and Nikraz 2012).

Another controversial aspect of this study is the presence of a constant value in the expression of the modulus ratio scale factor. The reviewers of the paper (Bahrami and Nikraz 2012) argued that this constant value might be a cause of numerical inaccuracies in FE model, a curve fitting aspect without any physical meaning or even an artifact of finite element. However, the authors decided to keep this constant in the equation and interpreted it as the limiting value of soil stiffness when the pile has very large (hypothetical) modulus of elasticity compared to soil shear modulus. As it will be shown in chapter 4, a theoretically based solution also contains such constant in the expression of Winkler spring stiffness with a value very close to what is obtained in the present chapter, and with clear physical meaning.

CHAPTER FOUR

4 CONTINUUM MECHANICS OF DYNAMICALLY LOADED PILES

In this section the problem of a dynamically loaded pile is approached via a continuum mechanics formulation. The soil is considered to be a linear elastic half-space continuum and the pile a slender flexible Euler-Bernouli beam. The objective is to find a closed-form solution for elastodynamic equations (section 2.1.1) that is more rigorous when compared to existing solutions. Although the topic of the thesis limits the present study to laterally loaded piles, it has shown the possibility of some improvement in the theory of axially loaded piles. Consequently, section 4.2 is dedicated to this topic in the belief that adding this section helps the thoroughness of this thesis and its application to the broader filed as originally planed.

4.1 Laterally loaded pile

Some of the existing solutions for the far field response of the pile-soil system are discussed in section 2.4. All of the methods have their own simplifying assumptions that lead to some degree of inaccuracy in the approximation. Kaynia's (1982) solution is probably the most accurate solution in the form of integral equations. The result, however, is in integral equation format which needs numerical and graphical declaration. The following sections provide more rigorous closed-form solutions to the elastodynamic equations which remove most of the weaknesses of the existing solutions of this type.

This chapter contains an improved solution to the problem studied by Nogami and Novak (1977). As discussed in section 2.4.3, their solution has certain weaknesses:

a) The vertical deformations in the soil media are ignored.
b) The effect of vertical shear stress is ignored.
c) The solution is only provided for two of the elastodynamic differential equations which only correspond to the equilibrium in horizontal directions.
d) The final solution is real-valued if the hysteretic damping of the pile is ignored, i.e. if no geometrical damping is included.
e) The modal form considered for the pile is valid only for certain end conditions of the pile.
f) The ground surface boundary conditions (i.e. zero traction) are not satisfied.
g) The solution is provided for a limited pile length in a soil layer overlaying rigid bedrock.

4.1.1 Assumptions

The following assumptions are made in solving the elastodynamic equations:

1- The soil and pile are assumed to be perfectly elastic, homogenous materials.
2- The soil is considered to be an elastic half-space. Lower half-space is considered to have a horizontal flat free (ground) surface as its boundary.
3- The pile is considered to be infinitely long, extending vertically downwards from the ground surface.
4- The pile is assumed to have a circular cross-section and be prismatic throughout its length.
5- The pile follows the Euler-Bernouli beam theory.
6- The soil and pile are considered to be fully connected (welded). No slippage or separation is allowed between the soil and the pile.
7- The pile is under steady-state vibrations in the horizontal 'x' direction. Transient vibrations are not considered.
8- Deformations are considered to be in cylindrical coordinates with the origin on the ground surface and 'z' axis heading downwards.

In order to be able to provide a solution to the general 3D form of elastodynamic equations, we make some simplifying assumptions which we call 'uncoupling of deflection'. It is assumed that the lateral deflection of the pile is composed of two independent components, a translation and a rotation (Figure 2-1). In general, these two components are interrelated. Here we uncouple the translation and rotation, i.e. they are independent to each other. We also assume that the translation only imposes lateral deformations while the rotation creates only vertical deformations in the soil. These assumptions play key role in providing solution to the elastodynamic equations.

4.1.2 Solving elastodynamic differential equations

The objective is to find a solution to elastodynamic differential equations (2.1–28), (2.1–29) and (2.1–30). The separation of variables technique is employed for solving the partial differential equations. The separation of the variable 'θ' is similar to what is explained in section 2.4.1 under the solution by Baranov (1967). We start the solution for horizontal deformation components in the soil by considering the following expansions:

$$u(r,\theta,z,t) = e^{-i\omega t}U(r)F(z)\cos\theta \qquad (4.1\text{–}1)$$

$$v(r,\theta,z,t) = e^{-i\omega t}[V(r) - U(r)]F(z)\sin\theta \tag{4.1–2}$$

$$w(r,\theta,z,t) = 0 \tag{4.1–3}$$

In the above expansions, the *'U(r)'* and *'F(z)'* are functions used to separate variables *'r'* and *'z'*, respectively. The function *'F(z)'* is like a shape function that defines variations of the horizontal displacements with depth. For this reason, the same function is considered for both radial and tangential displacements. The function *'U(r)',* defines the radial variations of the deformation component '$u(r,\theta,z,t)$' with *'r'*. A different function should define variations of the tangential component of soil deformation '$v(r,\theta,z,t)$' with *'r'*. Without loss of generality, this function is considered to be '$V(r) - U(r)$'. The reason for this choice becomes clear when considering that the deformation component in *'y'* direction should be zero at interface between the pile and the soil, because the vibrations are assumed to be in the *'x'* direction. This can be formulated as:

$$u(r_0,\theta,z,t)\sin\theta + v(r_0,\theta,z,t)\cos\theta = 0 \tag{4.1–4}$$

Substituting equations (4.1–1) and (4.1–2) into equation (4.1–4) results in:

$$e^{-i\omega t}V(r_0)F(z)\sin\theta\cos\theta = 0 \tag{4.1–5}$$

Equation (4.1–4) concludes:

$$V(r_0) = 0 \tag{4.1–6}$$

Later it will be shown that equation (4.1–6) establishes the basis for the dispersion of radiated SH-P waves in the soil.

Starting the solution of the elastodynamic equations, we first substitute equations (4.1–1), (4.1–2) and (4.1–3) into equation (2.4–32), which corresponds to vertical equilibrium in the soil. This leads to the following relationship between the functions *'V(r)'* and *'U(r)'*:

$$V(r) = -rU'(r) \tag{4.1–7}$$

Substituting equation (4.1–5) into equations (2.1–28) and (2.1–29) results in the following two equations:

$$F(z)[rU''(r) + 3U'(r) + r\varpi^2 U(r)] + F''(z)[rU(r)] = 0 \tag{4.1–8}$$

$$F(z)[rU^{(3)}(r)+4U''(r)+(3+r\varpi^2)U'(r)+\varpi^2U(r)]+F''(z)[U(r)+rU'(r)]=0 \qquad (4.1\text{–}9)$$

It can be verified that equation (4.1–9) is the derivative of equation (4.1–8) with respect to *'r'*. Therefore it is sufficient to consider only equation (4.1–8). Dividing equation (4.1–8) by *'U(r)F(z)'* and collecting *'r'* related terms to the left and *'z'* related terms to the right side of the equation, results in:

$$\frac{rU''(r)+3U'(r)+r\varpi^2U(r)}{rU(r)}=-\frac{F''(z)}{F(z)} \qquad (4.1\text{–}10)$$

This equation is valid only if both sides are constant. We equate the right-hand side of the above equation to a complex valued constant h^2. A solution to the right-hand side of the equation (4.1–10) is readily derived as:

$$F(z)=Ae^{ihz}+Be^{-ihz} \qquad (4.1\text{–}11)$$

'A' and *'B'* in the above equation are integration constants. The left-hand side of equation (4.1–10) can be written as:

$$r^2U''(r)+3rU'(r)+(\frac{a_0^2}{r_0^2}-h^2)r^2U(r)=0 \qquad (4.1\text{–}12)$$

This equation can be transformed into a Bessel equation by a change of variable: $U(r)=g(r)/r$.

$$r^2g''(r)+rg'(r)+[(\frac{a_0^2}{r_0^2}-h^2)r^2-1]g(r)=0 \qquad (4.1\text{–}13)$$

The solution to equation (4.1–13) can be expressed as Hankel functions of the first and the second kinds of order one.

$$g(r)\in\{H_1^{(1)}(\sqrt{a_0^2-h^2r_0^2}\,r/r_0),H_1^{(2)}(\sqrt{a_0^2-h^2r_0^2}\,r/r_0)\} \qquad (4.1\text{–}14)$$

In order to choose the right solution which reflects the physical reality of the problem, asymptotic expansions (Abramowitz and Stegun 1972) of the functions are investigated:

$$H_1^{(1)}(\sqrt{a_0^2 - h^2 r_0^2}\ \frac{r}{r_0}) \to \frac{\sqrt{2}}{\sqrt[4]{a_0^2 - h^2 r_0^2}\sqrt{\pi \frac{r}{r_0}}} Exp[i(\sqrt{a_0^2 - h^2 r_0^2}\ \frac{r}{r_0} - \frac{3}{4}\pi)] \tag{4.1–15}$$

$$H_1^{(2)}(\sqrt{a_0^2 - h^2 r_0^2}\ \frac{r}{r_0}) \to \frac{\sqrt{2}}{\sqrt[4]{a_0^2 - h^2 r_0^2}\sqrt{\pi \frac{r}{r_0}}} Exp[-i(\sqrt{a_0^2 - h^2 r_0^2}\ \frac{r}{r_0} - \frac{3}{4}\pi)] \tag{4.1–16}$$

It should be noted that the time harmonic term is considered as a negative complex exponential: $e^{-i\omega t}$. In combination with equation (4.1–11) the overall phase of the deformation field can be written as:

$$i(-\omega t + \sqrt{a_0^2 - h^2 r_0^2}\ \frac{r}{r_0} - \frac{3}{4}\pi \pm hz) \tag{4.1–17}$$

$$i(-\omega t - \sqrt{a_0^2 - h^2 r_0^2}\ \frac{r}{r_0} - \frac{3}{4}\pi \pm hz) \tag{4.1–18}$$

Equation (4.1–17) corresponds to the phase obtained for the Hankel function of the first kind while equation (4.1–18) corresponds to that of the Hankel function of the second kind. The phase velocity in the radial direction of the waves described by equation (4.1–15) is derived as:

$$V_{Phase-r-1} = \frac{\omega r_0}{\sqrt{a_0^2 - h^2 r_0^2}} \tag{4.1–19}$$

The phase velocity in the radial direction described by equations (4.1–16) can be written as:

$$V_{Phase-r-2} = -\frac{\omega r_0}{\sqrt{a_0^2 - h^2 r_0^2}} \tag{4.1–20}$$

It is seen that the waves described by the Hankel function of the first kind have positive phase velocity, meaning that the waves propagate towards positive ‘r’ direction, i.e. away from the pile, while the waves expressed by the Hankel function of the second kind have negative wave velocity, meaning that they travel towards the pile. It is evident that it is physically impossible for the latter waves to exist. A similar argument has already been made in section 2.4.1 in the discussion of Baranov’s (1967) solution. The difference between the present solution and Baranov’s solution is that in this solution a negative power for the

time dependent parameter is used, such that the Hankel functions of the first kind represent the propagating waves, while the choice of a positive time exponent in Baranov's solution leads to the Hankel functions of the second kind being the valid solution. It should be noted that the Hankel functions of the first and second kind are complex conjugates of each other, i.e. their imaginary parts are in opposite signs. Therefore, it is equally valid to choose either of them with the relevant choice of time exponent function.

Considering the above argument on the right choice of Hankel functions, the following expressions are derived for the functions '$U(r)$' and '$V(r)$':

$$U(r) = \frac{H_1^{(1)}(\sqrt{a_0^2 - h^2 r_0^2}\, r / r_0)}{r} \tag{4.1–21}$$

$$V(r) = \frac{\sqrt{a_0^2 - h^2 r_0^2}}{r_0} H_2^{(1)}(\sqrt{a_0^2 - h^2 r_0^2}\, r / r_0) \tag{4.1–22}$$

It has been mentioned before that equation (4.1–6) establishes dispersion conditions for radiated waves. Substituting equation (4.1–22) into equation (4.1–6) results in:

$$H_2^{(1)}(s) = 0, \quad s = s_R + i.s_I = \sqrt{a_0^2 - h^2 r_0^2} \tag{4.1–23}$$

In equation (4.1–23), *'s'* denotes all the roots of the Hankel function of the first kind of order 2 (i.e. infinite numbers). The numerical values of these roots are given in the literature (Döring 1965). The imaginary parts of all roots are negative and asymptotically approach the value of *'-0.5ln2'*. The real part of the first root is positive while all higher order roots have negative real values. The first five roots of equation (4.1–23) are given in Table 4-1.

Table 4-1 Complex roots of equation (4.1–23) and their squares

n	s_R	s_I	s_R^2-s_I^2	$2\, s_R\, s_I$
1	0.429	-1.281	-1.457	-1.101
2	-1.317	-0.836	1.035	2.202
3	-5.138	-0.372	26.256	3.825
4	-8.418	-0.356	70.73	5.992
5	-11.62	-0.351	134.901	8.167

Knowing the numerical values of *'s'*, the real and imaginary parts of factor *'h'* are written as:

$$\begin{cases} \mathrm{Re}(h) = \dfrac{1}{r_0}\sqrt{\dfrac{1}{2}[\sqrt{(a_0^2 + s_I^2 - s_R^2)^2 + (2s_I s_R)^2} + a_0^2 + s_I^2 - s_R^2} \\ \mathrm{Im}(h) = -\dfrac{|2s_I s_R|}{2s_I s_R}\dfrac{1}{r_0}\sqrt{\dfrac{1}{2}[\sqrt{(a_0^2 + s_I^2 - s_R^2)^2 + (2s_I s_R)^2} - a_0^2 - s_I^2 + s_R^2} \end{cases} \qquad (4.1\text{–}24)$$

Since there are infinite values for *'s'* satisfying equation (4.1–23), it is essential to determine which of these values are valid. The validity of a particular value of *'s'* is verified if the corresponding waves can physically exist. To investigate which of the *'s'* values can produce radiated waves and which cannot, we need to write the deformation field in standard wave form. We start with the function 'F(z)' and substitute the imaginary and real parts of *'h'* from equation (4.1–24) into equation (4.1–11):

$$F(z) = A \times e^{-\mathrm{Im}(h)z}\, Exp[i\,\mathrm{Re}(h)z] + B \times e^{+\mathrm{Im}(h)z}\, Exp[-i\,\mathrm{Re}(h)z] \qquad (4.1\text{–}25)$$

It is seen that function *'F(z)'* includes two harmonic terms corresponding to unknown factors *'A'* and *'B'*. The harmonic terms include exponential parts: $e^{\pm \mathrm{Im}(h)z}$. For the first value of *'s'* (which will be called *'s_1'*), the imaginary part of *'h'* is positive. Therefore the term corresponding to factor *'A'* shows damping with depth while the other term shows growth. Therefore it is physically impossible for the latter is to exist and it should be eliminated from equation (4.1–25), i.e. *'B=0'*. Now if we consider other values of *'s'* (which will be called

's_n') one may similarly conclude that the term corresponding to factor *'A'* should vanish. This leads us to two possible terrains of waves. The first terrain corresponds to *'s_1'* and the second terrain corresponds to all other values of *'s_n'*. In the following lines it will be shown that the second terrain of waves is physically impossible.

The function *'U(r)'* characterizes the transmission of waves in a radial direction. In distances far from the pile, asymptotic expansion of this function reads:

$$U(r)=\frac{H_1^{(1)}(s_1 r/r_0)}{r}\rightarrow\sqrt{\frac{2r_0}{\pi s_1 r^3}}Exp[i(\frac{s_1 r}{r_0}-\frac{3\pi}{4})] \tag{4.1–26}$$

The cosine function can also be written in terms of harmonic functions:

$$\cos\theta=\frac{1}{2}[Exp(i\theta)+Exp(-i\theta)] \tag{4.1–27}$$

Substituting equations (4.1–25), (4.1–26) and (4.1–27) into equation (4.1–1) results in equations for waves in radial direction. These equations are written for the first and the second terrains of waves separately:

$$u_1(r,\theta,z,t)=\frac{1}{2}A\times e^{-\mathrm{Im}(h_1)z}\left\{\begin{array}{l}Exp[-i(\omega t-\mathrm{Re}(h_1)z-\frac{s_1 r}{r_0}-\theta+\frac{3\pi}{4}]+\\+Exp[-i(\omega t-\mathrm{Re}(h_1)z-\frac{s_1 r}{r_0}+\theta+\frac{3\pi}{4}]\end{array}\right\} \tag{4.1–28}$$

$$u_n(r,\theta,z,t)=\frac{1}{2}B\times e^{\mathrm{Im}(h_n)z}\left\{\begin{array}{l}Exp[-i(\omega t+\mathrm{Re}(h_n)z-\frac{s_n r}{r_0}-\theta+\frac{3\pi}{4}]+\\+Exp[-i(\omega t+\mathrm{Re}(h_n)z-\frac{s_n r}{r_0}+\theta+\frac{3\pi}{4}]\end{array}\right\} \tag{4.1–29}$$

The phase velocities in the vertical direction for the first and the second terrains of waves are given in equation (4.1–30) and (4.1–31), respectively:

$$V_{Phase-z-1}=\frac{\omega}{\mathrm{Re}(h_1)} \tag{4.1–30}$$

$$V_{Phase-z-2}=-\frac{\omega}{\mathrm{Re}(h_n)} \tag{4.1–31}$$

Noting that *'Re(h)'* is always positive, it is evident that the first terrain of waves travels downwards while the second terrain travels upwards. Since the excitation of the pile takes

place at the ground surface, it is expected that the radiated waves travel downwards. In the absence of rigid bedrock or other boundaries that reflect these waves, there will be no waves travelling upwards in the soil media. Therefore the waves represented by equation (4.1–29) are unphysical, leading us to the conclusion that it is only possible for the first terrain of waves corresponding to the value of *'s_1'* to physically exist.

Substituting the numerical value of *'s_1'* into the equation (4.1–24) results in the following:

$$\begin{cases} \mathrm{Re}(h) = \dfrac{1}{r_0}\sqrt{\dfrac{1}{2}[\sqrt{(a_0^2+1.457)^2+1.211}+a_0^2+1.457} \\ \mathrm{Im}(h) = \dfrac{1}{r_0}\sqrt{\dfrac{1}{2}[\sqrt{(a_0^2+1.457)^2+(2s_1 s_R)^2}-a_0^2-1.457} \end{cases} \qquad (4.1\text{–}32)$$

It is convenient to introduce a non-dimensional radius parameter '$\hat{r} = r/r_0$' in the mathematical presentation of the displacement field:

$$u(r,\theta,z,t) = C \times e^{-i\omega t}\cos\theta \frac{H_1^{(1)}(s_1\hat{r})}{\hat{r}} Exp[-\mathrm{Im}(h)z + i\,\mathrm{Re}(h)z] \qquad (4.1\text{–}33)$$

$$v(r,\theta,z,t) = C \times e^{-i\omega t}\sin\theta[s_1 H_2^{(1)}(s_1\hat{r}) - \frac{H_1^{(1)}(s_1\hat{r})}{\hat{r}}]Exp[-\mathrm{Im}(h)z + i\,\mathrm{Re}(h)z] \qquad (4.1\text{–}34)$$

In the above equations, '*$C=A/r_0$*' is the wave amplitude. To eliminate the unknown factor *'C'* from the displacement equations, we substitute equation (4.1–28) into equation (2.1–46) and use a harmonic expression for pile deflection: $x(z,t) = X(z)e^{-i\omega t}$. The result is as follows:

$$C \times H_1^{(1)}(s_1)e^{-\mathrm{Im}(h)z + i\,\mathrm{Re}(h)z} = X(z) \qquad (4.1\text{–}35)$$

Eliminating the factor *'C'* among the equations (4.1–33), (4.1–34) and (4.1–35) results in the following equations that relate the displacement components in the soil to the lateral deflection of the pile:

$$u(r,\theta,z,t) = e^{-i\omega t}\cos\theta \frac{H_1^{(1)}(s_1\hat{r})}{\hat{r}H_1^{(1)}(s_1)} X(z) \qquad (4.1\text{–}36)$$

$$v(r,\theta,z,t) = e^{-i\omega t}\sin\theta[s_1 \frac{H_2^{(1)}(s_1\hat{r})}{H_1^{(1)}(s_1)} - \frac{H_1^{(1)}(s_1\hat{r})}{\hat{r}H_1^{(1)}(s_1)}]X(z) \qquad (4.1\text{–}37)$$

It is interesting to note that the horizontal components of deformation are non-dilatational. Therefore the waves represented by these components are non-dilatational or S-waves travelling vertically.

The solution of elastodynamic equations for uncoupled horizontal translation is complete at this point and we shall proceed to study the uncoupled rotation. In section 4.1.1 we assumed that the uncoupled rotation only imposes vertical deformations to the soil media. Similar to the horizontal components and due to the symmetry about the '*xz*' plane, the following expansion is considered for vertical deformations:

$$w(r,\theta,z,t) = e^{-i\omega t} W(r) Z(z) \cos(\theta) \tag{4.1–38}$$

Substituting equation (4.1–38) into equations (2.1–28), (2.1–29) and (2.1–30) leads to the following:

$$\frac{\lambda+\mu}{\mu}\cos(\theta) W'(r) Z'(z) = 0 \tag{4.1–39}$$

$$-\frac{\lambda+\mu}{\mu}\frac{1}{r}\sin(\theta) W(r) Z'(z) = 0 \tag{4.1–40}$$

$$\frac{1}{r^2}\cos(\theta)[\eta^2 r^2 W(r) Z''(z) + r^2 W''(r) Z(z) + r W'(r) Z(z) + (\varpi^2 r^2 - 1) W(r) Z(z)] = 0 \tag{4.1–41}$$

The first two equations can be satisfied simultaneously only if *'Z'(z)=0'*, i.e. '$w(r,\theta,z,t)$' is not a function of depth. However, it is evident that vertical deformations in the soil media should be depth-dependent. This discrepancy is caused by uncoupling the rotation from the lateral deformation of the pile. In this text, we ignore equations (4.1–39) and (4.1–40) and only consider the solution for equation (4.1–41), noting that the latter corresponds to the equilibrium equation in the vertical direction. Dividing both sides of equation (4.1–41) by $\eta^2 r^2 W(r) Z(z)$ results in:

$$-\frac{Z''(z)}{Z(z)} = \frac{r^2 W''(r) + r W'(r) + (\varpi^2 r^2 - 1) W(r)}{\eta^2 r^2 W(r)} \tag{4.1–42}$$

Equating the left-hand side of equation (4.1–42) to an arbitrary (complex-valued) constant *'f^2'* results in the following solution for *'Z(z)'*:

$$Z(z) = De^{ifz} \tag{4.1–43}$$

It should be noted that another solution to equation (4.1–43) also exists with the negative power of *'f'*. The right-hand side of the equation (4.1–42) can be transformed to a Bessel differential equation:

$$r^2W''(r) + rW'(r) + [(\varpi^2 - \eta^2 f^2)r^2 - 1]W(r) = 0 \tag{4.1–44}$$

The solutions to the above equation are Hankel functions of the first and second kinds of order 1. The Hankel function of the second kind is eliminated from the solution for reasons similar to the horizontal deformations which were explained before. The solution to equation (4.1–44) is therefore written as:

$$W(r) = H_1^{(1)}(\sqrt{a_0^2 - \eta^2 f^2 r_0^2}\, r / r_0) \tag{4.1–45}$$

The vertical component of the deformation field can now be written as:

$$w(r,\theta,z,t) = DH_1^{(1)}(\sqrt{a_0^2 - \eta^2 f^2 r_0^2}\, r / r_0)\cos(\theta)e^{-i\omega t}e^{ifz} \tag{4.1–46}$$

It is essential that vertical deformation satisfies equation (2.1–48) to ensure full connectivity between the pile surface and the soil. Substituting equation (4.1–46) into equation (2.1–48) results in:

$$w(r_0,\theta,z,t) = DH_1^{(1)}(\sqrt{a_0^2 - \eta^2 f^2 r_0^2})\cos(\theta)e^{-i\omega t}e^{ifz} = -r_0 X'(z)\cos\theta e^{-i\omega t} \tag{4.1–47}$$

Substituting for *'X(z)'* from equation (4.1–35) into equation (4.1–47) results in:

$$H_1^{(1)}(\sqrt{a_0^2 - \eta^2 f^2 r_0^2})(De^{-\mathrm{Im}(f)z + i\,\mathrm{Re}(f)z}) = -C(-\mathrm{Im}(h) + i\,\mathrm{Re}(h))r_0 e^{-\mathrm{Im}(h)z + i\,\mathrm{Re}(h)z} \tag{4.1–48}$$

Comparing the two sides of equation (4.1–48) concludes: *'f=h'*. In addition, the constant *'D'* can be written in terms of the pile rotation *'X'(z)'*, using the equation (4.1–47):

$$De^{ifz} = \frac{-r_0}{H_1^{(1)}(\sqrt{a_0^2 - \eta^2 h^2 r_0^2})} X'(z) \tag{4.1–49}$$

It is known from the definition of *'s'* that: $s_1^2 = a_0^2 - h^2 r_0^2$. Using this relationship and the fact that *'f=h'*, the factor *'f'* can be eliminated from equations (4.1–46) and (4.1–49):

$$\sqrt{a_0^2-\eta^2 f^2 r_0^2}\, r/r_0 = \sqrt{(1-\eta^2)a_0^2+\eta^2 s_1^2}\,\hat{r} \tag{4.1–50}$$

Substituting equations (4.1–49) and (4.1–50) into equation (4.1–46) results in the vertical component of the deformation field as a function of pile rotation:

$$w(r,\theta,z,t) = -e^{-i\omega t}\cos(\theta) r_0 \frac{H_1^{(1)}(\sqrt{(1-\eta^2)a_0^2+\eta^2 s_1^2}\,\hat{r})}{H_1^{(1)}(\sqrt{(1-\eta^2)a_0^2+\eta^2 s_1^2})} X'(z) \tag{4.1–51}$$

It is worth noting that the solution for the vertical deformation *'w'* results in nonzero dilatation. The dilatation reads:

$$\Delta = -r_0 \frac{H_1^{(1)}(\sqrt{(1-\eta^2)a_0^2+\eta^2 s_1^2}\,\hat{r})}{H_1^{(1)}(\sqrt{(1-\eta^2)a_0^2+\eta^2 s_1^2})} X''(z) \tag{4.1–52}$$

Vertical deformations being dilatational conclude that the vertical deformation field is a representative of P-waves travelling vertically.

The displacement field *'u,v,w'* should satisfy conditions of zero traction at the ground surface. The stresses at the free surface read:

$$\sigma_z\big|_{z=0} = e^{-i\omega t}\cos\theta\mu\eta^2 r_0 \frac{H_1^{(1)}(\sqrt{(1-\eta^2)a_0^2+\eta^2 s_1^2}\,\hat{r})}{H_1^{(1)}(\sqrt{(1-\eta^2)a_0^2+\eta^2 s_1^2})} X''(0) \tag{4.1–53}$$

$$\begin{aligned}\tau_{rz}\big|_{z=0} &= e^{-i\omega t}\cos\theta\mu \times \\ &\times\Big[\frac{H_1^{(1)}(\sqrt{(1-\eta^2)a_0^2+\eta^2 s_1^2}\,\hat{r}) - (\sqrt{(1-\eta^2)a_0^2+\eta^2 s_1^2}\,\hat{r})H_0^{(1)}(\sqrt{(1-\eta^2)a_0^2+\eta^2 s_1^2}\,\hat{r})}{\hat{r}H_1^{(1)}(\sqrt{(1-\eta^2)a_0^2+\eta^2 s_1^2})} + \\ &+ \frac{H_1^{(1)}(s_1\hat{r})}{\hat{r}H_1^{(1)}(s_1)}\Big] X'(0)\end{aligned} \tag{4.1–54}$$

$$\tau_{\theta z}\big|_{z=0} = e^{-i\omega t}\sin\theta\mu\Big[\frac{(s_1\hat{r})H_2^{(1)}(s_1\hat{r}) - H_1^{(1)}(s_1\hat{r})}{\hat{r}H_1^{(1)}(s_1)} + \frac{H_1^{(1)}(\sqrt{(1-\eta^2)a_0^2+\eta^2 s_1^2}\,\hat{r})}{\hat{r}H_1^{(1)}(\sqrt{(1-\eta^2)a_0^2+\eta^2 s_1^2})}\Big] X'(0) \tag{4.1–55}$$

It is clear that the above three stresses do not vanish at the free surface, unless certain end conditions are applied to the pile. Normal stress can be zero only if the curvature (and consequently the bending moment) of the pile at the ground surface is zero. The shear stresses, on the other hand, will be zero only if the pile rotation at the ground level is restricted. Since these conditions are not generally valid, the tractions at the free surface are

not zero. This remains a source of uncertainty in the solution. However, since the numerical value of the pile curvature and slope at the free surface are very small, the error is deemed negligible compared to other uncertainties involved in determining the elastic properties of the soil.

The following three stress components are applied at the pile-soil interface (i.e. at $r=r_0$) and are used in calculating the soil resistance on the pile:

$$\sigma_r\big|_{r=r_0} = e^{-i\omega t}\mu\cos\theta(\eta^2-2)r_0X''(z) \tag{4.1–56}$$

$$\tau_{r\theta}\big|_{r=r_0} = e^{-i\omega t}\mu\sin\theta\frac{1}{r_0}s_1^2X(z) \tag{4.1–57}$$

$$\tau_{rz}\big|_{r=r_0} = e^{-i\omega t}\cos\theta\mu[\sqrt{(1-\eta^2)a_0^2+\eta^2s_1^2}\frac{H_0^{(1)}(\sqrt{(1-\eta^2)a_0^2+\eta^2s_1^2})}{H_1^{(1)}(\sqrt{(1-\eta^2)a_0^2+\eta^2s_1^2})}]X'(z) \tag{4.1–58}$$

Using the equations (4.1–56) and (4.1–57) one can determine the soil reaction on the pile as:

$$q_x = -\int_{\theta=0}^{2\pi}(\sigma_r\cos\theta-\tau_{r\theta}\sin\theta)_{r=a}r_0d\theta = e^{i\omega t}\mu\pi[s_1^2X(z)-(\eta^2-2)r_0^2X''(z)] \tag{4.1–59}$$

The numerical value of 's_1^2' can be determined from Table 4-1 as: '$s_1^2=-1.457-i1.101$'. Vertical shear stress at the pile surface which is expressed by equation (4.1–58) imposes a distributed bending moment on the pile. The value of this bending moment is given in equation (4.1–60):

$$\begin{aligned} m_y &= \int_0^{2\pi}(r_0\cos\theta\tau_{rz})_{r=a}r_0d\theta = \\ &= e^{-i\omega t}r_0^2\pi\mu\sqrt{(1-\eta^2)a_0^2+\eta^2s_1^2}\frac{H_2^{(1)}(\sqrt{(1-\eta^2)a_0^2+\eta^2s_1^2})}{H_1^{(1)}(\sqrt{(1-\eta^2)a_0^2+\eta^2s_1^2})}X'(z) \end{aligned} \tag{4.1–60}$$

The equivalent distributed force on a beam under the simultaneous action of lateral load and distributed moment can be written using equation (2.2–23):

$$\begin{aligned} p_x &= -\frac{d}{dz}m_y+q_x = \\ &= e^{i\omega t}\mu\pi[s_1^2X(z)-(\eta^2-2-r_0^2\pi\mu\sqrt{(1-\eta^2)a_0^2+\eta^2s_1^2}\frac{H_2^{(1)}(\sqrt{(1-\eta^2)a_0^2+\eta^2s_1^2})}{H_1^{(1)}(\sqrt{(1-\eta^2)a_0^2+\eta^2s_1^2})})r_0^2X''(z)] \end{aligned} \tag{4.1–61}$$

4.1.3 Flexure equation of the pile

In the previous section, the displacement field in the soil was expressed as a function of pile lateral displacement and its second derivative (i.e. the pile curvature). In this section, the interaction between the pile and the soil is investigated by solving the flexure equation of the pile. Using the Euler-Bernouli beam theory, the flexure equation of the pile can be written as (Novak 1974):

$$E_p I_p \frac{\partial^4 x(z,t)}{\partial z^4} + N_{st} \frac{\partial^2 x(z,t)}{\partial z^2} + m_p \frac{\partial^2 x(z,t)}{\partial t^2} + c_p \frac{\partial x(z,t)}{\partial t} = p_x \tag{4.1–62}$$

Substituting equation (4.1–61) into equation (4.1–62) and setting $x(z,t) = e^{-i\omega t} X(z)$, leads to the following ordinary differential equation:

$$E_p I_p X^{(4)}(z) - k_{p\theta} X''(z) + k_{ps} X(z) = 0 \tag{4.1–63}$$

Where

$$k_{ps} = -\mu\pi s_1^2 - \omega^2 m_p - i\omega c_p \tag{4.1–64}$$

$$k_{p\theta} = \mu\pi r_0^2 [\eta^2 - 2 - \sqrt{(1-\eta^2)a_0^2 + \eta^2 s_1^2}\, \frac{H_2^{(1)}(\sqrt{(1-\eta^2)a_0^2 + \eta^2 s_1^2})}{H_1^{(1)}(\sqrt{(1-\eta^2)a_0^2 + \eta^2 s_1^2})} - \frac{\sigma_0}{\mu}] \tag{4.1–65}$$

Equation (4.1–65) is in the form of the Vlasov beam model (Vlasov and Leont'ev 1966) with complex-valued coefficients. Let us investigate an equivalent Winkler support model that results in the same deflected shape as the original beam. Such an equivalent beam with generalized spring stiffness (impedance) 'k_e' is expressed by the following flexure equation:

$$E_p I_p X^{(4)}(z) + k_e X(z) = 0 \tag{4.1–66}$$

The general solution to the above equation can be considered as a linear combination of exponential functions of the form e^{Dz}, where *'D's'* are four complex-valued roots of the algebraic equation:

$$E_p I_p D^4 + k_e = 0 \tag{4.1–67}$$

The function e^{Dz} should also satisfy equation (4.1–63), therefore:

$$E_p I_p D^4(z) - k_{p\theta} D^2 + k_{ps} = 0 \tag{4.1–68}$$

Eliminating *'D'* between equations (4.1–67) and (4.1–68) results in:

$$-k_e \mp k_{p\theta}\sqrt{\frac{-k_e}{E_p I_p}} + k_{ps} = 0 \tag{4.1–69}$$

After solving equation (4.1–69) for 'k_e' we will have:

$$k_e = k_{ps} - \frac{k_{p\theta}^2}{2E_p I_p}\left(1 + \sqrt{1 - 4E_p I_p \frac{k_{ps}}{k_{p\theta}^2}}\right) \cong k_{ps} - \frac{k_{p\theta}}{\sqrt{E_p I_p}}\sqrt{-k_{ps}} \tag{4.1–70}$$

In equation (4.1–70) the term '$I_s = \pi r_0^2 / 4$' holds for the second moment of inertia of the pile shaft. It is equal to the pile second moment of inertia *'I_p'* only if the pile cross-section is solid (non-tubular). It should be noted that in most practical cases, the order of magnitude of the term $E_p I_p / \mu I_s$ is very large compared to unity. Table 4-2 includes maximum and minimum values for soil and pile elastic modulus as well as calculated flexibility ratios. It can be seen that the value of $E_p I_p / \mu I_s$ has a minimum of 300 for solid concrete piles in soft clays. Compared to this value, the value of 1 in equation (4.1–70) can therefore be ignored. This is how the second approximate expression in the right-hand side of the equation (4.1–70) is derived.

Table 4-2 Maximum and minimum values for flexibility ratio of pile and soil

Value	μ (MPa)	E_p (GPa)	$\frac{E_p}{\mu}$	I_p/I_s	$\frac{E_p I_p}{\mu I_s}$	$\sqrt{\frac{\mu I_s}{E_p I_p}}$
Minimum	1(1)	30(3)	300	1(5)	300	5×10^{-2}
Maximum	100(2)	200(4)	200000	8 (6)	25000	6×10^{-3}

(1) Soft clays (Gunaratne 2006, Table 1.6)

(2) Dense gravel (sandy) (Gunaratne 2006, Table 1.6)

(3) Typical value for concrete piles

(4) Value for steel piles

(5) Value for solid concrete piles

(6) Value for tubular piles with diameter to thickness ratio of about 60

Substituting equations (4.1–64) and (4.1–65) into equation (4.1–70) results in:

$$k_e \cong \mu\pi\{-s_1^2 - \frac{\omega^2 m_p}{\mu\pi} - i\frac{\omega c_p}{\mu\pi} - 2[\eta^2 - 2 + \Omega\frac{H_2^{(1)}(\Omega)}{H_1^{(1)}(\Omega)} - \frac{\sigma_0}{\mu}]\sqrt{\frac{\mu I_s}{E_p I_p}}\sqrt{s_1^2 + \frac{\omega^2 m_p}{\mu\pi} + i\frac{\omega c_p}{\mu\pi}}\} \quad (4.1\text{–}71)$$

Where

$$\Omega = \sqrt{(1-\eta^2)a_0^2 + \eta^2 s_1^2} \quad (4.1\text{–}72)$$

4.1.4 Static stiffness of Winkler springs

The real part of equation (4.1–71) approaches the static value of the stiffness of Winkler springs for zero frequency:

$$k_e \cong \mu\pi\{-s_1^2 - 2s_1[\eta^2 - 2 - \frac{\sigma_0}{\mu} + \eta s_1\frac{H_2^{(1)}(\eta s_1)}{H_1^{(1)}(\eta s_1)}]\sqrt{\frac{\mu I_s}{E_p I_p}}\} \quad (4.1\text{–}73)$$

The term inside the brackets is difficult to evaluate in terms of simple functions, due to the presence of Hankel functions and the complex-valued factor *'s_1'*. It should be noted that when Poisson's ratio varies in the range of $0 \le \nu \le 0.5$, the factor η varies from $\sqrt{2}$ to 0. Curve fitting techniques are used to provide approximating functions for the real and imaginary parts of equation (4.1–73) with high accuracy:

$$\begin{aligned} &-2s_1[\eta^2 - 2 - \frac{\sigma_0}{\mu} + \eta s_1\frac{H_2^{(1)}(\eta s_1)}{H_1^{(1)}(\eta s_1)}] \cong \\ &3.432 - 0.316\eta + 25.002\eta^2 - 64.796\eta^3 + 39.355\eta^4 - 0.858\frac{\sigma_0}{\mu} + \\ &-i(10.248 + 2.132\eta - 26.778\eta^2 + 18.342\eta^3 + 2.562\frac{\sigma_0}{\mu}) \end{aligned} \quad (4.1\text{–}74)$$

The static Winkler spring stiffness is considered as the real part of equation (4.1–73), using the approximating function given in equation (4.1–74):

$$k_e^{Static} \cong$$

$$\mu\{4.577+\pi[3.432-0.316\eta+25.002\eta^2-64.796\eta^3+39.355\eta^4-0.858\frac{\sigma_0}{\mu}]\sqrt{\frac{\mu I_s}{E_p I_p}}\} \qquad (4.1\text{–}75)$$

Bahrami and Nikraz (2012) conducted a study into the static stiffness of Winkler springs by performing a large number of finite element analyses and applying curve fitting to the results. They proposed the following relationship for basic spring stiffness:

$$k_0=\mu[2.86+20.15(\frac{\mu}{E_p})^{0.40}][1+(\frac{\mu}{50E_p})^{0.0678}\frac{\nu}{1-\nu}] \qquad (4.1\text{–}76)$$

Equation (4.1–76) is comparable to equation (4.1–75) for its general form and parameters. Figure **4-1** plots the two equations over a practical range of modulus ratio. It can be seen that general agreement exists between the theoretical value and the values from the FE results, especially for stiffer soils.

Bothe theoretical curve and FE resulted curve show nonlinear relationship with modulus ratio. The FE resulted power of modulus ratio is 0.4 as stated in the equation (4.1–76). This is very close to the theoretically derived power of 0.5. Both theoretical and FE resulted curves have values for zero modulus ratio which are close in value.

For stiffer soils (i.e. modulus ratio greater than 5×10^{-3}) the values of theoretical and FE resulted carves are very close.

For softer soil, the theoretical relationship overestimates the FE values. The difference may be partly due to approximations included in the theory and partly due to the inaccuracies of the FE model, especially the finite length of the pile and the boundaries of the modeled soil.

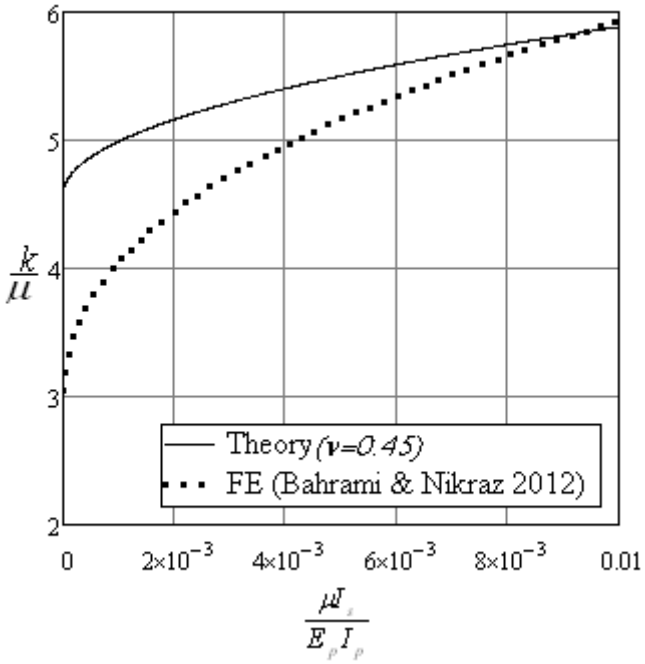

Figure 4-1 theoretical vs. FE values for Winkler spring stiffness

In section 3.2.4 the results of the FE study made in this thesis were compared to the most well-known stiffness values published in the literature. A similar comparison is made here also, using the Winkler spring stiffness derived in this section. The stiffness of a free-head pile with infinite length is given in Table 2-1 as:

$$K_h = 2E_p I_p \beta^3 \tag{4.1–77}$$

It is convenient to write equation (4.1–77) in terms of non dimensional parameters:

$$\frac{K_h}{\mu D} = \frac{\pi}{4} \frac{E_p I_p}{\mu I_s} \left(\frac{\mu I_s}{E_p I_p} \frac{k_e^{Static}}{\pi \mu}\right)^{\frac{3}{4}} \tag{4.1–78}$$

Figure 3-8 compares the stiffness values of some of the most well-known expressions published in the literature with the FE results reported in Chapter 3. Here we add the stiffness values from equation (4.1–78) to this figure for comparison (Figure 4-2). It can be seen that general agreement exists between the theoretically obtained stiffness and the other results.

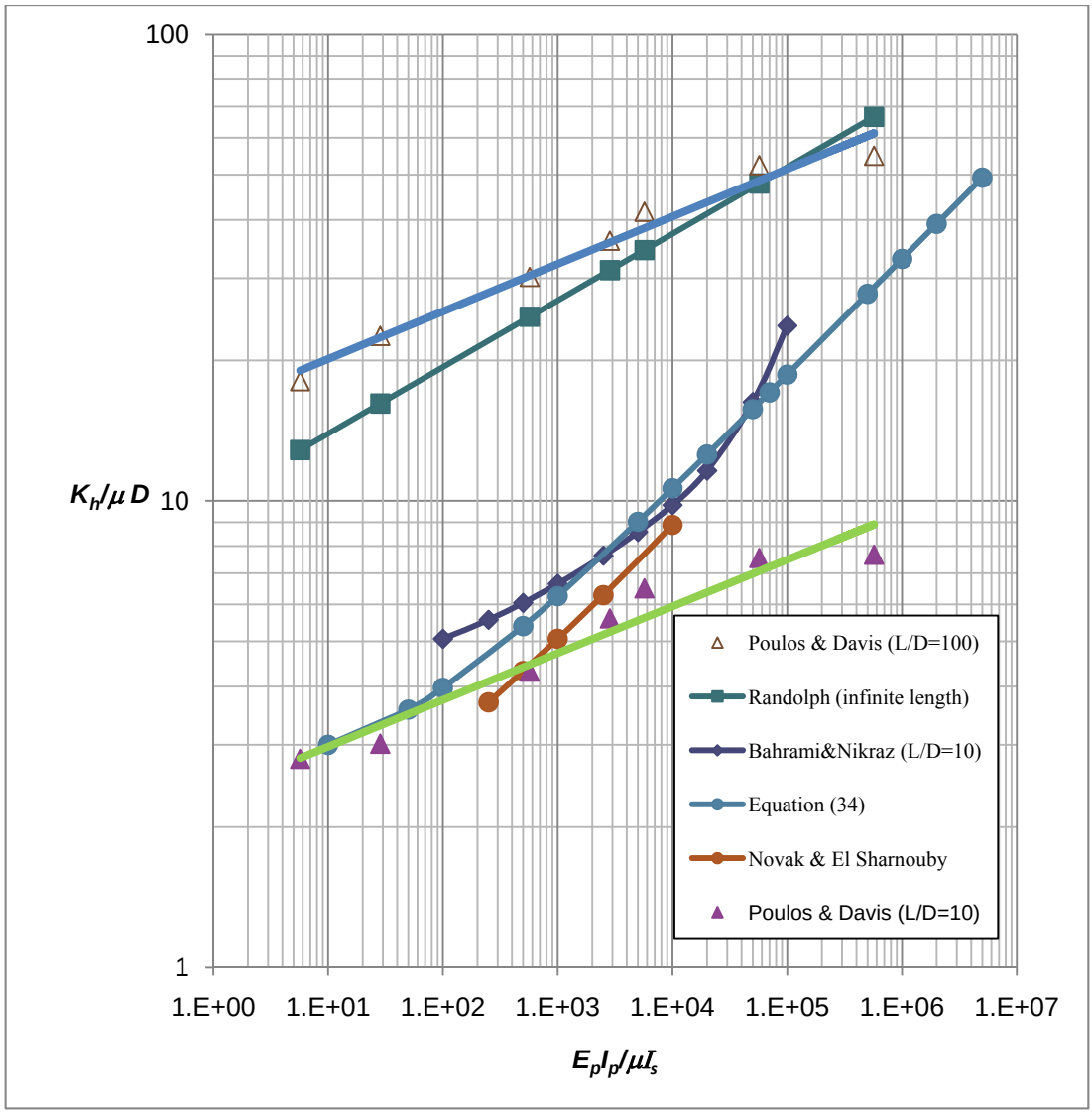

Figure 4-2 Non-dimensional stiffness ratio vs. pile modulus ratio by different authors

4.1.5 Low frequency limit for spring stiffness, soil mass and damping

In order to expand the Winkler spring properties for dynamic conditions, limiting frequencies are considered. We start with a low frequency limit which corresponds to vibrations with low frequencies. These frequencies are important in earthquake analysis. To define the low frequency limit, we consider the following expansions which provide two limiting expressions for the non-dimensional frequency factor:

$$\begin{cases} \sqrt{s_1^2+\dfrac{\omega^2 m_p}{\mu\pi}+i\dfrac{\omega c_p}{\mu\pi}}=\sqrt{s_1^2+\dfrac{a_0^2 m_p}{\rho A_s}+i\dfrac{a_0 c_p}{\sqrt{\pi\mu\rho A_s}}}\cong \\ \qquad\cong s_1+\dfrac{a_0^2 m_p}{2s_1\rho A_s}+i\dfrac{a_0 c_p}{2s_1\sqrt{\pi\mu\rho A_s}} \qquad if \quad a_0 << \sqrt{|s_1^2|\sqrt{\dfrac{\rho A_s}{m_p}}-\dfrac{c_p^2}{\pi\mu m_p}} \\ \Omega=\sqrt{(1-\eta^2)a_0^2+\eta^2 s_1^2}\cong \eta s_1 \qquad if \quad a_0 << \dfrac{\eta|s_1|}{\sqrt{1-\eta^2}}, \quad |s_1|=1.351 \end{cases} \tag{4.1–79}$$

The more stringent of the two limits given in equation (4.1–79) defines the low frequency limit for a particular problem. For most cases of saturated soils where Poisson's ratio is close to 0.5 (i.e. η is close to zero), the second limit governs. For nonsaturated soils there might be cases when the first condition governs.

After substituting expressions (4.1–79) into equation (4.1–71) we will have:

$$\mathrm{Re}(k_e^{Low})\cong k_e^{Static}+\pi\mu(a_0^2\frac{m_p}{\rho A_s}F_1-a_0\frac{c_p}{\sqrt{\pi\mu\rho A_s}}F_3)\sqrt{\frac{\mu I_s}{E_p I_p}}-\omega^2 m_p(1+F_2\sqrt{\frac{\mu I_s}{E_p I_p}}) \tag{4.1–80}$$

$$\begin{aligned}\mathrm{Im}(k_e^{Low})\cong{}&\mu\{3.453-\pi(10.248+2.132\eta-26.778\eta^2+18.342\eta^3+2.562\frac{\sigma_0}{\mu})\sqrt{\frac{\mu I_s}{E_p I_p}}\}+\\&-\omega[c_p-(c_p F_4+a_0 m_p F_3\sqrt{\frac{\pi\mu}{\rho A_s}})\sqrt{\frac{\mu I_s}{E_p I_p}}]\end{aligned} \tag{4.1–81}$$

In equations (4.1–80) and (4.1–81) the positive real-valued functions *'F_1'* to *'F_4'* are obtained by curve fitting on the calculated values. The accuracy of these functions is excellent:

$$\begin{cases} F_1=0.944+0.268\eta-2.274\eta^2+1.360\eta^3-0.236\dfrac{\sigma_0}{\mu} \\ F_2=\eta(9.630\eta^3-17.378\eta^2+8.336\eta-0.248) \\ F_3=2.808+0.713\eta-3.961\eta^2-1.796\eta^3+3.238\eta^4-0.702\dfrac{\sigma}{\mu} \\ F_4=0.944+0.515\eta+10.610\eta^2+18.739\eta^3-9.630\eta^4-0.236\dfrac{\sigma}{\mu} \end{cases} \tag{4.1–82}$$

The real part of the complex-valued stiffness is composed of two parts. The first part is the static stiffness plus a frequency-dependent term. The frequency-dependent terms have elements of relative mass of the pile 'm_p' and mass of the removed (displaced) soil 'ρA_s'. Material damping of the pile also exists in this term. The second term is expressed as a

constant value added to the mass of the pile. This term is interpreted as the contributing mass of the soil to the pile vibrations. It should be noted that the added mass vanishes for incompressible soils where Poisson's ratio equals 0.5 (e.g. saturated clays). The following relationships are proposed for the stiffness and the contributing mass of the soil:

$$k_s^{Low} = k_e^{Static} + \pi\mu(a_0^2 \frac{m_p}{\rho A_s} F_1 + a_0 \frac{c_p}{\sqrt{\pi\mu\rho A_s}} F_3)\sqrt{\frac{\mu I_s}{E_p I_p}} \tag{4.1–83}$$

$$m_s = m_p F_2 \sqrt{\frac{\mu I_s}{E_p I_p}} \tag{4.1–84}$$

The imaginary part of the complex-valued stiffness is considered to be damping. It can be seen from equation (4.1–81) that low frequency damping is also composed of two components. The first component is frequency-independent; therefore it can be interpreted as hysteretic damping. The second part is frequency-dependent; therefore it is analogous to viscous damping.

4.1.6 High frequency asymptotic values for spring stiffness, soil mass and damping

In a high frequency regime, we ignore the value of $\pi\mu s_1^2$ against $\omega^2 m_p + i\omega c_p$ under the square root sign of equation (4.1–71). Using asymptotic expansion of the Hankel function (Abramowitz and Stegun 1972) the following reads:

$$a_0 \to \infty \Rightarrow \quad \begin{cases} \sqrt{s_1^2 + \frac{\omega^2 m_p}{\mu\pi} + i\frac{\omega c_p}{\mu\pi}} \cong a_0 \sqrt{\frac{m_p}{\rho A_s}}(1 + i\frac{c_p}{2a_0 m_p}\sqrt{\frac{\rho A_s}{\mu\pi}}) \\ \Omega\frac{H_2^{(1)}(\Omega)}{H_1^{(1)}(\Omega)} = a_0\sqrt{1-\eta^2}\,\frac{H_2^{(1)}(a_0\sqrt{1-\eta^2})}{H_1^{(1)}(a_0\sqrt{1-\eta^2})} \cong \frac{3}{2} - ia_0\sqrt{1-\eta^2} \end{cases} \tag{4.1–85}$$

After substituting equation (4.1–85) into equation (4.1–71) we will have:

$$\begin{aligned} k_e \cong \mu\pi\{&-s_1^2 - \frac{\omega^2 m_p}{\mu\pi} - i\frac{\omega c_p}{\mu\pi} + \\ &-2a_0[\eta^2 - 3.5 - \frac{\sigma_0}{\mu} + ia_0\sqrt{1-\eta^2}](1 + i\frac{c_p}{2a_0 m_p}\sqrt{\frac{\rho A_s}{\mu\pi}})\sqrt{\frac{m_p}{\rho A_s}\frac{\mu I_s}{E_p I_p}}\} \end{aligned} \tag{4.1–86}$$

The real and imaginary parts of equation (4.1–86) are expressed as follows:

$$\mathrm{Re}(k_e^{High}) = 4.577\mu + \\ + \pi a_0[7\mu + 2\sigma_0 + \frac{c_p}{m_p}\sqrt{(1-\eta^2)\frac{\rho A_s}{\mu\pi}}]\sqrt{\frac{m_p}{\rho A_s}\frac{\mu I_s}{E_p I_p}} - \omega^2[m_p(1+\frac{2\eta^2}{a_0}\sqrt{\frac{\rho A_s}{m_p}\frac{\mu I_s}{E_p I_p}})] \quad (4.1\text{–}87)$$

$$\mathrm{Im}(k_e^{High}) = 3.459\mu + \\ + \pi(3.5\mu - \mu\eta^2 + \sigma_0)\frac{c_p}{\sqrt{\pi\mu m_p}}\sqrt{\frac{\mu I_s}{E_p I_p}} - \omega[c_p + 2a_0\sqrt{\pi\mu(1-\eta^2)m_p}\sqrt{\frac{\mu I_s}{E_p I_p}}] \quad (4.1\text{–}88)$$

In equation (4.1–87) we combined two frequency-related terms with the mass of the pile and, similarly for the low frequency regime, we interpreted these terms as the contributing mass of the soil. Unlike the low frequency case, the contributing mass of the soil is inversely related to the non-dimensional frequency.

The imaginary part of the Winkler springs stiffness is interpreted as damping. In a high frequency regime, the damping is composed of a hysteretic damping and a viscous damping. Table **4-3** summarizes characteristic values for stiffness, damping and mass of the soil in different frequency regimes.

Table 4-3 Summary of equivalent generalized Winkler springs properties

Factor	Low frequency limit	High frequency limit
k_s	$k_e^{Static} + \\ + \pi\mu(a_0^2 \frac{m_p}{\rho A_s} F_1 + a_0 \frac{c_p}{\sqrt{\pi\mu\rho A_s}} F_3)\sqrt{\frac{\mu I_s}{E_p I_p}}$	$4.577\mu + \\ + \pi a_0[7\mu + 2\sigma_0 + \frac{c_p}{m_p}\sqrt{(1-\eta^2)\frac{\rho A_s}{\mu\pi}}]\sqrt{\frac{m_p}{\rho A_s}\frac{\mu I_s}{E_p I_p}}$
m_s	$m_p F_2 \sqrt{\frac{\mu I_s}{E_p I_p}}$	$m_p \frac{2\eta^2}{a_0}\sqrt{\frac{\rho A_s}{m_p}\frac{\mu I_s}{E_p I_p}}$
c_h	$\mu\{3.459 - \\ \pi(10.248 + 2.132\eta - 26.778\eta^2 \\ + 18.342\eta^3 + 2.562\frac{\sigma_0}{\mu})\sqrt{\frac{\mu I_s}{E_p I_p}}\}$	$3.459\mu + \pi(3.5\mu - \mu\eta^2 + \sigma_0)\frac{c_p}{\sqrt{\pi\mu m_p}}\sqrt{\frac{\mu I_s}{E_p I_p}}$
c_s	$-(c_p F_4 + a_0 m_p F_3\sqrt{\frac{\pi\mu}{\rho A_s}})\sqrt{\frac{\mu I_s}{E_p I_p}}$	$2a_0\sqrt{\pi\mu(1-\eta^2)m_p}\sqrt{\frac{\mu I_s}{E_p I_p}}$

4.1.7 The properties of Winkler springs for a general range of frequencies

It is not possible to expand equation (4.1–71) to its real and imaginary parts for a general range of frequencies in terms of simple functions. In practical cases, one may evaluate equation (4.1–71) numerically and treat the real and imaginary parts as the impedance and the geometric damping. However, if this path is taken it is impossible to separate the stiffness and mass properties, as well as the hysteretic and viscous damping. It may be desirable to provide interpolating functions that give relevant values for stiffness, mass and damping of the soil for intermediate frequencies. Bahrami and Nikraz (2013) expanded the results of a plane strain solution (Baranov 1967) to stiffness, mass and damping parameters and presented the results in terms of elementary functions of non-dimensional frequency. A summary of this work appears in section 4.1.9.1. Their formulas for stiffness, mass and damping involved terms with powers of -1.5, -3 and -1 for non-dimensional frequency, respectively. Complying with their results, we propose the following interpolating functions:

$$m_s = \frac{m_s^{Low} + m_s^{High} a_0^3}{1 + a_0^3} \qquad (4.1–89)$$

$$k_s = \frac{k_s^{Low} + k_s^{High} a_0^{1.5}}{1 + a_0^{1.5}} \tag{4.1–90}$$

$$c = \frac{c^{Low} + c^{High} a_0}{1 + a_0} \tag{4.1–91}$$

In the above formulas the superscripts *'Low'* and '*High'* refer to low and high frequency limits of particular parameters included in Table 4-3

The term *'c'* holds for both hysteretic and viscous damping. Figure 4-3 compares low, high and intermediate stiffness formulas with the exact theoretical stiffness value obtained from equation (4.1-51). It can be seen that the high frequency limit approaches the exact value for larger frequencies. The low frequency formula provides good estimates for non-dimensional frequencies less than unity. The interpolating function given in equation (4.1–90) provides fair estimates for almost the entire range of frequencies. However, it is not as accurate as the low frequency formula for non-dimensional frequencies between 0.3 and 1.0. For practical purposes, equation (4.1–90) can be used to effectively calculate the stiffness of the Winkler springs. Similar conclusions may be made for damping and mass values.

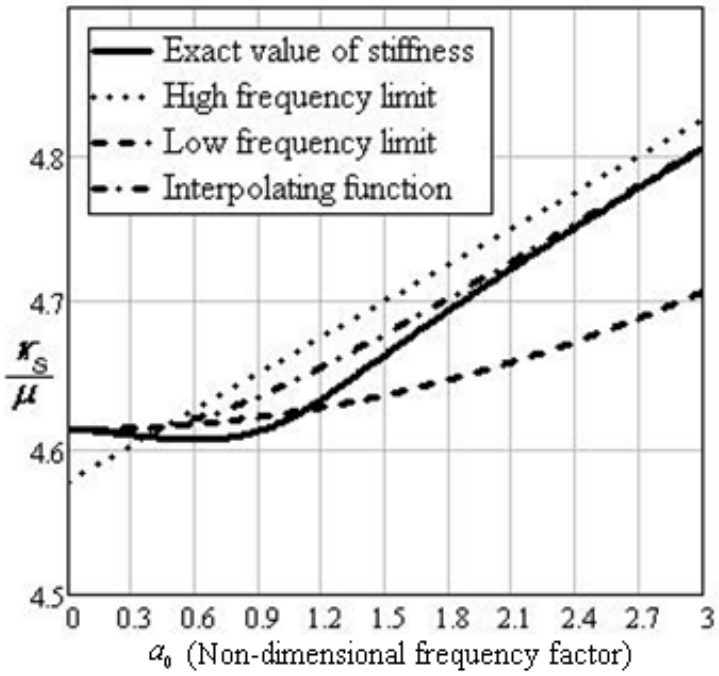

Figure 4-3 Frequency-dependent stiffness of Winkler springs

It should be noted that in order to obtain the stiffness, the inertia terms $\omega^2(m_p + m_s)$ should be eliminated from the real part of equation (4.1–71) such that the solid line in Figure 4-3 represents the stiffness of the Winkler springs which is always a positive values. If the inertia terms were not eliminated, the real part of equation (4.1–71) would become negative for most of the frequencies, especially for softer soils.

4.1.8 Effect of hysteretic damping of the soil

The energy dissipation behavior of soil can be best expressed by hysteretic damping properties (Verruijt 2010). One method of including hysteretic damping of the soil in elastodynamic equations is by introducing a complex-valued shear modulus $\mu' = \mu(1 + i2\xi_{sh})$ (e.g. Nogami and Novak 1977). After substitution and some algebraic manipulations we will have:

$$\begin{aligned} k'_{pe} &\cong (1 + i2\xi_{sh})[k_s - \omega^2 m_s - i(c_h + \omega c_s)] = \\ &= k_s + 2\xi_{sh}(c_h + \omega c_s) - \omega^2 m_s - i[c_h + \omega c_s - 2\xi_{sh}(k_s - \omega^2 m_s)] \end{aligned} \quad (4.1\text{–}92)$$

The real and imaginary parts of equation (40) determine the stiffness and damping of the soil.

4.1.9 Other solutions

In this section we will discuss and compare the results of the present theory with some existing solutions.

4.1.9.1 Plane strain model

The Baranov (1967) solution is used as the underlying theory for most plane strain models (section 2.4.1). The soil reaction on the side surface of a laterally loaded cylindrical embedded foundation is given for steady-state dynamic conditions. The soil reaction on the pile is considered to be a laterally distributed force *'q'* which is the result of normal stress and horizontal shear stress. Most plane strain models ignore the effect of vertical shear stress on the pile. In the case of a soft pile surface or very low skin friction, slippage may take place between the pile and the soil. In such cases the effect of shear stresses becomes minimal. The Baranov (1967) formulation for soil resistance on the pile is given in equation (2.4–15). Bahrami and Nikraz (Bahrami and Nikraz 2013) have rewritten factor *'c_2'* in equation (2.4–16) as follows:

$$c_2 = \pi\mu a_0^2 [1 + \frac{2H_2^{(2)}(a_0)}{H_0^{(2)}(a_0) + H_2^{(2)}(a_0)\dfrac{H_0^{(2)}(\eta a_0)}{H_2^{(2)}(\eta a_0)}}] \quad (4.1\text{–}93)$$

Consider a single degree of freedom (SDOF) system of a mass *'m'*, a linear spring *'k'* and a dashpot *'c'* vibrating with a constant frequency 'ω'. The force acting on the mass can be expressed as $(k - \omega^2 m + ic\omega)u_1 e^{i\omega t}$. By analogy, the real part of equation (4.1–93) can be interpreted as the sum of the soil stiffness and the combined mass of the pile and the soil.

The imaginary part of equation (4.1–93) serves as a measure of the geometrical damping of the soil, also known as radiation damping. It would be useful if we could write the real and imaginary parts of the equation (4.1–93) in a format that could be easily compared with an SDOF system. Due to the complexity of this equation, it is not possible to readily derive a simple representation of its real and imaginary parts. The limit of the term $H_0^{(2)}(sa_0)/H_2^{(2)}(sa_0)$ for $\nu \to 0.5$ (i.e. $\eta \to 0$) can be taken using the expansion of Hankel functions for small arguments (Abramowitz and Stegun 1972, Formulas 9.1.8 & 9.1.9). It is easy to prove that this limit exists and is equal to zero. After some mathematical manipulations, equation (4.1–93) can be written for soils with a Poisson's ratio equal to 0.5 as:

$$c_2 = \pi\mu\{[4\frac{J_1^2(a_0)+Y_1^2(a_0)}{J_0^2(a_0)+Y_0^2(a_0)} - \frac{J_2^2(a_0)+Y_2^2(a_0)}{J_0^2(a_0)+Y_0^2(a_0)}a_0^2] + ia_0[4\frac{J_1(a_0)Y_0(a_0)-J_0(a_0)Y_1(a_0)}{J_0^2(a_0)+Y_0^2(a_0)}] \quad (4.1\text{–}94)$$

Equation (4.1–94) is analogous to the force expression on an SDOF system. The imaginary part is written as a multiple of *'a_0'* and resembles the dashpot constant in the SDOF system. The real part is composed of a positive term and a negative term. The positive term resembles the stiffness of the SDOF system. The negative term which is a factor of a_0^2 resembles the mass of an SDOF system. Variations of these factors with non-dimensional frequency are shown in Figure 4-4.

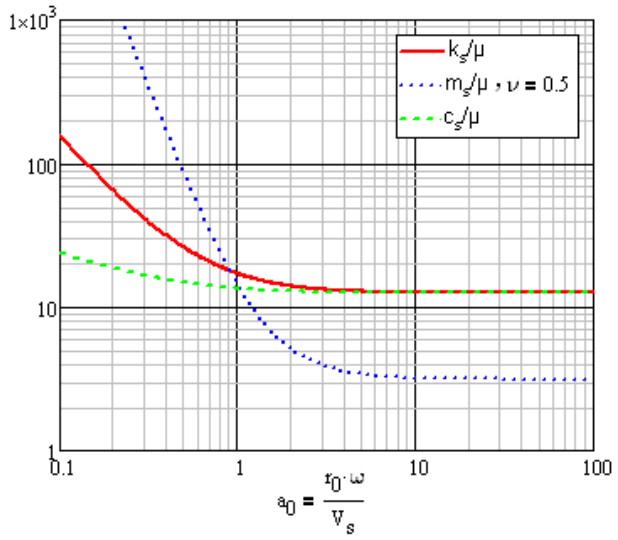

Figure 4-4- Stiffness, mass and damping of soil (plane strain model)

Formulas for stiffness, mass and damping are given in equation (4.1–95). Since these equations are in terms of Bessel functions, approximating functions based on elementary functions are proposed, using curve fitting techniques:

$$\begin{cases} k_s = 4\pi\mu \dfrac{J_1^2(a_0)+Y_1^2(a_0)}{J_0^2(a_0)+Y_0^2(a_0)} \cong 4\pi\mu(1+\dfrac{7}{20\sqrt{a_0^3}}) \\ m_s = \rho\pi r_0^2 \dfrac{J_2^2(a_0)+Y_2^2(a_0)}{J_0^2(a_0)+Y_0^2(a_0)} \cong \rho\pi r_0^2(1+\dfrac{4}{a_0^3}) \\ c_s = (2\rho V_s)(2\pi r_0)\dfrac{J_1(a_0)Y_0(a_0)-J_0(a_0)Y_1(a_0)}{J_0^2(a_0)+Y_0^2(a_0)} \cong 12.6\rho V_s r_0(1+\dfrac{1}{10a_0}) \end{cases} \quad (4.1\text{–}95)$$

The powers of the non-dimensional frequencies in the above functions are used in section 4.1.7 to establish interpolating functions. However, the values of stiffness and mass of the soil are overestimated by the plane strain model when compared to the similar values of the present theory.

4.1.9.2 Plane deformation model

Nogami and Novak (1977) developed a 3D solution which assumed zero vertical displacement in the soil media. Since their model only implements horizontal deformations, it could be seen as a plane deformation model. Their solution (section 2.4.3) is in the form of a generalized beam on Winkler support for each mode of vibration:

$$p(z) = \pi r_0 \mu \sum_{n=0}^{\infty} (1+iD_s) h_n^2 T_n U_n \sin(h_n z) \quad (4.1\text{–}96)$$

Where *'T_n'* is an expression in terms of modified Bessel functions with arguments of non-dimensional frequency. The expression of *'T_n'* is given in the abovementioned paper but is not repeated in this thesis for the sake of brevity. For a statically loaded pile (i.e. $\omega \to 0$) and for $\nu \to 0.5$, this expression reaches the following limit:

$$p(z) = \pi_0 \mu \sum_{n=1}^{\infty} h_n^2 r_0^2 [1 + \frac{4K_1(h_n r_0)}{h_n r_0 K_0(h_n r_0)}] U_n \sin(h_n z) \quad (4.1\text{–}97)$$

In equation (4.1–97) *'K_n'* is a modified Bessel function of the second kind of order *'n'*. For an infinitely deep layer of soil (i.e. $H \to \infty, h_n \to 0$), we will have:

$$p(z) = 4\pi\mu\sum_{n=1}^{\infty} U_n \sin(h_n z) = 4\pi\mu X(z) \qquad (4.1\text{–}98)$$

By analogy to the problem of a beam on Winkler springs, it can be concluded that the static stiffness of the springs equals the value of $4\pi\mu$ (for soils with a Poisson's ratio of 0.5). This value is equivalent to the stiffness value obtained from the plane strain model for very high frequencies. This similarity, however, cannot be justified as we have already noted that a plane strain model reaches zero stiffness at zero frequency. Equation (4.1–75) gives the static stiffness of Winkler supports which can be rewritten for $\nu \to 0.5$ as:

$$k_e^{Static} \cong \mu\{4.577 + \pi[3.432 - 0.858\frac{\sigma_0}{\mu}]\sqrt{\frac{\mu I_s}{E_p I_p}}\} \qquad (4.1\text{–}99)$$

The difference between equations (4.1–98) and (4.1–99) is considerable, especially for softer soils.

4.1.9.3 Simplified method

There are a number of simplified methods in the literature for calculating dynamic factors for pile analysis. Gazetas and Dobry (1984) have taken a simplified approach towards the evaluation of geometrical soil damping. Markis and Gazetas (1992) proposed the following values for stiffness and damping to be used in lateral pile analyses:

$$\begin{cases} k_s \approx 1.2E_s = 2.4(1+\nu)\mu \\ c_s \approx 6a_0^{-1/4}\rho V_s d + 2\xi_s \dfrac{k_s}{\omega} \end{cases} \qquad (4.1\text{–}100)$$

The stiffness value above is very close to the static value given in (4.1–99) for $\nu \to 0.5$, with a slight underestimation. The damping term of equation (4.1–100) has frequency terms in the denominator which results in a very high damping factor for low frequencies.

It is believed that the theory developed in the present thesis removes most of the weaknesses in the existing dynamic pile solutions. The good agreement with the FE results and the mathematical robustness for very high and very low frequencies (including zero frequency) lead us to believe that this theory can be considered a fundamental theory for soil-pile interaction analysis.

4.2 Axially loaded piles

A theory for axially loaded piles is developed in this section. Existing closed-form solutions for axially loaded piles have been briefly discussed in section 2.5. In this section we provide a solution to the soil-pile interaction problem in order to remove the shortcomings of the solution given by Nogami and Novak (1976).

4.2.1 Problem definition and assumptions

The pile is considered to be a prismatic vertical member extended through the full depth of the elastic homogeneous soil layer. Soil layer thickness is *'H'*, overlaying rigid bedrock. The pile is under axial excitation force $P_0 e^{i\omega t}$ at its head. The soil is considered uniform, i.e. its shear modulus is constant with depth. Soil density 'ρ' and Poisson's ratio 'ν' are also constant with depth. Figure 4-5 shows the configuration and main parameters of the problem. The aim of this section is to provide a solution to the elastodynamic equations, satisfying boundary conditions.

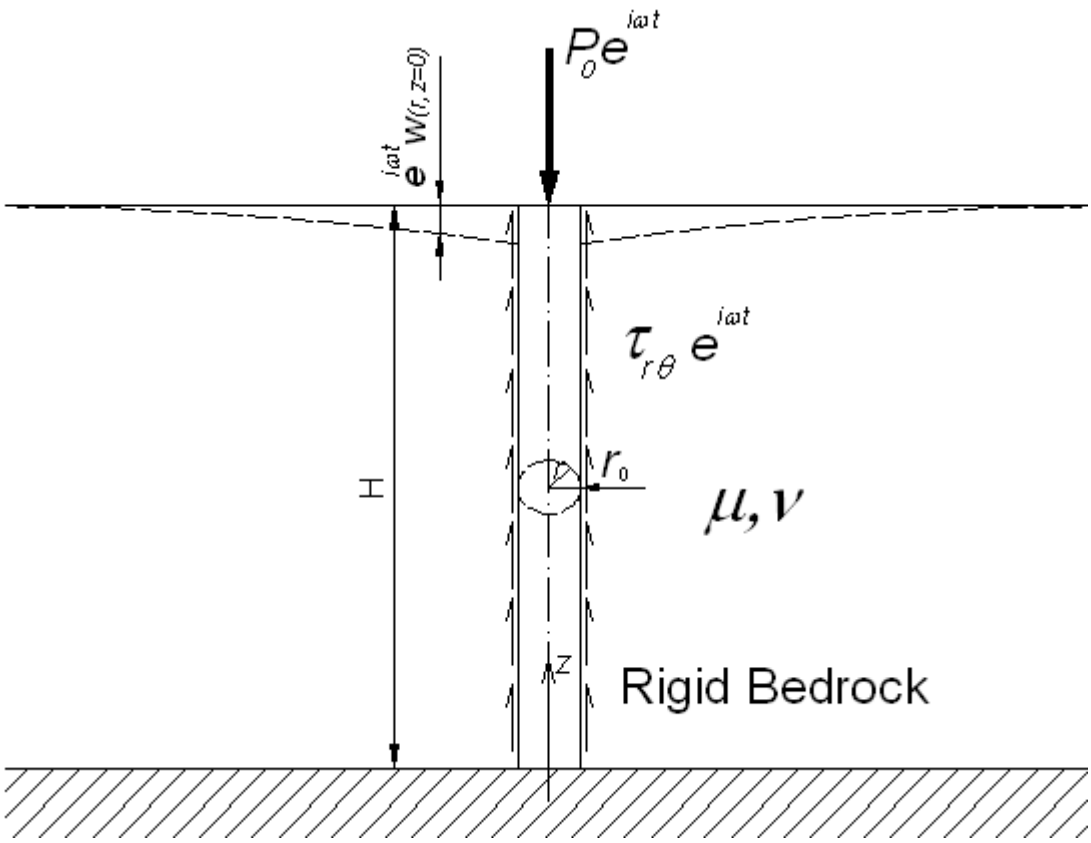

Figure 4-5 Pile under axial excitation force

4.2.2 Solution to elastodynamic equations

A solution to elastodynamic equations in the soil media has been provided by Nogami and Novak (1976):

$$w(r,z,t) = e^{i\omega t}\sum_{n=1}^{\infty} A_n K_0(q_n r)\sin(h_n z) \tag{4.2–1}$$

Where *'K_0'* denotes a modified Bessel function of the second kind of order zero and:

$$\begin{cases} h_n = (2n-1)\dfrac{\pi}{2H}, \quad n = 1,2,3...\infty \\ q_n^2 = \dfrac{(1+i2\xi_{sh})\eta^2 h_n^2 - (\omega/V_s)^2}{1+i2\xi_{sh}} \end{cases} \tag{4.2–2}$$

Note that in equation (4.2–1), the origin of the coordinate axis is located on the bedrock (i.e. 'z' points upwards). Factor *'A_n'* remained undetermined in the original paper of Nogami and Novak (1976). It can be determined, however, assuming that a perfect connection exists between the pile and the soil. If the vertical contraction (extension) of the pile is denoted as $v(z,t) = e^{i\omega t}V(z)$, the continuity condition between the pile and the adjacent soil can be written as:

$$V(z)e^{i\omega t} = e^{i\omega t}\sum_{n=1}^{\infty} A_n K_0(q_n r_0)\sin(h_n z) \tag{4.2–3}$$

Coefficient *'A_n'* can be determined by multiplying both sides of the above equation by '$\sin(h_n z)$' and integrating from zero to *'H'*:

$$A_n = \frac{2}{HK_0(q_n r_0)}\int_0^H V(z)\sin(h_n z)dz \tag{4.2–4}$$

The soil reaction on the pile is also derived (Nogami and Novak 1976) as:

$$p(z,t) = -2\pi r_0 \mu(1+2\xi_{sh}i)e^{i\omega t}\sum_{n=1}^{\infty} A_n q_n K_1(q_n r_0)\sin(h_n z) \tag{4.2–5}$$

The governing differential equation for the vertical pile deformation can be written as:

$$m_p \frac{\partial^2}{\partial t^2}v(z,t) + c_p \frac{\partial}{\partial t}v(z,t) - E_p A_p \frac{\partial^2}{\partial z^2}v(z,t) = p(z,t) \tag{4.2–6}$$

After some algebra the above equation simplifies to:

$$E_p A_p V''(z) + (m_p \omega^2 - i\omega c_p) V(z) = 2\pi r_0 \mu (1 + 2\xi_{sh} i) \sum_{n=1}^{\infty} C_n \sin(h_n z) \tag{4.2–7}$$

Where ' $C_n = A_n q_n K_1(q_n r_0)$ ' is a constant. The above equation should be solved for the following boundary conditions:

$$\begin{cases} V(z=0) = 0 \\ E_p A_p V'(z=H) = -P_0 \end{cases} \tag{4.2–8}$$

The first condition holds for zero displacement at the pile tip (bedrock) and the second is derived from vertical load applied at the pile head. Pile head deformation ' $V(\hat{z}=0) = V_0$ ' will be determined after the solution is completed. The Laplace transform method is employed in order to solve the differential equation (4.2–7). The following relationships are valid for the Laplace transform of function ' $V(\hat{z})$ ':

$$\int_0^{\infty} V(z) e^{-sz} dz = V(s) \tag{4.2–9}$$

$$\int_0^{\infty} V'(z) e^{-sz} dz = sV(s) - V(0) \tag{4.2–10}$$

$$\int_0^{\infty} V''(z) e^{-sz} dz = s^2 V(s) - sV(0) - V'(0) \tag{4.2–11}$$

$$\int_0^{\infty} \sin(h_n z) e^{-sz} dz = \frac{h_n}{s^2 + h_n^2}, \quad h_n = (2n-1)\frac{\pi}{2H} \tag{4.2–12}$$

$$f^2 = \frac{m_p \omega^2 - i\omega c_p}{E_p A_p} \tag{4.2–13}$$

$$g^2 = r_0 \frac{\mu(1 + 2\xi_{sh} i)}{E_p} \frac{1}{A_p} \tag{4.2–14}$$

Taking the Laplace transform of equation (4.2–7) and using the above relationships leads to the following equation in terms of the Laplace transform of ' $V(s)$ ':

$$V(s) = V'(0) \frac{1}{s^2 + f^2} + 2\pi g^2 \sum_{n=1}^{\infty} C_n \frac{h_n}{f^2 - h_n^2} \left(\frac{1}{s^2 + h_n^2} - \frac{1}{s^2 + f^2} \right) \tag{4.2–15}$$

Note that 's' in the above equations is the Laplace transform parameter and will disappear as soon as the inverse transform is derived.

Using tables of Laplace transforms (e.g. Pipes and Harvill 1970), the inverse transform of equation (4.2–15) is found to be:

$$V(z) = V'(0)\frac{1}{f}\sin(fz) + 2\pi g^2 \sum_{n=1}^{\infty} C_n \frac{1}{f^2 - h_n^2}[\sin(h_n z) - \frac{h_n}{f}\sin(fz)] \qquad (4.2\text{–}16)$$

Taking the derivative of the above equation and applying the boundary condition at the pile head (i.e. $V'(z = H) = -\frac{P_0}{E_p A_p}$) leads to:

$$V'(0) = -\frac{P_0}{E_p A_p \cos(fH)} + 2\pi g^2 \sum_{n=1}^{\infty} C_n \frac{h_n}{f^2 - h_n^2} \qquad (4.2\text{–}17)$$

The resonant frequencies of the pile can be determined as the frequencies that, in the absence of damping, cause infinite deformation. The resonance frequency associates with $f = h_n = (2n-1)\pi / 2H$ which results in:

$$\omega_r = \frac{1}{H}\sqrt{(2n-1)\pi \frac{E_p A_p}{2m_p}} \qquad (4.2\text{–}18)$$

Substituting equation (4.2–17) into equation (4.2–16) leads to:

$$V(z) = -\frac{P_0}{E_p A_p}\frac{\sin(fz)}{f\cos(fH)} + 2\pi g^2 \sum_{n=1}^{\infty} C_n \frac{1}{f^2 - h_n^2}\sin(h_n z) \qquad (4.2\text{–}19)$$

The constant *'A_n'* can now be determined. Multiplying equation (4.2–19) by '$\sin(h_n z)$' and integrating it from *0* to *H* yields:

$$\int_0^H V(z)\sin(h_n z)dz = (-1)^n \frac{P_0}{E_p A_p}\frac{1}{f^2 - h_n^2} + \pi g^2 H C_n \frac{1}{f^2 - h_n^2} \qquad (4.2\text{–}20)$$

Substituting equation (4.2–20) into equation (4.2–4) and noting that: '$C_n = A_n q_n K_1(q_n r_0)$' yields:

$$A_n = (-1)^n \frac{P_0}{E_p A_p H}\frac{2}{K_0(q_n r_0)(f^2 - h_n^2) - 2\frac{\mu(1 + i2\xi_{sh})}{E_p A_p}(q_n r_0)K_1(q_n r_0)} \qquad (4.2\text{–}21)$$

It should be noted that solution (4.2–1) for deformations in soil media holds for a progressive (downwards) wave and its reflection from the bedrock. This can be investigated by writing the sine function in its exponential form: $\sin(h_n z) = (e^{ih_n z} - e^{-ih_n z})/2i$ which leads to a series of progressive waves in the form of $e^{i(\omega t - h_n z)}$ and reflected waves in the form of $e^{i(\omega t + h_n z)}$. The latter reflect again from the free surface. The equation for reflected waves is similar to that for progressive waves with a reversed sign of time (i.e. the term $e^{-i\omega t}$ should be used instead of $e^{i\omega t}$). The response of the pile to the reflected wave is similar to the response to the progressive waves. Therefore, the solution procedure and the results are also similar. The only difference is in the application of boundary conditions. Since the stress at the pile head is used once when deriving the response to the progressive waves, it should not be included again in the response to the reflected waves. Therefore we may write:

$$V_R'(0) = 2\pi g^2 \sum_{n=1}^{\infty} C_n \frac{h_n}{f^2 - h_n^2} \tag{4.2–22}$$

Index *'R'* in the above equation holds for the response to reflected waves from the free surface. The response to the reflected wave is written as:

$$v_R(z,t) = 2e^{-i\omega t}\pi g^2 \sum_{n=1}^{\infty} C_n \frac{\sin(h_n z)}{f^2 - h_n^2} \tag{4.2–23}$$

The total response of the pile will be equal to the sum of the responses to the progressive and reflected waves:

$$v(z,t) = -e^{i\omega t}\frac{P_0}{E_p A_p}\frac{\sin(fz)}{f\cos(fH)} + 4\cos(\omega t)\pi g^2 \sum_{n=1}^{\infty} C_n \frac{1}{f^2 - h_n^2}\sin(h_n z) \tag{4.2–24}$$

It is evident that the response to the progressive waves (4.2–24) is in phase with the applied load and the response to the reflected waves is behind (or ahead of) the applied load by half a period (180^o phase difference with the applied load).

It is helpful to investigate the variation of in-phase pile head vertical movements with frequency, ignoring material damping of the soil and the pile.

$$V_h = -\frac{P_0 H}{E_p A_p}\left[\frac{\sin(fH)}{fH\cos(fH)} + \right.$$
$$\left. -2\pi\frac{\mu}{E_p}\frac{H^2}{A_p}\sum_{n=1}^{\infty}\frac{2}{\frac{K_0(q_n r_0)}{(q_n r_0)K_1(q_n r_0)}(f^2-h_n^2)H^2 - 2\frac{\mu H^2(1+i2\xi_{sh})}{E_p A_p}}\times\frac{1}{(f^2-h_n^2)H^2}\right] \quad (4.2\text{–}25)$$

The value of the term under the summation sign is very small if the excitation frequency is not close to the resonance frequency. Therefore, for most practical purposes it is convenient to ignore this term and consider the in-phase pile head vertical deformation as:

$$V_h = -\frac{P_0 H}{E_p A_p}\frac{\tan(fH)}{fH} \quad (4.2\text{–}26)$$

Figure 4-6 shows variations in pile head deformation with frequency. It can be seen that the deformations grow exponentially if the frequency approaches the value of the resonance frequency. Insight may be gained by considering typical numerical values for piles. Considering the solid (non-tubular) cross-section of a concrete pile with a density of 2.4 tons/m^3 and a modulus of elasticity of 30 GPa, in a soil layer 10m deep, we will have:

$$fH = \sqrt{\frac{m_p}{E_p A_p}}H\omega = \omega H\sqrt{\frac{\rho_p}{E_p}} = (2.828\times10^{-3})\omega \quad (4.2\text{–}27)$$

Equating this to the critical value of ' $fH = \pi/2$ ' we obtain an angular frequency of 555 rad/s (88 Hz) as the critical frequency of a typical pile.

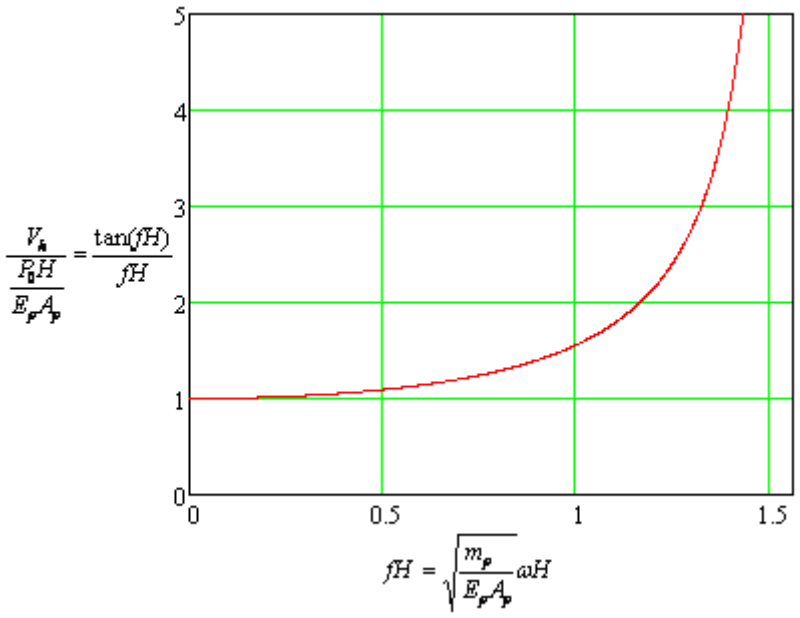

Figure 4-6 Variations in pile head deformation with frequency (no damping)

4.2.3 Static loading

Response of a pile-soil system to a static axial load can be obtained by letting '$\omega \to 0$' in the solution derived in the previous section. The vertical deformation of the pile expressed in equation (4.2–25) becomes:

$$V_{Static}(z) = -\frac{P_0 H}{E_p A_p}\left[\frac{z}{H} - 4\pi \frac{\mu}{E_p}\frac{H^2}{A_p}\sum_{n=1}^{\infty}\frac{2(-1)^{n-1}\sin(h_n z)}{\frac{K_0(\eta h_n r_0)}{(\eta h_n r_0)K_1(\eta h_n r_0)}H^2 h_n^2 + 2\frac{\mu H^2}{E_p A_p}} \times \frac{1}{H^2 h_n^2}\right] \qquad (4.2\text{–}28)$$

The axial strain in the pile is calculated by taking the derivative of static deformation with respect to *'z'*. The stress is obtained by multiplying the strain by the modulus of elasticity of the pile. The axial force at any depth is obtained by multiplying the stress by the pile's cross-sectional area. The axial force at the tip of the pile can be calculated by letting *'z=0'* in the final formulation:

$$P_{Static}(z=0) = -P_0\left(1 - 4\frac{\mu}{E_p}\frac{H^2}{A_p}\sum_{n=1}^{\infty}\frac{2(-1)^{n-1}}{\frac{H}{r_0}\frac{K_0(\eta h_n r_0)}{\eta K_1(\eta h_n r_0)}Hh_n + 2\frac{\mu H^2}{E_p A_p}}\frac{1}{Hh_n}\right) \qquad (4.2\text{–}29)$$

The term in the parentheses is a factor which is less than unity. It represents the percentage of the axial load which is transferred to the bedrock in an end-bearing pile. That portion of

the axial load which is transferred to the soil media is a function of the relative soil/pile modulus, the Poisson's ratio of the soil, the pile's slenderness ratio and the thickness of the soil layer. Poulos and Davis (1980) called this the load transfer proportion 'β' and represented it in the form of graphs. We can write the load transfer proportion 'β' in terms of a number of dimensionless factors, using equation (4.2–29):

$$\beta = 1 - \frac{16}{\pi}\frac{1}{1+\nu}\left(\frac{E_s}{E_p}\right)\left(\frac{\pi D^2}{4A_p}\right)\left(\frac{D}{H}\right)^2 \sum_{n=1}^{\infty} \frac{(-1)^{n+1}}{\dfrac{(2n-1)\pi K_0[H\eta(2n-1)\pi/4D]}{(2s\eta)K_1[H\eta(2n-1)\pi/4D]} + \dfrac{4}{\pi}\left(\dfrac{E_s}{E_p}\right)\left(\dfrac{\pi r_0^2}{A_p}\right)\left(\dfrac{D}{H}\right)^2 \dfrac{1}{1+\nu}} \times \frac{1}{(2n-1)\pi} \qquad (4.2\text{–}30)$$

The load transfer factor is drawn vs. pile soil modulus ratio for a soil Poisson's ratio of 0.4 (Figure 4-7). The graph is very similar to the one reported by Poulos and Davis (1980).

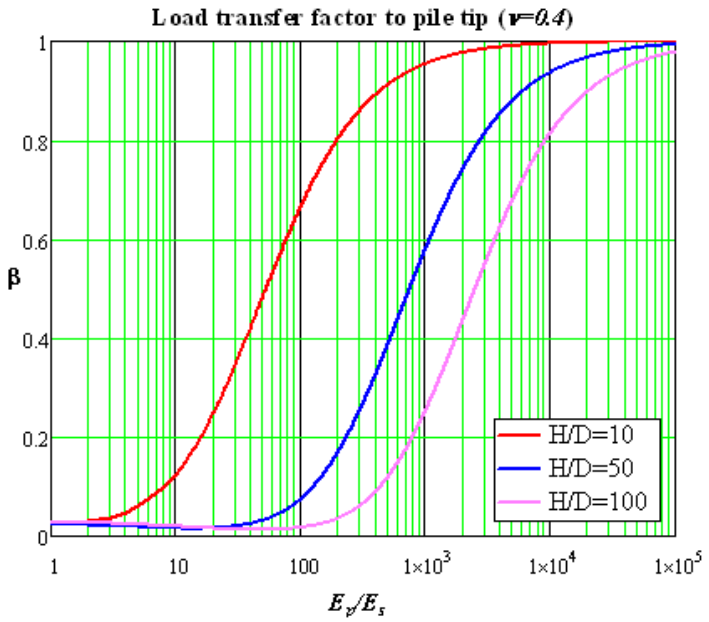

Figure 4-7 Load transfer factor vs. pile/soil modulus ratios

4.2.4 Application to layered soil

A two-layered soil is shown in Figure 4-8. The Poisson's ratio and the thickness of the layers are assumed to be constant, but they each have a different shear modulus.

The vertical deformation of each layer can be established as follows, following the proposed solution of Nogami and Novak (1976):

$$w_1(r,z,t) = e^{i\omega t} K_0(qr)[A_1 \sin(hz) + B_1 \cos(hz)] \tag{4.2–31}$$

$$w_2(r,z,t) = e^{i\omega t} K_0(qr) A_2 \sin(hz) \tag{4.2–32}$$

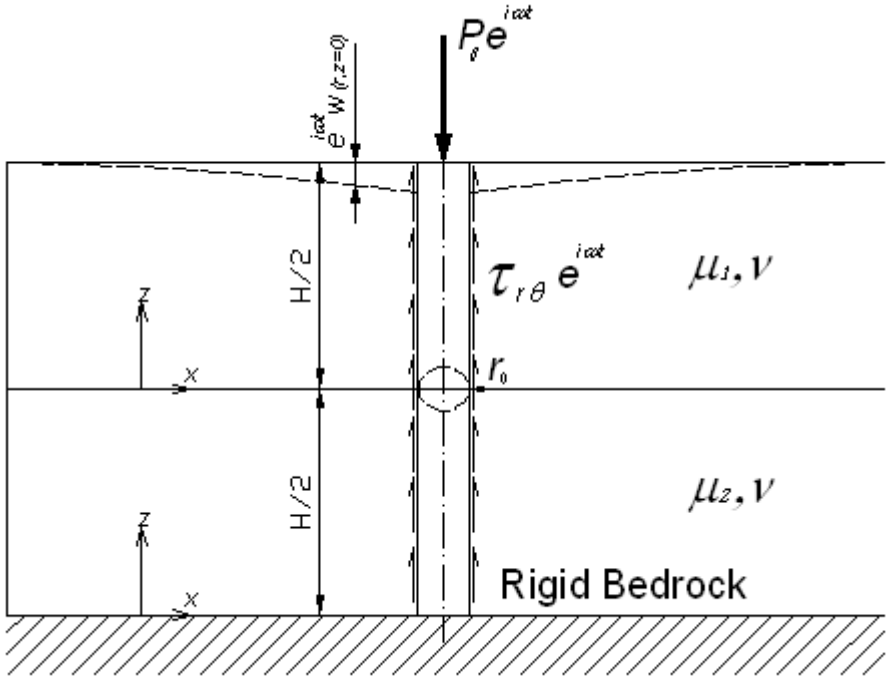

Figure 4-8 Two-layered soil

The deformations and stresses between the two layers should be equal:

$$w_1(r,0,t) = w_2(r,H/2,t) \Rightarrow B_1 = A_2 \sin(hH/2) \tag{4.2–33}$$

$$\mu_1 \frac{2(1-\nu)}{1-2\nu} \frac{\partial}{\partial z} w_1(r,0,t) = \mu_2 \frac{2(1-\nu)}{1-2\nu} \frac{\partial}{\partial z} w_2(r,H/2,t) \Rightarrow A_1 = \frac{\mu_2}{\mu_1} A_2 \cos(hH/2) \tag{4.2–34}$$

On the ground surface, the normal stress should be zero, i.e.:

$$\mu_1 \frac{\partial}{\partial z} w_1(r,H/2,t) = 0 \Rightarrow A_1 \cos(hH/2) - B_1 \sin(hH/2) = 0 \tag{4.2–35}$$

Substituting from equations (4.2–33) and (4.2–34) into equation (4.2–35) results in:

$$\frac{\mu_2}{\mu_1}\cos^2(hH/2)-\sin^2(hH/2)=0 \Rightarrow \tan(hH/2)=\pm\sqrt{\frac{\mu_2}{\mu_1}} \qquad (4.2\text{–}36)$$

This equation leads to determination of the factor *'h'*:

$$h_n=\frac{1}{H}(n\pi-2\tan^{-1}\sqrt{\frac{\mu_2}{\mu_1}}) \qquad (4.2\text{–}37)$$

Note that if '$\mu_2=\mu_1$' the problem simplifies to a single layer homogeneous soil with thickness *'H'* and the value of *'h'* becomes equal to equation (4.2–2). The expressions for the deformation of soil in each layer become:

$$w_1(r,z,t)=e^{i\omega t}\sum_{n=1}^{\infty}K_0(q_n r)A_n[\frac{\mu_2}{\mu_1}\cos(h_n H/2)\sin(h_n z)+\sin(h_n H/2)\cos(h_n z)] \qquad (4.2\text{–}38)$$

$$w_2(r,z,t)=e^{i\omega t}\sum_{n=1}^{\infty}K_0(q_n r)A_n\sin(h_n z) \qquad (4.2\text{–}39)$$

In the above equations, *'A_n'* is used in place of *'A_2'* without loss of generality.

The solution process is similar to that for uniform soil. The solution should be performed for two parts of the pile embedded in each soil layer and unknown constants to be derived from continuity conditions. This process will be laborious and time-consuming with few rewards. A better approach is to make an analogy with the case of a column to which longitudinal springs, dashpots and masses are connected continuously.

4.2.5 Analogy with column with continuous spring, mass and dashpot

Figure 4-9 shows the equivalent column with longitudinal generalized springs. This model should have the same dynamic properties as the continuum model.

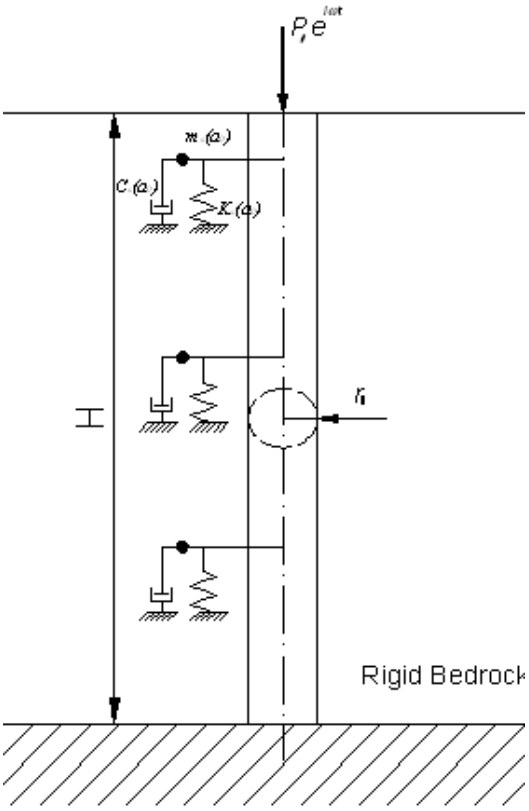

Figure 4-9 Equivalent column with longitudinal generalized springs

The governing differential equation of the deformations for the structure in Figure 4-9 is written as:

$$(m_p + m_s)\frac{\partial^2}{\partial t^2}v(z,t) + (c_p + c_s)\frac{\partial}{\partial t}v(z,t) - E_p A_p \frac{\partial^2}{\partial z^2}v(z,t) = -k_s v(z,t) \tag{4.2–40}$$

Considering the steady-state vibration: $v(z,t) = e^{i\omega t}V(z)$, the above equation is simplified to:

$$E_p A_p V''(z) + [(m_p + m_s)\omega^2 - i\omega(c_p + c_s) - k_s]V(z) = 0 \tag{4.2–41}$$

The following is a solution to the differential equation (4.2–41):

$$V(z) = \frac{P_0}{E_p A_p}\frac{\sin\lambda z}{\lambda\cos\lambda H} \tag{4.2–42}$$

Where

$$\lambda^2 = \frac{(m_p + m_s)\omega^2 - i\omega(c_p + c_s) - k_s}{E_p A_p} \tag{4.2–43}$$

The axial force at the pile tip is calculated from equation (4.2–42):

$$P(z=0) = \frac{P_0}{\cos \lambda H} \tag{4.2–44}$$

At first glance, it appears that the force on the bottom is greater than the force at the top of the pile due to the presence of the cosine term in the denominator. A closer look, however, proves otherwise. Let us consider the case of static loading. We can obtain factor 'λ' by substituting zero for the frequency in equation (4.2–43):

$$\lambda^{Static} = i\sqrt{\frac{k_s}{E_p A_p}} \tag{4.2–45}$$

It can be seen that for the static case, the expression for 'λ' is purely imaginary. Therefore the cosine function changes to the hyperbolic cosine function. It is known that hyperbolic cosine is always greater than or equal to unity. The static force at the pile tip becomes:

$$P_{static}(z=0) = \frac{P_0}{\cosh\sqrt{\frac{k_s H^2}{E_p A_p}}} \tag{4.2–46}$$

Equating the above equation to equation (4.2–30) results in determination of the stiffness factor:

$$\frac{1}{\cosh\sqrt{\frac{k_s H^2}{E_p A_p}}} = \beta \quad \Rightarrow \quad k_s = E_p \frac{A_p}{H^2}[\cosh^{-1}(\frac{1}{\beta})]^2 \tag{4.2–47}$$

The simple equivalent model is capable of modelling the correct load transfer to the bedrock in static conditions. However, it has major deficiencies in a dynamic analysis that makes it unsuitable for this kind of usage. The model cannot simulate the reflected wave from the bedrock. It is possible to modify the simple model such that these effects are simulated.

Rewriting equations (4.2–1) and (4.2–5) in a fashion that shows the progressive and reflected waves gives:

$$w(r,z,t) = -\frac{i}{2}\sum_{n=1}^{\infty} A_n K_0(q_n r) e^{i(\omega t - h_n z)} + \frac{i}{2}\sum_{n=1}^{\infty} A_n K_0(q_n r) e^{i(\omega t + h_n z)} \tag{4.2–48}$$

$$p(z,t) = -2\pi r_0 \mu (1 + 2\xi_{sh} i)\frac{i}{2}[-\sum_{n=1}^{\infty} C_n e^{i(\omega t - h_n z)} + \sum_{n=1}^{\infty} C_n e^{i(\omega t + h_n z)}] \tag{4.2–49}$$

The objective is to show a linear relationship between the soil reaction and the vertical pile deformation that can be interpreted as spring/damper-type behaviour. In the present format, the above two equations do not show such a relationship. In a modal format, however, it is possible to establish a linear relationship between the modal deformations and modal soil reaction. Writing the term relating to the progressive wave in equation (4.2–48) on pile surface in a modal form yields:

$$w(r_0,z,t) = e^{i\omega t}\sum_{n=1}^{\infty} w_n = -\frac{i}{2} e^{i\omega t}\sum_{n=1}^{\infty} A_n K_0(q_n r_0) e^{i h_n z} \tag{4.2–50}$$

In the above equation, 'w_n' is the modal shape of the soil deformation at the interface between the pile and the soil. Comparing equation (4.2–50) with equation (4.2–49) results in the following:

$$p(z,t) = 2\pi r_0 \mu (1 + i2\xi_{sh} i)\frac{i}{2}\sum_{n=1}^{\infty} A_n q_n K_1(q_n r_0) e^{i(\omega t - h_n z)} = -2\pi\mu (1 + i2\xi_{sh}) e^{i\omega t}\sum_{n=1}^{\infty} w_n \frac{(q_n r_0) K_1(q_n r_0)}{K_0(q_n r_0)} \tag{4.2–51}$$

From there modal impedance can be derived as:

$$I_n = 2\pi\mu (1 + i2\xi_{sh})\frac{(q_n r_0) K_1(q_n r_0)}{K_0(q_n r_0)} \tag{4.2–52}$$

The above equation includes stiffness, damping and mass terms. Asymptotic expansions can be used to uncouple different components of the impedance. For large values of q_n we can write:

$$\lim_{q_n r_0 \to \infty} \quad K_m(q_n r_0) \cong \sqrt{\frac{\pi}{2 q_n r_0}} e^{-q_n r_0} \tag{4.2–53}$$

Therefore, equation (4.2–52) is written for large arguments as:

$$(I_n)_{q_n r_0 \to \infty} = 2\pi\mu(1+i2\xi_{sh})(q_n r_0) = 2\pi r_0 \mu(1+i2\xi_{sh})\sqrt{\eta^2 h_n^2 - \frac{(\omega/V_s)^2}{1+i2\xi_{sh}}} = \\ = 2\pi\mu(1+i2\xi_{sh})\eta h_n r_0 \sqrt{1 - \frac{1}{1+i2\xi_{sh}}(\frac{\omega}{\eta h_n V_s})^2} \qquad (4.2\text{–}54)$$

If the value of $\frac{1}{1+i2\xi_{sh}}(\frac{\omega}{\eta h_n V_s})^2$ is less than unity, binomial approximation can be used to expand the square root term. Using binomial approximation further simplifies equation (4.2–54):

$$(I_n)_{q_n r_0 \to \infty} = 2\pi\mu(1+i2\xi_{sh})\eta h_n r_0 [1 - \frac{1}{2}\frac{1}{1+i2\xi_{sh}}(\frac{\omega}{\eta h_n V_s})^2] = 2\pi\mu(1+i2\xi_{sh})\eta h_n r_0 - \pi\mu\eta h_n r_0 (\frac{\omega}{\eta h_n V_s})^2 \qquad (4.2\text{–}55)$$

From there modal stiffness, damping and mass components are recognized as follows:

$$\begin{cases} (k_n)_{q_n r_0 \to \infty} = (2n-1)\pi^2 \mu\eta \dfrac{r_0}{H} \\ (c_n)_{q_n r_0 \to \infty} = 2(2n-1)\pi^2 \xi_{sh} \mu\eta \dfrac{r_0}{H}\dfrac{1}{\omega} \\ (m_n)_{q_n r_0 \to \infty} = \dfrac{2}{2n-1}\eta\rho H r_0 \end{cases} \qquad (4.2\text{–}56)$$

The above formulas are accurate for higher modes of vibration. They are also good approximations for lower modes when there are low excitation frequencies and deep soil layers.

Another condition that must be considered is the case of resonance. Under resonance conditions, the excitation frequency approaches one of the natural frequencies of the system. Resonance conditions can be formulated as follows, assuming that the hysteretic damping of the soil is very small:

$$\omega r_0 / V_s \to \eta h_n r_0 \sqrt{1 + 4\xi_{sh}^2} \qquad (4.2\text{–}57)$$

The following limiting expressions are valid for modified Bessel functions of the second kind (Abramowitz and Stegun 1972):

$$\begin{cases} [K_0(q_n r_0)]_{q_n r_0 \to 0} \cong -\ln(q_n r_0) \\ [K_1(q_n r_0)]_{q_n r_0 \to 0} \cong \dfrac{1}{q_n r_0} \end{cases} \qquad (4.2\text{–}58)$$

The impedance equation (4.2–52) can be written for resonance frequency as:

$$(I_n)_{\mathrm{Re}sonance} = -2\pi\mu(1+i2\xi_{sh})\frac{1}{\ln(q_n r_0)} \tag{4.2–59}$$

The argument in exponential form: $q_n r_0 = |q_n r_0| e^{i\varphi}$, using equation (4.2–2) is as follows:

$$\begin{cases} |q_n r_0| = \sqrt{[\eta^2 h_n^2 r_0^2 - \dfrac{a_0^2}{1+4\xi_{sh}^2}]^2 + \dfrac{4\xi_{sh}^2}{(1+4\xi_{sh}^2)^2}} \\ \varphi = \dfrac{1}{2}\tan^{-1}\dfrac{2\xi_{sh}a_0^2}{\eta^2 h_n^2 r_0^2(1+4\xi_{sh}^2) - a_0^2} \end{cases} \tag{4.2–60}$$

Note that in resonance we have $\varphi \cong \pi/4$ and $|q_n r_0| \cong \dfrac{2\xi_{sh}}{1+4\xi_{sh}^2}$, therefore the logarithmic part of the equation (4.2–59) is written as:

$$\ln(q_n r_0) = \ln(\frac{2\xi_{sh}}{1+4\xi_{sh}^2}) + i\frac{\pi}{4} \tag{4.2–61}$$

Substituting this result into equation (4.2–59) leads to:

$$(I_n)_{\mathrm{Re}sonance} = -\frac{2\pi\mu}{[\ln(\frac{2\xi_{sh}}{1+4\xi_{sh}^2})]^2 + \frac{\pi^2}{16}}[\ln(\frac{2\xi_{sh}}{1+4\xi_{sh}^2}) + \frac{\pi}{2}\xi_{sh} + i(2\xi_{sh}\ln(\frac{2\xi_{sh}}{1+4\xi_{sh}^2}) - \frac{\pi}{4})] \tag{4.2–62}$$

From there, stiffness and damping can be written for the resonance conditions:

$$\begin{cases} (k_n)_{\mathrm{Re}sonance} = -\dfrac{2\pi\mu}{[\ln(\frac{2\xi_{sh}}{1+4\xi_{sh}^2})]^2 + \frac{\pi^2}{16}}[\ln(\frac{2\xi_{sh}}{1+4\xi_{sh}^2}) + \frac{\pi}{2}\xi_{sh}] \\ (c_n)_{\mathrm{Re}sonance} = -\dfrac{2\pi\mu}{[\ln(\frac{2\xi_{sh}}{1+4\xi_{sh}^2})]^2 + \frac{\pi^2}{4}}[2\xi_{sh}\ln(\frac{2\xi_{sh}}{1+4\xi_{sh}^2}) - \frac{\pi}{4}] \end{cases} \tag{4.2–63}$$

Note that the resonance stiffness and damping values are positive for all ranges of hysteretic damping. Figure 4-10 shows stiffness and damping under resonance conditions.

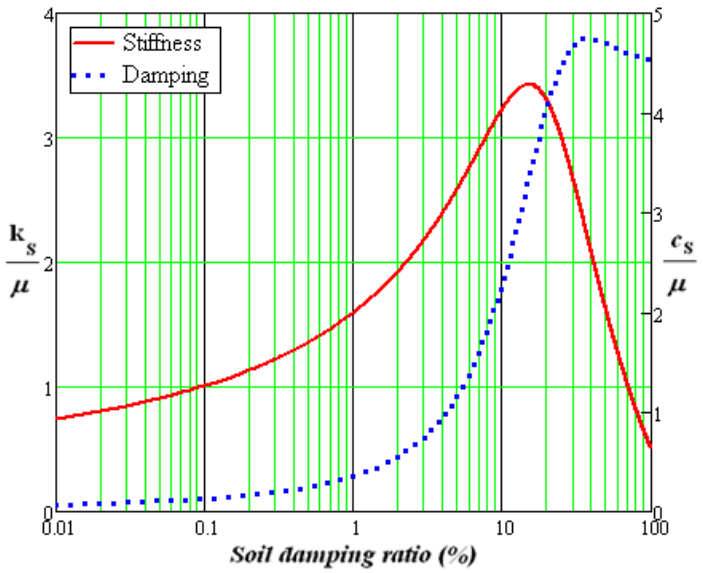

Figure 4-10 Stiffness and damping values under resonance conditions

An analytical model is proposed based on the analysis made in this section. Figure 4-11 shows the proposed model which is composed of four Kelvin-Voigt models with masses. Each Voigt block consists of a spring, a damper and a mass of soil which contributes to the modal vibration. The first Voigt block represents the progressive wave from the pile. In order to correctly model the reflected wave from the bedrock and the free surface, the response of the Voigt block needs to be given 180 degrees phase delay. This is achieved by adding two unit dampers after the first block. This adds two more degrees of freedom to the model. The second Voigt block represents the reflected wave from the bedrock. The reflected wave from the bedrock is again reflected by the ground surface (the third Voigt block).

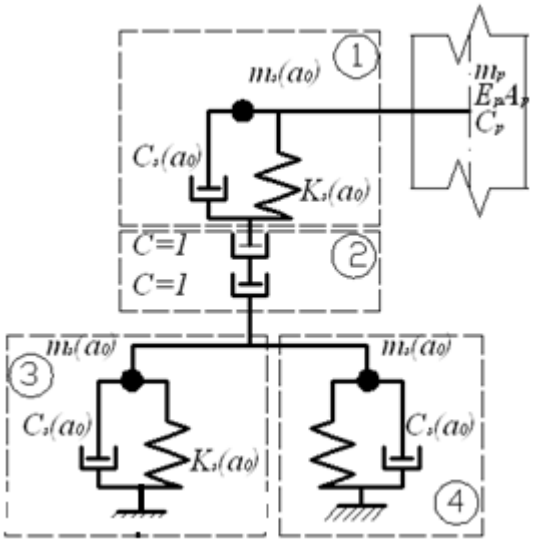

Figure 4-11 Proposed model for modal analysis of the pile

Notes on Figure 4-11:

1) First Voigt block representing progressive wave from the pile.
2) Two unit dampers adding 180 degrees phase to the progressive wave.
3) Voigt block representing reflected wave from the bedrock.
4) Voigt block representing the reflected wave from the ground surface.

4.3 Application

The applications of the results of this chapter are demonstrated via some solved examples.

4.3.1 Example 1

The test pile discussed in section 3.3: site Mathura I as reported by Boominathan and Ayothiraman (2006) is dynamically analysed in this section. The type of dynamic analysis we perform in this section is Eigen value analysis which is aimed to obtain free vibration frequencies of the pile. For this type of analysis it is essential to attribute mass and damping coefficients to the pile and to determine the stiffness of soil springs using the results of the present chapter. Since these values are frequency dependent, an iterative procedure should be followed. Soil mass is calculated for each layer and is added to the pile material density. The damping constant should be translated in terms of damping ratio in order to input as a material property. Typical value of damping ratio of the concrete is 5%. The damping ratio is

determined as the damping constant divided by the factor '$2m_p\omega$'. The calculations are performed via a Mathcad (2009) spreadsheet.

Input data

Pile diameter $D := 500mm$

Concrete nominal compressive strength $f_c := 25MPa$

Concrete mass per volume $\rho_p := 2400kg \cdot m^{-3}$

Material damping ratio of pile (assumed) $\zeta_p := 5\%$

Soil Poisson's ratio (assumed) $\nu := 0.3$

Number of soil layers- layer index $i := 0,1..2$

Soil shear modulus for each layer $\mu := \begin{pmatrix} 64.08 \\ 84.86 \\ 170.37 \end{pmatrix} MPa$

Soil shear wave velocity $V_s := \begin{pmatrix} 190.52 \\ 210.24 \\ 292.60 \end{pmatrix} \frac{m}{s}$

Simple calculations

Pile modulus of elasticity (ACI 318) $E_p := 4700MPa\sqrt{\frac{f_c}{1MPa}}$

$E_p = 23.5GPa$

Mass of pile cap (750 x 750 x 750) $M_{cap} := (0.75m)^3 \cdot \rho_p$

Soil density $\rho_i := \frac{\mu_i}{(V_{s_i})^2}$

$\rho = \begin{pmatrix} 1.77 \\ 1.92 \\ 1.99 \end{pmatrix} tonne \cdot m^{-3}$

Pile cross sectional area $A_p := \frac{\pi}{4} \cdot D^2$

Pile second moment of inertia $I_p := \frac{\pi}{64} \cdot D^4$

Shaft cross sectional area $A_s := \frac{\pi}{4} \cdot D^2$

Shaft second moment of inertia $I_s := \frac{\pi}{64} \cdot D^4$

Factor η $\eta := \sqrt{\frac{1 - 2\nu}{2(1 - \nu)}}$

Pile mass per unit length $m_p := \rho_p \cdot A_p$ $m_p = 471 \frac{kg}{m}$

Frequency related functions declaration

Spil springs static stiffness

$$k_{e.stat_i} := \mu_i \cdot \left[4.577 + \pi \cdot \left(3.432 - 0.316 \cdot \eta + 25.002\eta^2 - 64.796\eta^3 + 39.355\eta^4 \right) \cdot \sqrt{\frac{\mu_i \cdot I_s}{E_p \cdot I_p}} \right]$$

$$k_{e.stat} = \begin{pmatrix} 332 \\ 448 \\ 949 \end{pmatrix} MPa$$

Non - dimensional frequency

$$a_0(\omega) := \begin{pmatrix} \frac{\omega \cdot D}{2 \cdot V_{s_0}} \\ \frac{\omega \cdot D}{2 \cdot V_{s_1}} \\ \frac{\omega \cdot D}{2 \cdot V_{s_2}} \end{pmatrix}$$

Pile damping factor $c_p(\omega) := 2m_p \cdot \omega \cdot \zeta_p$

Correlation factors F_1 to F_4

$F_1 := 0.944 + 0.268 \cdot \eta - 2.274 \cdot \eta^2 + 1.360\eta^3$ $F_1 = 0.645$

$F_2 := \eta \cdot \left(9.630\eta^3 - 17.378\eta^2 + 8.336\eta - 0.248 \right)$ $F_2 = 0.381$

$F_3 := 2.808 + 0.713\eta - 3.961\eta^2 - 1.796\eta^3 + 3.238\eta^4$ $\quad F_3 = 2.047$

$F_4 := 0.944 + 0.515\eta + 10.610\eta^2 + 18.739\eta^3 - 9.63\eta^4$ $\quad F_4 = 6.326$

Added soil mass to the pile mass per unit volume $\quad \rho_{s_i} := \rho_p \cdot F_2 \cdot \sqrt{\frac{\mu_i \cdot I_s}{E_p \cdot I_p}}$

$$\rho_s = \begin{pmatrix} 48 \\ 55 \\ 78 \end{pmatrix} \frac{kg}{m^3}$$

Equivelent mass of the pile when soil mass is added $\quad \rho_e := \rho_p + \rho_s$

$$\rho_e = \begin{pmatrix} 2448 \\ 2455 \\ 2478 \end{pmatrix} \frac{kg}{m^3}$$

Dynamic stiffness of soil springs (low frequency limit

$$k_{e.dyn}(\omega) := \begin{bmatrix} k_{e.stat_0} + \pi \cdot \mu_0 \cdot \left[\left(a_0(\omega)_0 \right)^2 \cdot \frac{m_p}{\rho_0 \cdot A_s} \cdot F_1 + a_0(\omega)_0 \cdot \frac{c_p(\omega)}{\sqrt{\pi \cdot \mu_0 \cdot \rho_0 \cdot A_s}} \cdot F_3 \right] \cdot \sqrt{\frac{\mu_0 \cdot I_s}{E_p \cdot I_p}} \\ k_{e.stat_1} + \pi \cdot \mu_1 \cdot \left[\left(a_0(\omega)_1 \right)^2 \cdot \frac{m_p}{\rho_1 \cdot A_s} \cdot F_1 + a_0(\omega)_1 \cdot \frac{c_p(\omega)}{\sqrt{\pi \cdot \mu_1 \cdot \rho_1 \cdot A_s}} \cdot F_3 \right] \cdot \sqrt{\frac{\mu_1 \cdot I_s}{E_p \cdot I_p}} \\ k_{e.stat_2} + \pi \cdot \mu_2 \cdot \left[\left(a_0(\omega)_2 \right)^2 \cdot \frac{m_p}{\rho_2 \cdot A_s} \cdot F_1 + a_0(\omega)_2 \cdot \frac{c_p(\omega)}{\sqrt{\pi \cdot \mu_2 \cdot \rho_2 \cdot A_s}} \cdot F_3 \right] \cdot \sqrt{\frac{\mu_2 \cdot I_s}{E_p \cdot I_p}} \end{bmatrix}$$

Viscous damping factor $\quad c_s(\omega) := \begin{bmatrix} \left(c_p(\omega) \cdot F_4 + a_0(\omega)_0 \cdot F_3 \cdot m_p \cdot \sqrt{\frac{\pi \cdot \mu_0}{\rho_0 \cdot A_s}} \right) \cdot \sqrt{\frac{\mu_0 \cdot I_s}{E_p \cdot I_p}} \\ \left(c_p(\omega) \cdot F_4 + a_0(\omega)_1 \cdot F_3 \cdot m_p \cdot \sqrt{\frac{\pi \cdot \mu_1}{\rho_1 \cdot A_s}} \right) \cdot \sqrt{\frac{\mu_1 \cdot I_s}{E_p \cdot I_p}} \\ \left(c_p(\omega) \cdot F_4 + a_0(\omega)_2 \cdot F_3 \cdot m_p \cdot \sqrt{\frac{\pi \cdot \mu_2}{\rho_2 \cdot A_s}} \right) \cdot \sqrt{\frac{\mu_2 \cdot I_s}{E_p \cdot I_p}} \end{bmatrix}$

Viscous damping ratio of soil $\quad \zeta_{v.h}(\omega) := \frac{c_s(\omega)}{2 m_p \cdot \omega}$

Total joint damping ratio of soil and pile $\quad \zeta_e(\omega) := \zeta_p + \zeta_{v.h}(\omega)$

Test equipment setup as described and depicted by Boominathan and Ayothiraman (2006) is given in Figure 4-12. The capacity of the mechanical oscillator is given as 5 tonnes, but the exact amount of its mass during each test is not given. The analysis is typically performed for 1 tonne oscillator mass (20% capacity).

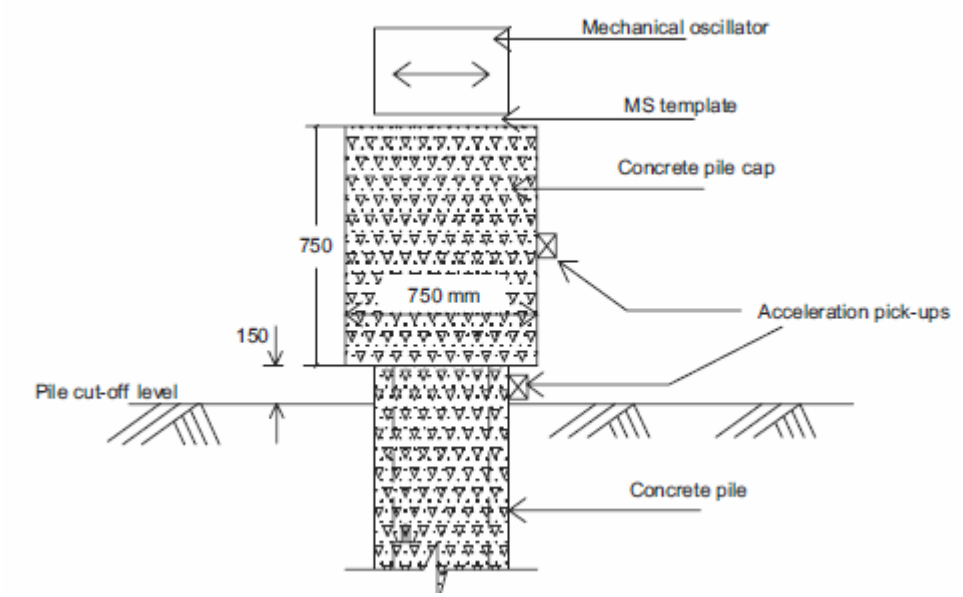

Figure 4-12 Set up for forced vibration test (Boominathan and Ayothiraman 2006)

The analysis model is similar to what is described in section 3.3 and with the same computer program. An above ground extension of 150 mm and a pile cap are added to the model. Mass of the oscillator is also added to the top of the pile cap. The values of spring stiffness are calculated for each element, using the values obtained from the Mathcad spreadsheet. Iterative procedure is followed to include the effects of frequency dependent stiffness and damping values. For the first trial, the frequency of 20 Hz is used. Relevant calculations are performed in a Mathcad spreadsheet.

Modal analysis is performed via the computer program. The first twelve modal frequencies are calculated by the software (Table 4-4). The value of the first modal frequency is 22.524 Hz. This is close to the guess value of 20 Hz which is used in the first iteration.

Iterative procedure

Trial 1

$f_1 := 20Hz$

$\omega_1 := 2\pi \cdot f_1$

Check if the low frequency limit is valid for all layers

$$Frequency_i := \begin{cases} \text{"low"} & \text{if } a_{0.}(\omega_1)_i < \frac{1}{3} \cdot \frac{\eta \cdot 1.351}{\sqrt{1-\eta^2}} \\ \text{"is not low"} & \text{otherwise} \end{cases}$$

$$Frequency = \begin{pmatrix} \text{"low"} \\ \text{"low"} \\ \text{"low"} \end{pmatrix}$$

$$k_{e.dyn}(\omega_1) = \begin{pmatrix} 332.767 \\ 448.436 \\ 950.011 \end{pmatrix} \cdot MPa$$

$$\zeta_e(\omega_1) = \begin{pmatrix} 0.12 \\ 0.131 \\ 0.164 \end{pmatrix}$$

$$a_o := a_{0.}(\omega_1) = \begin{pmatrix} 0.165 \\ 0.149 \\ 0.107 \end{pmatrix}$$

Table 4-4 Modal periods frequencies resulted from modal analysis

Mode No. (---)	**Period, *T*** Sec	**Frequency, *f*** Hz	**ω** rad/sec	**Eigen value** rad2/sec2
1	0.044397	22.524	141.52	20029
2	0.017083	58.538	367.81	135280
3	0.008479	117.94	741.06	549160
4	0.007854	127.33	800.02	640030
5	0.006859	145.8	916.06	839170
6	0.00561	178.26	1120.1	1254500
7	0.005379	185.9	1168	1364300
8	0.004506	221.94	1394.5	1944600
9	0.004462	224.12	1408.2	1983100
10	0.004202	237.96	1495.2	2235500
11	0.003706	269.84	1695.5	2874600
12	0.003295	303.46	1906.7	3635500

Trial 2

$$f_2 := 22.524\text{Hz}$$

$$\omega_2 := 2\pi \cdot f_2$$

Check if the low frequency limit is valid for all layers

$$\text{Frequency}_i := \begin{cases} \text{"low"} & \text{if } a_{0.}(\omega_2)_i < \frac{1}{3} \cdot \frac{\eta \cdot 1.351}{\sqrt{1-\eta^2}} \\ \text{"is not low"} & \text{otherwise} \end{cases}$$

$$\text{Frequency} = \begin{pmatrix} \text{"low"} \\ \text{"low"} \\ \text{"low"} \end{pmatrix}$$

$$k_{e.dyn}(\omega_2) = \begin{pmatrix} 332.856 \\ 448.538 \\ 950.156 \end{pmatrix} \text{MPa}$$

$$\zeta_e(\omega_2) = \begin{pmatrix} 0.12 \\ 0.131 \\ 0.164 \end{pmatrix}$$

$$a_o := a_{0.}(\omega_2) = \begin{pmatrix} 0.186 \\ 0.168 \\ 0.121 \end{pmatrix}$$

It is seen that the change in stiffness value and damping ratio in the second trial are negligible therefore another analysis is not required. The free vibration frequencies reported for this site by Boominathan and Ayothiraman (2006) was varing from 19.7 Hz to 23.5 Hz. This is in very good agreement with the calculated frequency of 22.524 Hz.

This example shows how the results of the present chapter can be used to determine the free vibration frequency of pile in layered soils.

4.3.2 Example 2

This example is provided to show applicability of the results obtained for vertically loaded pile and to compare the results with other well established methods (i.e. Poulos and Davis 1980).

An end-bearing pile in a uniform soil with 10m depth is considered. The pile diameter is 1m, i.e. the diameter to length ratio is 0.1. The soil to pile modulus is assumed to be of the order

of 100. The soil Poisson's ratio is assumed 0.4. Equation (4.2–30) gives a value of ' $\beta = 0.664$ ' for the load transfer proportion.

Poulos and Davis (1980) presented the load transfer proportion for an end-bearing pile as the product of four factors:

$$\beta = \beta_0 C_K C_b C_\nu \tag{4.3–1}$$

Using the graphs given in the abovementioned reference, the following are obtained:

$$\begin{cases} \beta_0 = 0.12 \\ C_K = 0.8 \\ C_b = 7.5 \\ C_\nu = 0.85 \end{cases} \tag{4.3–2}$$

This leads to a value of ' $\beta = 0.12 \times 0.8 \times 7.5 \times 0.85 = 0.612$ ' which is very close to the value obtained from equation (4.2–30). Possible causes of the difference could be:

1- General approximation due to working with graphs;
2- The effect of the relative stiffness of the bedrock on the soil (Poulos and Davis (1980) did not solve for completely rigid bedrock. A relative stiffness value of 1000 is used in the present calculations).

4.4 Summary Chapter four

This chapter involves solution of elastodynamic equations for an idealized soil-pile system. The soil is considered as a linearly elastic half space. The pile is modelled as a classical Euler-Bernouli beam.

The solution to the elastodynamic equations is made in two stages. In the first stage, it is assumed that every cross section of the beam has a lateral movement (translation) without rotation. It should be noted that this assumption does not conclude rigid body motion as different pile cross sections can have different translations. This assumption implies a continuous rotational restraint on all pile cross sections. In the second stage, the rotational restraint is removed while the restraint is applied on the translation. Solutions to elastodynamic equations for the two stages are combined using the principle of superposition.

Soil reactions are applied on the pile and the flexure equation is written for it. It is seen that the flexure equation is in the form of a Vlasov (1966) beam. In this model, the soil reaction

is related to both beam lateral deflection and local curvature. Therefore Winkler's hypothesis (section 2.2.1) is not valid for a pile. However, generalized equivalent Winkler beam can be defined such that a beam on Winkler support has the same deflected shape and stiffness properties as the exact model.

The equivalent Winkler spring constant is a complex value. The real part of the stiffness (impedance) is comprised of stiffness and inertia effects. The imaginary part of it is interpreted as damping. The three main parameters: stiffness, mass and damoing are frequency dependent. They are expressed in closed mathematical form for low frequency and high frequency limits separately. Interpolating functions are introduced to estimate the values of stiffness, mass and damping for intermediate frequencies. A published full scale dynamic pile tests is analysed as a beam on springs using the proposed values for stiffness, mass and damping. Very good agreement found between the calculated and measured free vibration frequency values.

An axially vibrating pile is also considered in this chapter. An existing solution to a pile under oscillating axial force is modified to remove some of its shortcomings. The original solution to elastodynamic is unchanged. However, the modal analysis approach to the soil-pile interaction which leads to erroneous results is abandoned. In this chapter Laplace transform (e.g. Pipes and Harvill 1970) method is employed to solve the differential equation of soil-pile interaction. An example for the special case of a statically loaded pile is provided to show the validity of this approach and its compliance with existing studies.

CHAPTER FIVE

5 DISCUSSION

The main objective of this study is to determine the contribution of the soil mass in lateral pile vibrations. In the course of the study, other important factors like the stiffness and the geometrical damping of the soil have also been derived. In this section, we focus on the contributing mass of soil and discuss the results obtained in the previous section in more details.

The contributing soil mass is derived via analogy with a single degree of freedom (SDOF) vibrating mass. Each element of the pile is considered as an SDOF mass which vibrates in a lateral direction. The spring stiffness and damping is caused by the presence of the soil. In addition, we assume that a mass of soil should also contribute to the vibrations.

The solution to the elastodynamic equations provides soil reaction on the pile. This reaction is seen to be proportional to the pile deflection and curvature. Therefore an SDOF may not correctly represent the interaction between the soil and the pile. However, an equivalent SDOF model is established such that it has the same stiffness characteristics as the true model.

The next sections discuss the results obtained in Chapter 4 with particular attention to the contributing soil mass.

5.1 Low frequency upper limit

Formulas for the contributing soil mass are given in Table **4-3**. The formulas from the table are given here in a modified format that shows the ratio of the contributing mass to the mass per unit length of the pile. For low frequency limit we may write:

$$\frac{m_s^{Low}}{m_p} = \eta(9.630\eta^3 - 17.378\eta^2 + 8.336\eta - 0.248)\sqrt{\frac{\mu I_s}{E_p I_p}} \qquad (5.1\text{–}1)$$

Equation (5.1–1) is valid only for certain frequencies. It is essential to determine the range of frequencies for which this equation is valid. An upper limit for the frequency is established in equation (4.1–79) and can be rewritten as:

$$a_0^{Low} << Min\left\{\sqrt{3.652\sqrt{\frac{\rho A_s}{m_p}}-\frac{c_p^2}{\pi\mu m_p}},\frac{\eta|s_1|}{\sqrt{1-\eta^2}}\right\},\quad |s_1|=1.351 \qquad (5.1\text{–}2)$$

Different factors contribute to the low frequency limit. Ignoring the pile material damping, the main factors are the replaced mass ratio $(\rho A_s / m_p)$ and the Poisson's ratio of the soil. The replaced mass ratio is the relative mass of soil removed (displaced) due to the installation of the pile to the mass per unit length of the pile. For solid (non-tubular) pile cross-sections, this ratio equals the ratio of the densities of the soil and the pile. In most of the cases, the replaced mass ratio is less than unity for solid pile cross-sections. Considering typical values is useful. Cast-in-place concrete piles have solid cross-sections. Normal weight concrete has a typical density of 2.4 tones/m^3. Soil density may vary from 1.6 tones/m^3 to 2.2 tones/m^3, depending on the soil type. A typical value of 1.8 tones/m^3 is quite common in practical cases. Using these numerical values, the first value for the low frequency limit for a typical cast-in-place concrete pile is determined as:

$$a_0 << |s_1|\sqrt[4]{\frac{\rho A_s}{m_p}} = 1.257\ , \qquad \text{for solid concrete piles} \qquad (5.1\text{–}3)$$

Similar calculations can be made for non-tubular (i.e. I-, H-shape) steel piles, knowing that the density of steel is about 7.850 tones/m^3:

$$a_0 << |s_1|\sqrt[4]{\frac{\rho A_s}{m_p}} = 1.997\ , \qquad \text{for non-tubular steel piles} \qquad (5.1\text{–}4)$$

The Poisson's ratio, in general, may vary from 0 for fully compressible to 0.5 for fully incompressible materials. Saturated sands and clays may have typical Poisson's ratio values of 0.35 and 0.45 respectively. Therefore, the second limit in equation (5.1–2) for the low frequency can be considered as:

$$a_0 << \frac{\eta|s_1|}{\sqrt{1-\eta^2}} = \begin{cases} 0.740 & Sand \\ 0.427 & Clay \end{cases} \qquad (5.1\text{–}5)$$

It is evident that for non-tubular concrete and steel piles, the second criterion of equation (5.1–5) governs. Tubular piles have been widely used in offshore and onshore projects. Precast concrete piles are made hollow to reduce their weight and increase the ease of handling. The use of precast concrete piles is restricted due to limitations in length and

difficulties with pile driving. Steel tubular piles of greater length are also used, especially in offshore installations. In order to investigate the low frequency limit for tubular steel piles, it is convenient to introduce a thickness to diameter ratio:

$$\alpha = t / D \tag{5.1–6}$$

This enables us to write the pile cross-sectional area in terms of the shaft cross-sectional area:

$$A_p = \pi D t = \pi D^2 \alpha = A_s (4\alpha) \tag{5.1–7}$$

The American Petroleum Institute (API-RP-2A 2007) specified minimum pile thicknesses for commonly used pile sizes. Table **5-1** is an extract from this publication.

Minimum Pile Wall Thickness			
Pile Diameter		Nominal Wall Thickness, *t*	
in.	mm	in.	mm
24	610	1/2	13
30	762	9/16	14
36	914	5/8	16
42	1067	11/16	17
48	1219	3/4	19
60	1524	7/8	22
72	1829	1	25
84	2134	1 1/8	28
96	2438	1 1/4	31
108	2743	1 3/8	34
120	3048	1 1/2	37

Table 5-1 Minimum pile wall thickness from (API-RP-2A 2007)

It is concluded from the values in Table 5-1 that the thickness to diameter ratio may vary from 0.021 to 0.012 for tubular steel piles (minimum values). Using equation (5.1–7) and the maximum value of 0.021 for thickness to diameter ratio, a lower bound for the first low frequency limit for steel tubular piles is obtained:

$$a_0 << \sqrt{3.652\sqrt{\frac{\rho}{4\rho_s \alpha}}} = 2.825\,, \qquad \text{for tubular steel piles} \tag{5.1–8}$$

It is seen that this value is still smaller than the value given in equation (5.1–5), therefore the latter governs.

The sign: '<<' in equation (5.1–5) means much smaller. In order to quantify the phrase 'much smaller', we should establish an acceptable error limit for the parameters. For instance, consider accepting 1% computational error in the calculations. Since all of our low frequency approximation is made to simplify the terms under the square root sign, we consider the following classical square root and its approximate value derived from the Newton binomial:

$$\sqrt{1+x} \cong 1+0.5x \qquad (5.1–9)$$

The relative error of using the right-hand side of the above equation to the exact left-hand side expression is given as:

$$Error = 1-\frac{1+0.5x}{\sqrt{1+x}} \qquad (5.1–10)$$

Figure 5-1 shows the error vs. the value of the main variable. It is seen that 1% error takes place for $x \cong 1/3$.

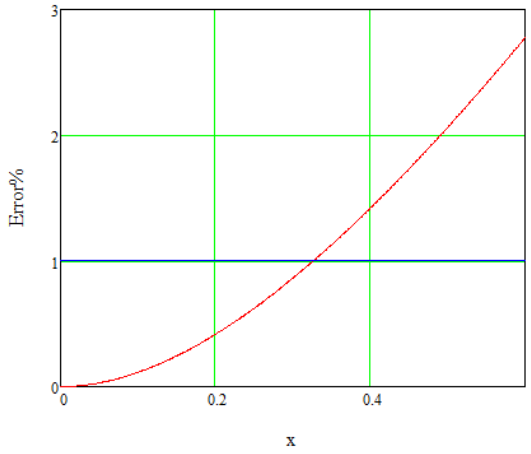

Figure 5-1 Relative error arising from using small expansion approximation

Considering the above argument, we can change the sign '<<'in equation (5.1–5) to the sign '<' in equation (5.1–11) by using 1/3 of the values in the right hand side:

$$a_0 < \begin{cases} 0.25 & Sand \\ 0.14 & Clay \end{cases} \qquad (5.1–11)$$

Equation (5.1–11) establishes a convenient means to determine whether a particular frequency lies in the 'small frequency' category.

5.2 High frequency lower limit

A high frequency limit is defined as a frequency that is great in value such that the constant value under the square root of equation (4.1–85) can be ignored against the frequency-related term. Considering the first equation of (4.1–85) and making the high frequency limit approximation (ignoring pile material damping) gives:

$$\sqrt{s_1^2+\frac{\omega^2 m_p}{\mu\pi}}=\sqrt{s_1^2+a_0^2\frac{m_p}{\rho A_s}}=a_0\sqrt{\frac{m_p}{\rho A_s}}\times\sqrt{1+\frac{s_1^2}{a_0^2}\frac{\rho A_s}{m_p}}\cong a_0\sqrt{\frac{m_p}{\rho A_s}}\quad if\quad \frac{|s_1|}{a_0}\sqrt{\frac{\rho A_s}{m_p}}<<1 \qquad (5.2\text{–}1)$$

With arguments similar to those for low frequency, we propose the following values for the solid concrete and tubular piles:

$$a_0>3|s_1|\sqrt[4]{\frac{\rho A_s}{m_p}}=\begin{cases}3.772 & Solid\quad concrete\quad pile\\ 5.992 & Tubular\quad steel\quad pile\end{cases} \qquad (5.2\text{–}2)$$

The second equation of (4.1–85) results in:

$$\sqrt{(1-\eta^2)a_0^2+\eta^2 s_1^2}=a_0\sqrt{1-\eta^2}\times\sqrt{1+\frac{\eta^2 s_1^2}{(1-\eta^2)a_0^2}}\quad if\quad \frac{\eta|s_1|}{\sqrt{1-\eta^2}\,a_0}<<1 \qquad (5.2\text{–}3)$$

Similarly to the low frequency limit, we may change the sign '<<' to the more definite sign '<' by accepting 1% computational error:

$$a_0>3\frac{\eta s_1}{\sqrt{1-\eta^2}}=\begin{cases}2.22 & Sand\\ 1.281 & Clay\end{cases} \qquad (5.2\text{–}4)$$

It can be seen that, unlike the low frequency limit which was governed by the soil Poisson's ratio, the high frequency limit is governed by the replaced mass ratio. A reliable value for the high frequency limit can be established using equation (5.2–2).

The relationship of the contributing mass to the mass per unit length of the pile in the high frequency regime is written as:

$$\frac{m_s^{High}}{m_p}=m_p\frac{2\eta^2}{a_0}\sqrt{\frac{\rho A_s}{m_p}\frac{\mu I_s}{E_p I_p}} \qquad (5.2\text{–}5)$$

5.3 General frequency range – lateral vibrations

The expressions for stiffness, mass and damping are generally derived in section 4.1.7, using values for low and high frequency regimes and interpolating functions. The relationship for contributing mass is repeated here after some algebraic simplification:

$$\frac{m_s}{m_p} = \frac{\eta}{1+a_0^3}(9.630\eta^3 - 17.378\eta^2 + 8.336\eta - 0.248 + 2\eta a_0^2\sqrt{\frac{\rho A_s}{m_p}})\sqrt{\frac{\mu I_s}{E_p I_p}} \qquad (5.3\text{–}1)$$

Figure **5-2** shows the variations in relative mass given in equation (5.3–1) vs. the non-dimensional frequency for solid concrete piles.

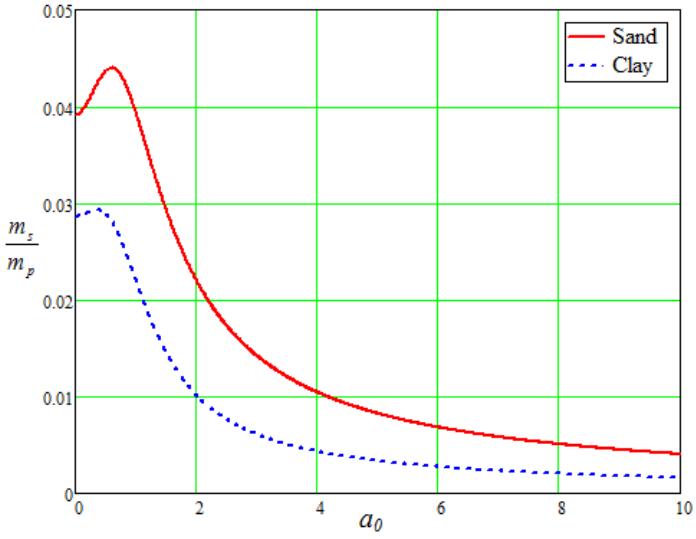

Figure 5-2 Relative mass vs. non-dimensional frequency, solid concrete pile, $\mu I_s / E_p I_p = 0.01$

Figure **5-3** shows the variations in relative mass of the tubular steel piles vs. the non dimensional frequency factor.

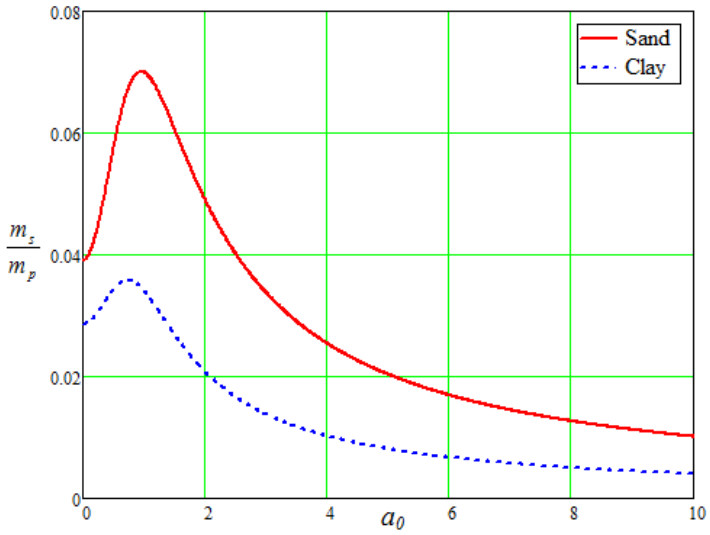

Figure 5-3 Relative mass vs. non-dimensional frequency, steel tubular pile, $\mu I_s / E_p I_p = 0.01$

The contributing soil mass is strongly related to frequency. It can be seen that the contributing soil mass can add 7% to the pile mass for tubular steel piles in sand. The contributing soil mass has its maximum effect in the (non-dimensional) frequency range of 0.4 to 1.0. The effect of mass reduces as the frequency increases and approaches zero at very high frequencies ($a_0>>10$). The effect for steel tubular piles is more important than for solid concrete piles. This can be explained by the fact that steel tubular piles are lighter than the concrete piles for the same shaft diameter.

Another important factor in the contributing mass is the modulus ratio of the soil and the pile '$\mu I_s / E_p I_p$'.

5.4 Lumped mass model for a laterally vibrating pile

So far, the inertia effects in soil are attributed to pile in a distributed bases, i.e. a continuous mass per unit length of the pile is added to the system to include soil mass. This approach is particularly useful when analysis based on beam on Winkler model for layered or variable soils are carried out (see section 4.3.1). In this section we investigate a simple model in which the combined effect of soil-pile mass are attributed to the pile top as a lumped mass. The pile mass per unit length is considered as 'm_p' and the soil mass 'm_s' is obtained from Table 4-3. The pile cap is considered as a lumped mass of 'm_c' on the top of the pile at the ground surface. For simplicity, mass moment of inertia of the pile cap and the damping of soil are ignored. Using these assumptions, the equation (4.1–66) turns to a real valued beam on elastic foundation equation with the foundation modulus determined as:

$$k_e = k_s - \omega^2 (m_p + m_s) \tag{5.4–1}$$

In this section only free vibration of the pile is considered and as it is shown in section 4.3.1 first free vibration frequency usually lies in low frequency range. Variations of soil stiffness with the frequency are not significant in low frequency range. Therefore the factor 'k_s' can be assumed constant. General solution of a beam on elastic foundation with infinite length is given in the equation (2.2–4) and repeated here:

$$X(z) = e^{-\beta z}(A\cos\beta z + B\sin\beta z) \tag{5.4–2}$$

The factor β in the equation (5.4–2) is defined in terms of effective Winkler spring stiffness;

$$\beta = \sqrt[4]{\frac{k_s - \omega^2 (m_p + m_s)}{4E_p I_p}} \tag{5.4–3}$$

The shear (horizontal) force 'V_0' acting on pile head due to free vibration of the pile cap with frequency ω is:

$$V_0 = m_c \omega^2 X(0) \tag{5.4–4}$$

It is seen that the shear force depends on the lateral deflection at pile top. Since the mass moment of inertia is ignored and the mass is applied at the ground level, the moment at pile head is zero (i.e. M_0=0). The constants 'A' and 'B' in the equation (5.4–2) are determined in the equations (2.2–9) and (2.2–10):

$$B = 0 \tag{5.4–5}$$

$$A = \frac{V_0}{2E_p I_p \beta^3} \tag{5.4–6}$$

Substituting the equations (5.4–4) to (5.4–6) into the equation (5.4–2) results in the following equation:

$$X(z) = \frac{m_c \omega^2 X(0)}{2E_p I_p \beta^3} e^{-\beta z}\cos\beta z \tag{5.4–7}$$

Taking the value of the equation (5.4–7) at 'z=0' leads to the following equation for the free vibration frequency:

$$\frac{m_c\omega^2}{2E_pI_p\beta^3}=1 \tag{5.4–8}$$

If the pile and the soil were mass less, the free vibration frequency became:

$$\omega_0^2=\frac{\sqrt[4]{2E_pI_pk_s^3}}{m_c} \tag{5.4–9}$$

The equation (5.4–9) is only useful for comparison and does not have any application. Substituting from the equation (5.4–3) in the equation (5.4–8) results in the following characteristic equation for free vibration frequency:

$$m_c\omega^2=(2E_pI_p)^{1/4}[k_s-\omega^2(m_p+m_s)]^{3/4} \tag{5.4–10}$$

The equation (5.4–10) can be simplified to a fourth order algebraic equation in terms of the frequency. Such equation can only be solved numerically. Here we follow another path and will simplify the equation by making some approximation. Let us assume that the following inequality is valid:

$$\omega^2\frac{m_p+m_s}{k_s}<<1 \tag{5.4–11}$$

The write hand side of the equation (5.4–10) is simplified using Newton binomial:

$$m_c\omega^2\cong(2E_pI_p)^{1/4}(k_s)^{3/4}(1-\frac{3}{4}\frac{m_p+m_s}{k_s}\omega^2) \tag{5.4–12}$$

The free vibration frequency is derived from the equation (5.4–12) as:

$$\omega^2\cong\frac{\sqrt[4]{2E_pI_pk_s^3}}{m_c+\frac{3}{4}\sqrt[4]{\frac{2E_pI_p}{k_s}}(m_p+m_s)} \tag{5.4–13}$$

Comparing the equation (5.4–13) with the equation (5.4–9) shows that the combined soil-pile mass can be assumed as a lumped mass applied to the pile head with the value of:

$$m_{Lump} \cong \frac{3}{4}\sqrt[4]{\frac{2E_pI_p}{k_s}}(m_p + m_s) \tag{5.4–14}$$

A similar procedure shall be followed for the limped mass moment of inertia. This time a hypothetical mass with only moment of inertia of 'I_c' is applied at the top of the pile. The moment at the pile due to the vibration of the mass is expressed as:

$$M_0 = I_c\omega^2 X'(0) \tag{5.4–15}$$

Where $X'(0)$ is the rotation at the pile head at the level of the ground. The factors 'A' and 'B' are determined as:

$$B = \frac{M_0}{2E_pI_p\beta^2} \tag{5.4–16}$$

$$A = -\frac{M_0}{2E_pI_p\beta^2} \tag{5.4–17}$$

The derivative of the deflected curve of the pile is given in equation (2.2–5). Substituting for 'A' and 'B' from equations (5.4–15), (5.4–16) and (5.4–17) in the equation (2.2–5) leads:

$$X'(z) = \frac{I_c\omega^2 X'(0)}{E_pI_p\beta}e^{-\beta z}\cos\beta z \tag{5.4–18}$$

Taking the value of the equation (5.4–18) at 'z=0' results in the following equation for the frequency:

$$\frac{I_c\omega^2}{E_pI_p\beta} = 1 \tag{5.4–19}$$

Assuming that the pile and soil had no mass, a hypothetical frequency was obtained which will be used only for comparison:

$$\omega_1^2 = \frac{\sqrt[4]{\frac{(E_pI_p)^3}{4}k_s}}{I_c} \tag{5.4–20}$$

The true equation for the free vibration frequency when the pile and soil masses are included is derived as:

$$\omega^2 \cong \frac{\sqrt[4]{(E_p I_p)^3 \frac{k_s}{4}}}{I_c + \frac{1}{4}\sqrt[4]{\frac{(E_p I_p)^3}{4k_s^3}}(m_p + m_s)} \tag{5.4–21}$$

Comparison the equations (5.4–20) and (5.4–21) shows that the effect of combined soil-pile mass can be considered as a lumped mass moment of inertia to the pile head at the ground line:

$$I_{Lump} \cong \frac{1}{4}\sqrt[4]{\frac{(E_p I_p)^3}{4k_s^3}}(m_p + m_s) \tag{5.4–22}$$

Now that the equivalent lumped mass for the soil and the pile are derived we can consider the free vibration frequency of the system with a general mass/ mass moment of inertia on its top. The effective mass and mass moment of inertia on the top of a mass less soil-pile system is written as follows. The mass of soil-pile system is transferred to the centre of mass of the cap which is located at height ‘d’ above the ground line:

$$\begin{cases} m'_c = m_c + m_{Lump} \\ I'_c = I_c + I_{Lump} + m_{Lump} d^2 \end{cases} \tag{5.4–23}$$

The shear force and bending moment on the pile head at the ground line are as follows, assuming that the centre of mass of the pile cap is located a distance ‘*d*’ above the ground line and the pile cap is rigid:

$$\begin{cases} V_0 = m'_c \, \omega^2 [X(0) - X'(0).d] \\ M_0 = I'_c \, \omega^2 X'(0) - V_0 d \end{cases} \tag{5.4–24}$$

The constants ‘A’ and ‘B’ are determined from the equations (2.2–9), (2.2–10) and (5.4–24):

$$B = \frac{M_0}{2E_p I_p \beta^2} \tag{5.4–25}$$

$$A = \frac{V_0}{2E_p I_p \beta^3} - \frac{M_0}{2E_p I_p \beta^2} \tag{5.4–26}$$

Substituting the equations (5.4–24), (5.4–25) and (5.4–26) in the equations (2.2–4) and (2.2–5) reads:

$$X(z) = e^{-\beta z}[(\frac{V_0}{2E_pI_p\beta^3} - \frac{M_0}{2E_pI_p\beta^2})\cos\beta z + \frac{M_0}{2E_pI_p\beta^2}\sin\beta z] \quad (5.4\text{–}27)$$

$$X'(z) = -\beta e^{-\beta z}[(\frac{V_0}{2E_pI_p\beta^3} - \frac{M_0}{2E_pI_p\beta^2})(\cos\beta z + \sin\beta z) - \frac{M_0}{2E_pI_p\beta^2}(\cos\beta z - \sin\beta z)] \quad (5.4\text{–}28)$$

Taking the value of the equations (5.4–27) and (5.4–28) at 'z=0' and some algebraic simplification leads to the following system of homogenous algebraic equations in terms of *X(0)* and *X'(0)*:

$$(1 - \omega^2 m'_c \frac{1+\beta d}{2E_pI_p\beta^3})X(0) + \omega^2 \frac{\beta I'_c + m'_c d(1+\beta d)}{2E_pI_p\beta^3} X'(0) = 0 \quad (5.4\text{–}29)$$

$$\omega^2 m'_c \frac{1+2\beta d}{2E_pI_p\beta^2} X(0) + (1 - \omega^2 \frac{2\beta I'_c + m'_c d(1+2\beta d)}{2E_pI_p\beta^2})X'(0) = 0 \quad (5.4\text{–}30)$$

It is known that for a system of linear homogeneous equations to have non trivial answers the determinant of the coefficients must be zero. This will lead to the characteristic equation of the free vibration frequency:

$$(I'_c m'_c)\omega^4 + 2E_pI_p\beta[m'_c(1+2\beta^2d^2+2\beta d) + 2\beta^2 I'_c]\omega^2 + 4(E_pI_p)^2\beta^4 = 0 \quad (5.4\text{–}31)$$

Solving the equation (5.4–31) leads to:

$$\omega^2 = \frac{2E_pI_p\beta^3[1 + m'_c \frac{1+2\beta d+2\beta^2d^2}{2\beta^2 I'_c} - \sqrt{1 + (m'_c \frac{1+2\beta d+2\beta^2d^2}{2\beta^2 I'_c})^2 + 2\frac{m'_c d}{I'_c}\frac{1+\beta d}{\beta}}]}{m'_c} \quad (5.4\text{–}32)$$

General formula for the free vibration frequency of a SDOF system is given as:

$$\omega^2 = \frac{K_d}{m'_c} \quad (5.4\text{–}33)$$

Where 'K_d' is dynamic stiffness of the system translated to the centre of mass. Comparison between the equations (5.4–32) and (5.4–33) concludes that the dynamic stiffness of the pile reads:

$$K_d = 2E_pI_p\beta^3\left[1+m'_c\frac{1+2\beta d+2\beta^2d^2}{2\beta^2I'_c}-\sqrt{1+\left(m'_c\frac{1+2\beta d+2\beta^2d^2}{2\beta^2I'_c}\right)^2+2\frac{m'_c\,d}{I'_c}\frac{1+\beta d}{\beta}}\right] \quad (5.4\text{–}34)$$

The term $2E_pI_p\beta^3$ in the equation (5.4–34) is the static stiffness of a free head pile at the ground line (see Table 2-1). It is seen that the stiffness is reduced for two main reasons:

- The existence of the mass moment of inertia
- The height of the centre of mass above the ground line

A stiffness reduction factor is introduced here:

$$SR = 1+m'_c\frac{1+2\beta d+2\beta^2d^2}{2\beta^2I'_c}-\sqrt{1+\left(m'_c\frac{1+2\beta d+2\beta^2d^2}{2\beta^2I'_c}\right)^2+2\frac{m'_c\,d}{I'_c}\frac{1+\beta d}{\beta}} \quad (5.4\text{–}35)$$

This factor may become significant in practical situations in multistory buildings where centre of mass is located in considerable height above the ground.

It should be noted that the equation (5.4–32) is suited for undamped vibration. The damped free vibration frequency can be approximately obtained using the following simple formula for SDOF system (Clough and Penzien 1995):

$$\omega_D = \omega\sqrt{1-\xi^2} \quad (5.4\text{–}36)$$

Where ‘ ω ’ is the frequency calculated from the equation (5.4–33), ‘ ξ ’ is the damping ratio of the system and ‘ ω_D ’ is the damped free vibration frequency.

5.5 Application

To check the validity of the results obtained in this chapter and to demonstrate their application to practical problems the same published test results as discussed in previous chapters is considered. The critical length of the pile in Mathura I (Boominathan and Ayothiraman 2006) is derived in section 2.7 to be 2.565 meters. The soil properties in this depth are almost invariable. Therefore the soil properties of the first layer are taken as the characteristic values. Values calculated in section 4.3.1 are used to avoid repeated calculations. Calculations are made in Mathcad spreadsheet and given in the following pages. The result is in excellent agreement with the Eigen value analysis performed via compiter program (section 4.3.1). Table 5-2 summarizes the calculated and test results.

Table 5-2 Back analysis results for the first free vibration frequency of test pile

Derivation method	Formulas in Section 5.4	FEA (section 4.3.1)	Full scale dynamic test- Mathura I (Boominathan and Ayothiraman 2006)
Frequency (Hz)	22.325	22.524	19.7-23.5

Input data

$x := 750mm$ Cap length

$y := 750mm$ Cap height

$z := 750mm$ Cap Thickness

$c := 150mm$ Clearance to ground line

$D := 500mm$ Pile diameter

$\rho := 2.4tonne \cdot m^{-3}$ Density of concrete

$M_o := 1tonne$ Oscillator mass

Data from section 4.3.1

$E_p := 23.5\ GPa$ Modulus elasticity of concrete

$m_p := 471 \frac{kg}{m}$ Pile mass per unit length

$k_s := 332.767MPa$ Soil stiffness factor for the first layer

$\zeta_s := 0.12$ combined soil-pile damping ratio

$\rho_s := 48kg \cdot m^{-3}$ Soil adding density to the concrete pile

Calculations

$d := c + \frac{x}{2}$

$I_p := \frac{\pi}{64} \cdot D^4$ Pile second moment of inertia

$A_p := \frac{\pi}{4} \cdot D^2$

$M_{cap} := x \cdot y \cdot z \cdot \rho$ $M_{cap} = 1.012 \times 10^3 kg$ Pile cap mass

$I_{cap} := M_{cap} \cdot \left(\frac{x^2 + y^2}{12} \right)$ Pile cap mass moment of inertia

$M_c := M_{cap} + M_o$ $M_c = 2.013 \cdot tonne$ Total mass at centre of pile cap

$I_c := I_{cap} + M_o \cdot (c + y)^2$ Total mass moment of inertia at centre of pile cap

$I_c = 904.922\, m^2 \cdot kg$

$m_s := A_p \cdot \rho_s$ Soil mass per unit length of pile

$$m_{Lump} := \frac{3}{4}\left(\frac{2 \cdot E_p \cdot I_p}{k_s}\right)^{\frac{1}{4}} \cdot (m_p + m_s)$$ Lumped mass of the soil-pile system

$m_{Lump} = 292.34\, kg$

$$I_{Lump} := \frac{1}{4} \cdot \left[\frac{(E_p \cdot I_p)^3}{4 \cdot k_s^3}\right]^{\frac{1}{4}} \cdot (m_p + m_s)$$ Lumped mass moment of inertia of soil-pile system

$I_{Lump} = 26.97\, m^2 \cdot kg$

$m_{pc} := M_c + m_{Lump}$ Total lumped mass

$I_{pc} := I_c + I_{Lump} + m_{Lump} \cdot d^2$ Total mass moment of inertia

$$\beta := \left(\frac{k_s}{4E_p \cdot I_p}\right)^{\frac{1}{4}}$$ Parameter β

$K_h := 2E_p \cdot I_p \cdot \beta^3$ Pile free head stiffness

$$SR := 1 + \frac{m_{pc} \cdot (1 + 2\beta \cdot d + 2\beta^2 \cdot d^2)}{2\beta^2 \cdot I_{pc}} - \sqrt{\left[1 + \left[\frac{m_{pc} \cdot (1 + 2\beta \cdot d + 2\beta^2 \cdot d^2)}{2\beta^2 \cdot I_{pc}}\right]\right]^2 + 2\frac{m_{pc} \cdot d}{I_{pc}} \cdot \frac{1 + \beta \cdot d}{\beta}}$$

$SR = 0.287$ Stiffness reduction factor

$K_d := SR \cdot K_h$ $\frac{1}{2\pi}\cdot\sqrt{\frac{K_h}{M_c}} = 44.951\,\frac{1}{s}$

$\omega := \sqrt{1-\zeta_s^2}\cdot\sqrt{\frac{K_d}{m_{pc}}}$ $\omega = 140.272\,\frac{1}{s}$ $K_h = 1.605\times10^5\cdot\frac{kN}{m}$

$f := \frac{\omega}{2\pi}$ $f = 22.325\,\frac{1}{s}$ $K_d = 4.601\times10^4\cdot\frac{kN}{m}$

5.6 Summary chapter five

The results of the solutions obtained in chapter four are discussed in this chapter. Clear limits for low and high frequency regimes are established. Considerations are made to the pile and soil types. It is seen that the low frequency upper limit is governed by the soil type and is slightly different for clays and sands. Equation (5.1–11) establishes the upper limit for low frequency regime.

High frequency lower limits are also established in this chapter. Again the soil type was governing for both cast in place concrete piles and tubular steel piles. Equation (5.2–4) establishes the high frequency lower limit. Table 5-3 summarizes the limits for different frequency regimes.

Table 5-3 Summary low and high frequency limits

Soil type	Low frequency regime	Intermediate	High frequency regime
Clay	$a_0 \leq 0.14$	$0.14 < a_0 < 1.281$	$a_0 \geq 1.281$
Sand	$a_0 \leq 0.25$	$0.25 < a_0 < 2.22$	$a_0 \geq 2.22$

In chapter four the soil mass is determined as a distributed mass which is added to the pile mass per unit length. In this chapter, an equivalent lumped mass that can be added to the centre of mass of the pile cap is determined. It should be noted that the proposed formulae for the lumped mass is only valid for low frequency vibrations. Equations (5.4–14) and (5.4–21) express the lumped mass and mass moment of inertia of the soil-pile system, respectively.

A simple formula for free vibration frequency of pile is obtained using the results of section 2.2.1 and combining them with the results of the present chapter. It is shown that the free head pile stiffness should be reduced by a factor which depends on the mass moment of inertia and height of the centre of mass of pile cap in order to obtain the true dynamic

stiffness of the pile. This considerably simplifies calculations of the free vibration frequency. The agreement with FE analysis and test results is excellent.

CHAPTER SIX

6 SUMMARY AND CONCLUSIONS

The elastic dynamic analysis of piles has been discussed in this thesis. A solution to elastodynamic equations has been found for semi-infinite soil under the vibrations of a laterally loaded pile. The solution mathematically expressed the horizontal and vertical deformations in the soil media which were interpreted as radiated waves. It was shown that the horizontal components of deformations in the soil are non-dilatational; therefore they represent SH-waves. The vertical component of deformations in the soil is dilatational and represents the pressure P-waves. Both sets of waves travel in a vertical direction in the soil media.

The resistance of soil against the lateral deflection of the pile was investigated. It is observed that soil resistance comprises of two components:

1- A lateral distributed force which is proportional to pile local lateral deflection
2- A distributed bending moment which is proportional to pile local curvature

An equivalent beam on Winkler supports is proposed to represent the interaction between the soil and the pile. This model is composed of a beam representing the piles and set of distributed springs, masses and dashpots representing the soil.

Simple formulas are proposed for stiffness, mass and damping of the Winkler supports. It has been shown that these quantities are highly frequency-dependent. The formulas are given for low-frequency and high-frequency regimes. Interpolating functions are also proposed in order to estimate the values of stiffness, mass and damping for the general case of vibration frequencies.

A number of researchers have investigated the lateral stiffness of piles. Each study has its own approach, limitations and approximations. A finite element analysis (FEA) was conducted in the course of the present research in order to establish an independent view on the stiffness of Winkler supports. General agreement between the FEA, the published data and the theoretically-developed values in this thesis verified the soundness of the present approach. There were also similarities between the damping values obtained from the theory and those used and reported by others.

Contributing soil mass was the main subject of this thesis. This parameter was clearly determined within the solution process. It was shown that the contributing soil mass can be

as high as 7% of the mass of the pile for steel tubular piles. The effect of the contributing mass is more significant for low vibration frequencies and for tubular piles in stiff soils.

Although the subject of this thesis was limited to laterally vibrating piles, attention was also paid to the problem of axially vibrating piles. There is room for improvement in the existing theories for piles under axially vibrating loads. These solutions were given for an end-bearing pile in a layer of soil overlaying rigid bedrock. An improved solution was proposed for this problem which also formulated the concept of the contributing soil mass in vertical pile vibrations. The added soil mass was derived for each mode of vibration in a modal analysis. The reflection of waves from the bedrock and from the free surface were discussed and included in the proposed solution. A model composed of three generalized Kelvin-Voigt models was proposed such that the reflected waves from the bedrock and the free surface can be successfully modeled.

The results of this research can be used in the dynamic analysis of piles and soil-pile-structure interaction problems. The pile may be modeled as a beam on generalized Winkler support composed from springs, masses and dampers. If nonlinear effects need to be included in the analysis, they can be modeled in the near-field region, either by finite elements or by inclusion of p-y springs. The spring, mass and dampers as determined in the present study should be added to such model to represent the far-field zone. This will lead to a great deal of simplification as well as increased accuracy in a typical FE model.

The application of the results of this study is demonstrated via back analyzing of published full scale pile test results. A selected test pile is modeled via a commercial FEA computer program. Soil springs are added to the model with stiffness values obtained in the present study. Mass and damping properties of the soil are added to similar values of the pile material. Free vibration analysis (Eigen value analysis) is performed. The same pile is also re-analyzed using the simple formulas obtained for free vibration. Since the chosen pile was in stiff clay which behaved almost elastically, the results of both analyses closely matched each other and the test results.

The proposed solution in this study is an improvement to the existing continuum solutions to the laterally vibrating pile problem. Although such solutions have limited applicability, they provide insight to the problem and light the way towards solving more complex ones. The results of this thesis may be used in the study of propagating SH-P waves, pile group analysis and pile-soil-pile interaction analysis. These aspects could not be covered in the present study due to the limited space and time, but may be considered as future fields of research.

REFERENCES

Abramowitz, M. and I. A. Stegun (1972). Handbook of Mathematical Functions With Formulas, Graphs, and Mathematical Tables. Washington DC, US Department of Commerce

ACI-Committee-318 (2011). Building Code Requirements for Structural Concrete and Commentary. Frmingtom Hills, American Concrete Institute.

API-RP-2A (2007). Recommended Practice for Planning, Designing and Constructing Fixed Offshore Platforms-Working Stress Design (21 st Edition), . Washington D.C., API Publishing Services.

Ashford, S. A. and T. Juirnarongrit (2003). "Evaluation of pile diameter effect on initial modulus of subgrade reaction." Journal of Geotechnical and Geoenvironmental Engineering **129**(3): 234-242.

Bahrami, A. and H. Nikraz (2012). "Effect of shaft diameter of pile on lateral Winkler springs' stiffness." Journal of Earthquake Engineering **16**(5): 595–606.

Bahrami, A. and H. Nikraz (2013). A mathematically developed dynamic model for laterally loaded piles. State of The Art of Pile Foundation and Pile Case Histories. P. P. Rahardjo, D. Choudhury and B. Widjaja. Bandung, Indonesia**:** C3-1–C3-6.

Banerjee, P. K. (1978). Analysis of Axially and Laterally Loaded Pile Groups. Developments in Soil Mechanics. C. R. Scott. London, Applied Science Publishers.

Banerjee, P. K. and T. G. Davies (1978). "The behaviour of axially and laterally loaded single piles embedded in nonhomogeneous soils." Géotechnique **28**(3): 309 - 328.

Baranov, V. A. (1967). "On the calculation of excited vibrations of an embedded foundation." Voprosy Dynamiki Prochnocti **14**: 195 - 209.

Berger, E., S. Mahi and R. Pyke (1977). Simplified Method for Evaluating Soil-Pile-Structure Interaction Effects. Proceedings of Offshore Technology Conference, 2 - 5 May, Houston, Texas.

Biot, M. A. (1922). "Bending of an Infinite Beam on an Elastic Foundation." Zeitschrift fiir Angewandte Maihematik und Mechanik **2**(3): 165 - 184.

Blaney, G. W., E. Kausel and J. M. Roesset (1976). Dynamic Stiffness of Piles. Proceedings of the Second International Conference on Numerical Methods in Geotechnical Engineering. New York, ASCE**:** 1001 - 1012.

Boominathan, A. and R. Ayothiraman (2006). "Dynamic response of laterally loaded piles in clay." Proceedings of the Institution of Civil Engineers - Geotechnical Engineering **159**(GE3): 233-241.

Bowles, J. E. (1997). Foundation Analysis and Design. New York, McGraw-Hill, Inc.

Butterfield, R. and P. K. Banerjee (1971a). "The elastic analysis of compressible piles and pile groups." Geotechnique **21**(1): 43 - 60.

Butterfield, R. and P. K. Banerjee (1971b). "The problem of pile group-pile cap interaction." Geotechnique **21**(2): 135 -142.

Carter, D. P. (1984). A non-linear soil model for predicting lateral pile response. C. E. D. Rep. No. 359, Univ. of Auckland, New Zealand.

Clough, R. W. and J. Penzien (1995). Dynamics of Structures. Berkeley, Computers & Structures, Inc.

Dobry, R., I. Oweis and A. Urzua (1976). "Simplified procedures for estimating the fundumental period of a soil profile." Bulletin of the Seismological Society of America **66**(4): 1293 -1321.

Döring, B. (1965). "Complex zeros of cylinder functions." Math. Comp. **20**: 215-222.

Douglas, J. D. and E. H. Davis (1964). "The movement of buried footings due to moment and horizontal load and the movement of anchor plates." Geotechnique **14**: 115 -132.

El Naggar, M. H. and M. Novak (1994). "Nonlinear lateral interaction in pile dynamics." Soil Dynamics and Earthquake Engineering **14**: 141 -157.

El Naggar, M. H. and M. Novak (1995). "Nonlinear analysis for dynamic lateral pile response." Soil Dynamics and Earthquake Engineering **15**: 233 - 244.

Gazetas, G. and R. Dobry (1984). "Horizontal Response of Piles in Layered Soils." Journal of Geotechnical Engineering (ASCE) **110**(1): 20 - 40.

Gazetas, G., K. Fan and A. M. Kaynia (1992). "Dynamic response of pile groups with different configurations." Soil Dynamics and Earthquake Engineering **12**: 239 - 257.

Georgiadis, M. (1983). Development of p-y Curves for Layered Soils. Conference on Geotechnical Practice in Offshore Engineering,April 27-29, 1983. Austin Texas, American Society of Civil Engineers**:** 536 - 545.

Gunaratne, M., Ed. (2006). The Foundation Engineering Handbook. Boca Raton, Taylor & Francis.

Hetenyi, M. (1946). Beams on Elastic Foundation. Ann Arbor, University of Michigan Press.

Hetnarski, R. B. and J. Ignaczak (2004). Mathematical Theory of Elasticity. New York, Taylor & Francis.

Howe, R. J. (1955). A Numerical Method for Predicting the Behaviour of Laterally Loaded Piling, Exploration and Production Research Divison Publication No. 412

Houston, Texas., Shell Oil Co.

Johnson, K. L. (1985). Contact Mechanics. Cambridge, UK, Cambridge University Press.

Kausel, E. (2006). Fundamental Solutions in Elastodynamics: A Compendium. Cambridge, UK, Cambridge University Press.

Kaynia, A. M. (1982). Dynamic stiffness and seismic response of pile groups, Doctoral Thesis. Massachusetts, USA, Department of Civil Engineering, Massachusetts Institute of Technology

Kaynia, A. M. and E. Kausel (1980). Dynamic Stiffness and Seismic Response of Sleeved Piles, Report No. R80-12, Massachusetts Institute of Technology.

Kaynia, A. M. and E. Kausel (1991). "Dynamics of piles and pile groups in layered soil media." Soil Dynamics and Earthquake Engineering **10**(8): 386 - 401.

Kuhelmeyer, R. L. (1979). "Static and dynamic laterally loaded floating piles." Journal of geotechnical engineering division (ASCE) **105**(2): 289-304.

Lamb, H. (1904). "On the propagation of tremors over the surface of an elastic solid " Phillosophical Transactions of the Royal Society of London **A**: 203.

Lenci, C., J. Maurice and F. Madigner (1968). "Pieu vertical sollicite horizontalement." Annales des Ponts et Chaussees **I**: 337 - 383.

Love, A. E. H. (1944). A Treatise on the Mathematical Theory of Elasticity. New Yorke, Dover Publications.

Markis, N. and G. Gazetas (1992). "Dynamic pile-soil-pile interaction II: Lateral and seismic response." Earthquake Engineering and Structural Dynamics **21**: 145-162.

Matlock, H. (1970). Correlations for Design of Laterally Loaded Piles in Soft Clay. Offshore Technology Conference OTC 1204, Houston, Texas.

Matlock, H. and L. C. Reese (1960). "Generalized solutions for laterally loaded piles." Journal of the Soil Mechanics and Foundations Division (ASCE) **86**(5): 63 - 94.

Matthewson, C. D. (1969). The Elastic Behaviour of a Laterally Loaded Pile. Civil Engineering Department. Christchurch, University of Canterbury, N.Z. **Ph.D.**

Maxfield, B. (2009). Essential Mathcad for Engineering, Science, and Math. Amsterdam, Elsevier.

McClelland, B. and J. A. Focht (1958). "Soil modulus for laterally loaded piles." Transactions of American Society of Civil Engineers **123**: 1049 -1086.

Michell, J. (1899). "On the direct determination of stress in an elastic solid with application to the theory of plates." Proc. London Math. Soc. **31**: 100 -124.

Mindlin, R. D. (1936). "Force at a point in the interior of a semi-infinite solid." Physics **7**: 195 - 202.

Nogami, T. (1980). Dynamic Stiffness and Damping of Pile Groups in Inhomogeneous Soil. Dynamic Response of Pile Foundations: Analytical Aspects.Proceedings of a Session Sponsored by the Geotechnical Engineering Division at the ASCE National Convention, 30 October 1980. M. W. O'Neill and R. Dobry. Florida, American Society of Civil Engineers**:** 31-52.

Nogami, T. and K. Konagai (1986). "Time domain axial response of dynamically loaded single piles." Journal of Engineering Mechanics **112**(11): 1241 -1252.

Nogami, T. and K. Konagai (1988). "Time domain flexural response of dynamically loaded single piles." Journal of Engineering Mechanics **114**(9): 1512 -1525.

Nogami, T., K. Konagai and H. L. Chen (1992). "Nonlinear soil-pile interaction model for dynamic lateral motion." Journal of Geotechnical Engineering (ASCE) **118**(1): 89 - 106.

Nogami, T. and M. Novak (1976). "Soil-Pile Interaction in Vertical Vibration." Earthquake Engineering & Structural Dynamics **4**(277-293): 277-293.

Nogami, T. and M. Novak (1977). "Resistance of soil to a horizontally vibrating pile." Earthquake Engineering and Structural Dynamics **5**: 249 - 261.

Novak, M. (1974). "Dynamic stiffness and damping of piles." Canadian Geotechnical Journal **11**: 574 - 598.

Novak, M. and F. Aboul-Ella (1978). "Impedance functions of piles in layered media." Journal of Engineering Mechanics **104**: 643 - 661.

Novak, M. and F. Aboul-Ella (1997). PILAY: A Computer Program for Calculation of Stiffness and Damping of Piles in Layered Media, University of Western Ontario, Canada, 1997,Report No. SACDA 77-30

Novak, M. and Y. O. Beredugo (1972). "Vertical vibration of embedded footings." Canadian Geotechnical Journal **9**(4): 477- 497.

Novak, M. and B. El Sharnouby (1983). "Stiffness constants of single piles." Journal of Geotechnical Engineering **109**(7): 961 - 974.

Novak, M. and T. Nogami (1977). "Soil-pile interaction in horizontal vibration." Earthquake Engineering and Structural Dynamics **5**: 263 - 281.

Novak, M., T. Nogami and F. Aboul-Ella (1978). "Dynamic soil reactions for plane strain case." Journal of the Engineering Mechanics Division (ASCE) **104**(EM4): 953 - 959.

Novak, M. and M. Sheta (1980). Approximate approach to contact problems of piles. Proceeding of Geotechnical Engineering Division, National Convention, Dynamic Response of Pile Foundations: Analytical Aspects, 30 October 1980. Florida, ASCE**:** 53 - 79.

Novak, M. and M. Sheta (1982). Dynamic Response of Piles and Pile Groups. 2nd International Conference of Numerical Methods in Offshore Piling, April 29-30, 1982. Austin, Texas**:** 1 - 18.

Novak, M., M. Sheta, L. El-Hifnawy, H. El-Marsafawi and O. Ramadan (1991). DYNA3: A computer program for calculation of foundation response to dynamic loads. London, Geotechnical Research Centre, the University of Western Ontario.

O'Rourke, M. J. and R. Dobry (1979). Spring and Dashpot Coefficient for Machine Foundations on Piles. Proceedings of the American Concrete Institute International Symposium on Foundation for Equipment and Machinery, Milwaukee, Wisc.

O'Neill, M. W. and J. M. Murchison (1983). An Evaluation of p-y Relationships in Sands. Report PRAC 82-41-1, Prepared for the American Petroleum Institute Houston, Texas, University of Houston.

Pak, R. Y. S. (1985). Dynamic Response of a Partially Embedded Bar under Transverse Excitations. Report No. EERL 85-04, Earthquake Engineering Research Laboratories. Pasedena, California, California Institute of Technology.

Pak, R. Y. S. and B. B. Guzina (1999). "Seismic soil-structure interaction analysis by direct boundary element methods." Int. J. Solids Struct. **36**: 4743-4766.

Pak, R. Y. S. and P. C. Jennings (1987). "Elastodynamic response of pile under transverse excitation." Journal of Engineering Mechanics **113**(7): 1101 - 1116.

Pender, M. J., D. P. Carter and S. Pranjoto (2007). "Diameter effects on pile head lateral stiffness and site investigation requirements for pile foundation design." Journal of Earthquake Engineering **11**: 1 -12.

Pipes, L. A. and L. R. Harvill (1970). Applied Mathematics for Engineers and Physicists. New York, McGraw-Hill Book Company.

Poulos, H. G. (1971a). "Behaviour of laterally loaded piles: I-single piles." Journal of Soil Mechanics and Foundations Division (ASCE) **97**(SM5): 711 - 731.

Poulos, H. G. (1971b). "Behaviour of laterally-loaded piles: II-pile groups." Journal of Soil Mechanics and Foundations Division (ASCE) **97**(SM5): 733 - 751.

Poulos, H. G. (1973). "Load -deflection prediction for laterally loaded piles." Australian Geomechanics Journal **G3**(1): 1 - 8.

Poulos, H. G. and E. H. Davis (1980). Pile Foundation Analysis and Design. New York, John Wiley & Sons.

Rajapakse, R. K. N. D. and Y. Wang (1990). "Load-transfer problem for transversely isotropic elastic media." Journal of Engineering Mechanics **116**(12): 2643 - 2662.

Randolph, M. (1981). "The response of flexible piles to lateral loading." Geotechnique **31**(2): 247 - 259.

Reese, L. C. and W. R. Cox (1975). Field Testing and Analysis of Laterally Loaded Piles in Stiff Clay. Proceedings of the Seventh Annual Offshore Technology Conference, May 5-8. Houston, Texas**:** OTC 2312.

Reese, L. C. and H. Matlock (1956). Non-dimensional solutions for laterally-loaded piles with soil modulus assumed proportional to depth. Proceedings of the 8th Texas Conference on Soil Mechanics and Foundation Engineering, September 14 and 15. Austin, Texas**:** 1-41.

Reese, L. C. and W. F. Van Impe (2001). Single Piles and Pile Groups Under Lateral Loading. Leiden,, A.A. Balkema Publishers.

Sadd, M. H. (2009). Elasticity Theory, Applications, and Numerics. New York, Elsevier.

Salencon, J. (2001). Handbook of Continuum Mechanics: General Concepts - Thermoelasticity. Heildelberg, Springer.

Spillers, W. R. and R. D. Stoll (1964). "Lateral response of piles." J.S.M.F.D., ASCE **90**(SM6): 1 - 9.

Takemiya, H. and Y. Yamda (1981). "Layered soil-pile structure dynamic interaction." Earthquake Engineering and Structural Dynamics **9**: 437 - 457.

Timoshenko, S. P. (1934). Strength of Materials. New York, Van Nostrand Company.

Timoshenko, S. P. and J. N. Goodier (1970). Theory of Elasticity. New York, McGraw-Hill Book Company.

Vallabhan, C. V. G. and Y. C. Das (1988). "Parametric study of beams on elastic foundations." Journal of Engineering Mechanics (ASCE) **114**(12): 2072 - 2083.

Vallabhan, C. V. G. and Y. C. Das (1991). "Modified Vlasov model for beams on elastic foundations." Journal of Geotechnical & Geoenvironmental Engineering (ASCE) **117**(6): 856 - 967.

Velez, A., G. Gazetas and Krishnan. R (1982). "Lateral dynami response of constrained-head piles." Journal of Geotechnical Engineering **109**(8): 1063 - 1081.

Verruijt, A. (2010). An Introduction to Soil Dynamics. Heidelberg, Springer.

Vesic, A. S. (1961). Beam on elastic subgrade and the Winkler hypothesis. Proceedings of the 5th International Conference on Soil Mechanics and Foundation Engineering, 17th to 22nd July. Paris. **1:** 845 - 850.

Vlasov, V. Z. and N. N. Leont'ev (1966). Beams, plates and shells on elastic foundations. Israel Program for Scientific translations, Jerusalem. (Translated from Russian)

Winkler, E. (1867). "Die Lehre von der Elastizität und Festigkeit." H. Dominicus: 182-184.

Xu, K. J. and H. G. Poulos (2000). "General elastic analysis of piles and pile groups." International Journal for Numerical and Analytical Methods in Geomechancis **24**: 1109-1138.

Zimmermann, H. (1888). Die Berechnung des Eisenbahn Oberbaues. Berlin.

Every reasonable effort has been made to acknowledge the owners of copyright material. I would be pleased to hear from any copyright owner who has been omitted or incorrectly acknowledged.